MARITIME TRANSPORTATION RESEARCH AND EDUCATION CENTER
TIER 1 UNIVERSITY TRANSPORTATION CENTER
U.S. DEPARTMENT OF TRANSPORTATION

Effect of Permeability Variation of Expansive Yazoo Clay at the Maritime and Multimodal Transportation Infrastructure in Mississippi

October 01, 2018, to December 31, 2019

Prepared by:

Sadik Khan, Ph.D., P.E.
John Ivoke, S.M.ASCE
Masoud Nobahar, S.M, ASCE
Department of Civil and Environmental Engineering,
Jackson State University,
1400 J. R. Lynch St, Box 17068
Jackson, MS, 39217
Phone: 601-979-6373
Email: J00797693@jsums.edu

January 2020

FINAL RESEARCH REPORT
Prepared for:
Maritime Transportation Research and Education Center

University of Arkansas
4190 Bell Engineering Center
Fayetteville, AR 72701
479-575-6021

ACKNOWLEDGEMENT

This material is based upon work supported by the U.S. Department of Transportation under Grant Award Number 69A3551747130. The work was conducted through the Maritime Transportation Research and Education Center at the University of Arkansas.

DISCLAIMER

The contents of this report reflect the views of the authors, who are responsible for the facts and the accuracy of the information presented herein. This document is disseminated in the interest of information exchange. The report is funded, partially or entirely, by a grant from the U.S. Department of Transportation's University Transportation Centers Program. However, the U.S. Government assumes no liability for the contents or use thereof.

ABSTRACT

The existence of Yazoo clay soil in Mississippi frequently causes distress to the pavement and cause deformation at the slopes in highways and levees, which are a critical component in Maritime and multimodal transportation infrastructure. Each year, fixing the pavement requires a significant maintenance budget of MDOT. Also, the infiltration of the rainwater in the highway and levee slopes leads to landslides, which require millions of maintenance dollars each year. Due to the shrinkage and swelling behavior of the Yazoo clay, the hydraulic conductivity varies over the different seasons and has higher vertical permeability during the dry season. With high vertical permeability, the rainwater can easily percolate in the pavement subgrade and slopes, which accelerates the failure. However, a limited study is available on the change in hydraulic permeability of Yazoo clay soil. The current study investigates the change in unsaturated vertical and horizontal permeability and its effect on the maritime and multimodal infrastructures, especially on the pavement and slopes of highway embankment and levees. Highly plastic Yazoo clay soil samples were collected from highway slope sites and then tested in the laboratory to investigate the changes in the hydraulic conductivity with different wet-dry cycles. Mini Disk Infiltrometer and instant profile method were utilized to determine the hydraulic conductivity of Yazoo clay with 1, 2, and 3 numbers of wet-dry cycles. The laboratory test results indicated that the hydraulic conductivity of Yazoo clay is very low at a fully compacted phase (~10^{-6} cm/s). However, with an increment in the wet-dry cycles, the hydraulic conductivity of Yazoo clay increases (~10^{-4} cm/s) after the sample is exposed to 3 numbers of wet-dry cycles. Flow analysis was performed on a highway and a levee embankment, to investigate the effect of the changes of the hydraulic conductivity on the infiltration behavior with the presence of different rainfall volume. The flow analysis was performed using the finite element method, using Plaxis 2D. The flow analysis results indicated that with an increase in the hydraulic conductivity, the rate of infiltration increases along the slopes, and it only influences the highway pavement near the shoulder. However, the increase in hydraulic conductivity severely affects the infiltration behavior of the levee. At high hydraulic conductivity, the low intensity and long duration rainwater infiltrated through the levee and saturated the levee section. Due to the rapid infiltration of the rainwater in the levee, the matric suction value almost disappears, which leads to saturated conditions of the levee. Even though the changes in the hydraulic conductivity affect the saturation behavior which influences the stability of the highway embankment and levee slopes, it is mostly ignored in the design. It is highly recommended to include the variation of hydraulic conductivity in the design of the Maritime and Multimodal Transportation Infrastructures on Yazoo clay.

TABLE OF CONTENT

LIST OF FIGURES

LIST OF TABLES

Chapter 1: INTRODUCTION

1.1 Research Challenge

Expansive soils cover more than 25% of the total area of the United States. The expansive clay experience volumetric deformation, which affects the stability and performance of the structures constructed on it. Expansive subgrade soils can induce significant deterioration on pavements including surficial distresses, edge cracks, shoulder drop-offs, shrinkage cracks and overall serviceability loss. Expansive soils are a very significant problem in many parts of the United States and are responsible for the application of premature maintenance and rehabilitation activities on many miles of roadway each year (Christopher et al. 2006). The destructions are more visible in low volume hot mix asphalt pavements which usually have light loading and traffic; therefore, premature failure usually occurs as a result of environmental factors (Wanyan et al., 2010). Post-construction damages can be significantly reduced if this issue is addressed during the design stage. Therefore, an accurate understanding of soil behavior and the potential effect on pavement performance is necessary.

Expansive soil problems typically occur due to water content changes in the upper several feet (Nelson and Miller 1992). The water content in these upper layers is significantly influenced by climatic and environmental factors and is generally termed as the zone of seasonal fluctuations or active zone, as presented in Figure 1.1. In general, negative pore water pressures exist in the active zone; however, excess water addition through the surface will increase the water content, and heave will occur in expansive clay. On the other hand, dissipation of the soil moisture occurs during the dry period and cause shrinkage of the soil. The active zone can vary significantly with climate conditions with depths up to 15 ft. (Biddle, 2001).

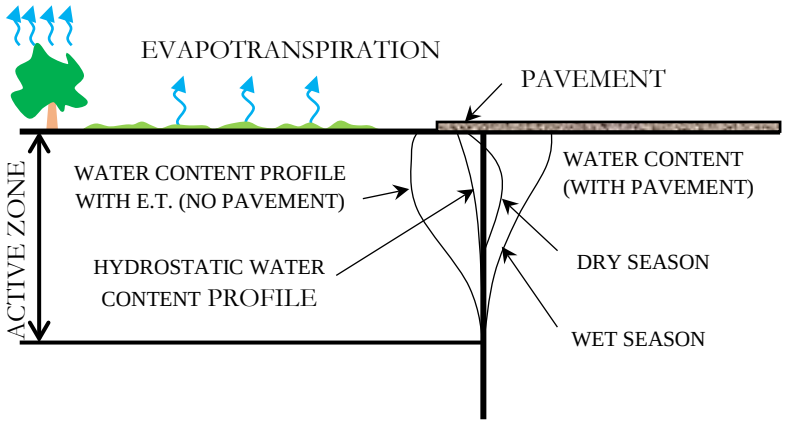

Figure 1.1 Water content profiles in Active Zone (redrawn after Nelson and Miller, 1992)

Fredlund et al., 2006 presented that the distress of pavement on an expansive subgrade is caused by the loss of support condition. The soil outside the pavement is more exposed and subjected to more moisture variation. During the wet period, water infiltrates through the side of the pavement, which may saturate and cause the perimeter soil to become wetter than the soil underneath the pavement. As a result, a differential moisture variation may occur resulting in differential swelling at expansive clay underneath the pavement. The differential movement increases stress concentration inside the pavement structure and may initiate the crack, which propagates with time and load repetitions. Consequently, during the dry

season, the soil loses moisture and causes the shrinkage of the expansive soil. As the soil shrinks, the slab's edge might separate from the supporting soil. Separation of the slab increases stress concentration in the slab and causes the slab to develop top-down cracking (Luo, 2007).

The Yazoo Formation containing Yazoo clay is geologically defined within the Jackson Group and has been identified throughout the southeastern and southwestern United States. The upper stratigraphy of the Jackson Group that contains Yazoo clay (or its geological equivalent) extends in regional locations across Alabama, Louisiana, and Mississippi. The geographical extent of the Yazoo clay lies within the central Mississippi counties of Yazoo, Holmes, Hinds, Rankin, Madison, Scott, Newton, Smith, Jasper, and Wayne. The horizontal width of the surface outcrop varies from approximately 35 miles on the west to less than 10 miles on the east, whereas; the metropolitan Jackson area is located directly on top of the Yazoo clay (Lee 2012). Yazoo Clay is indicated to have a very high shrink/swell potential and moisture changes result in expansive, swelling, shrinkage, and otherwise, destructive behavior causes the detrimental effect to the roads, foundations, and related infrastructure in the central Mississippi region (Douglas and Dunlap, 2000; Lee 2012). The change of volume of the Yazoo clay between the liquid limit and oven-dry moisture contents is ranged from 100 to 235 percent. On the other hand, swell pressures have been measured by more than 25,000 psf (Johnson 1973).

The Mississippi Department of Transportation (MDOT) has significant maintenance issues on their pavements due to the existence of the highly plastic Yazoo clay soil. Moreover, there are Levee System in Mississippi, especially along the Mississippi River, which face significant damages due to the presence of Yazoo clay in it. The levee system is a critical component of the Maritime and Multimodal Transportation System. During the seasonal moisture and temperature variation, the expansive Yazoo clay subgrade attains shrink-swell behavior, which deteriorated the pavement condition, as well as the condition of the levee system over time. As presented in Figure 1.2, the Jackson metroplex in Mississippi has highly plastic Yazoo clay soil, which experiences high precipitation (>60 inches) annually and also subjected to severe drought. Due to the high precipitation and severe drought, the highly plastic Yazoo clay soil experience significant shrinkage and swelling, which affects the hydraulic conductivity of the soil. During the summertime, the excessive drought causes shrinkage cracks in the Yazoo clay, which increases the vertical permeability of the high PI clay. On the other hand, the rainfall after the summertime can infiltrate easily in the levee embankment and highway pavement, which cause distress (Figure 1.2 (d)).

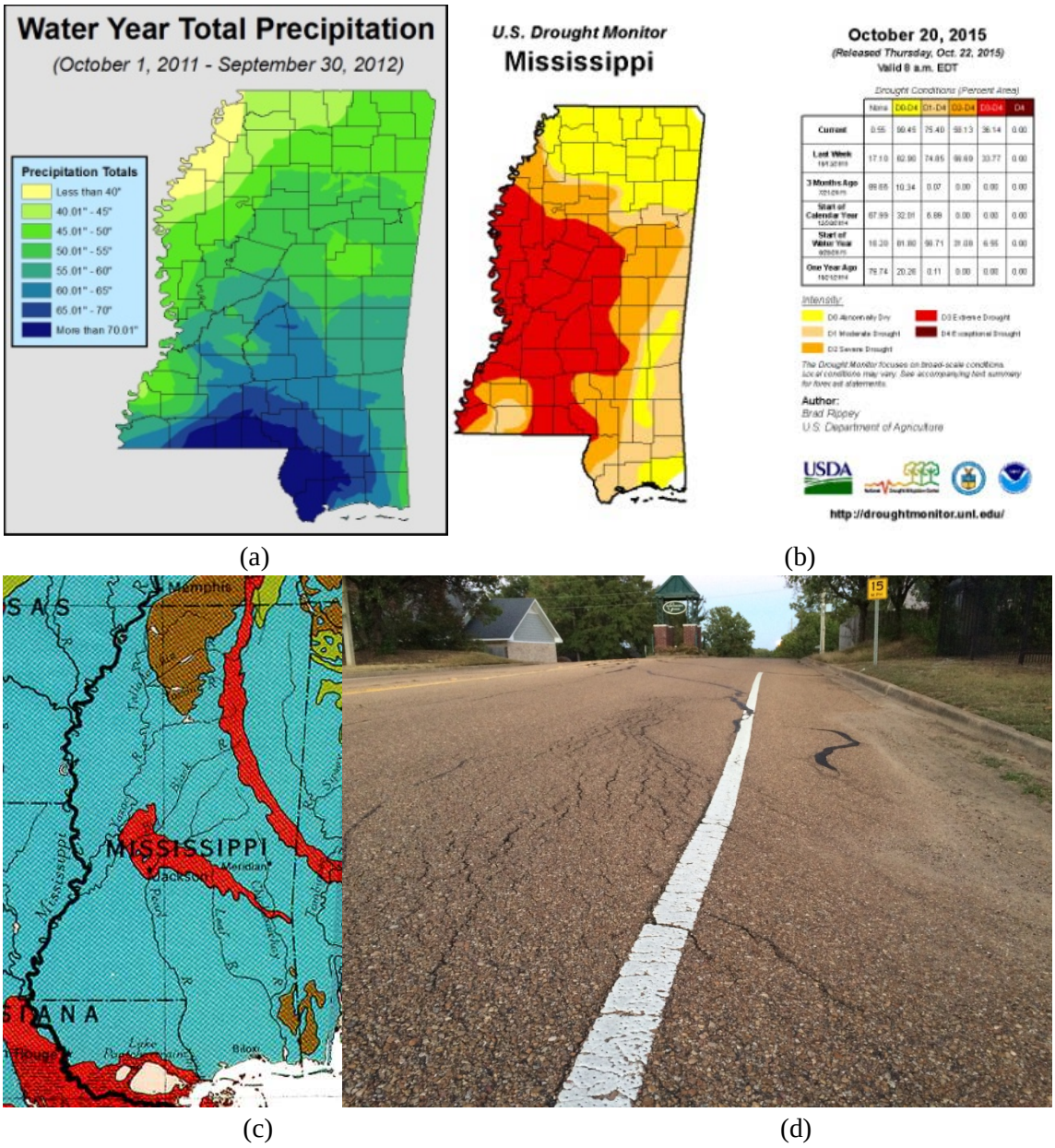

Figure 1.2 a. Total Precipitation map, b. Drought map, c. Yazoo clay profile in Mississippi, d. Typical Pavement distress

At present, the state-of-the-practice at Mississippi for characterizing the expected pavement subgrade or foundation soil behavior at expansive Yazoo clay soil locations solely relies on a standard operating procedure using Atterberg limit and percentage volume change (VC%) results from laboratory testing where the borehole vertical sampling interval typically ranges from 30 inches to 60 inches (Lee, 2012). Based on the laboratory test parameters, the design and construction over the expansive subgrade are undertaken. A usual practice at the state of Mississippi is to conduct a 3 ft. excavation as open trench underneath roadway pavement and the fill section should be backfilled with not expansive soil. In addition, the cut slopes are constructed as 6H: 1V and embankment slopes are constructed as 5H: 1V to minimize the risk of future slope failure (Lee, 2012). A schematic of road-way alignment for both cut and fill

geometry is illustrated in Figure 1.3. Besides the roadway pavement, a similar problem exists in the levees built by Yazoo clay. Every year, the MS Levee board and USACE spend millions of dollars on repairing the distress on the levees, which is induced by precipitation, infiltration of the slopes and softening behavior of the expansive Yazoo clay soil.

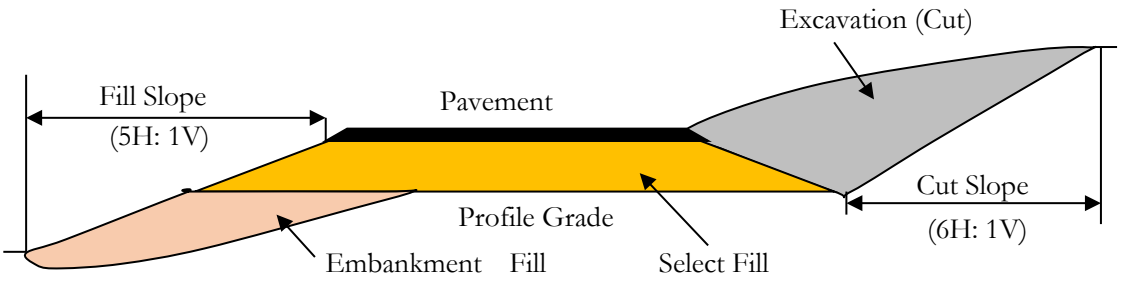

Figure 1.3 State of Practice of roadway on Yazoo clay at the state of Mississippi (redrawn after Lee, 2012)

Due to Moisture Infiltration, heave damage has been observed in the roadway pavement with 3 ft. excavation and backfilling with select fill at the Jackson area. Moreover, shallow to deep-seated slope failure takes place on the levee system with prolonged rainfall events. Both of the failures are triggered by the moisture variations due to the infiltration of rainwater. Even though the permeability of Yazoo clay is high, the presence of the desiccation cracks severely influences infiltration behavior. However, a minimal understanding of current exists to define the infiltration behavior of the Yazoo clay. The current study is focused on investigating the changes in permeability with wet-dry cycles and its associated effect on the highway pavement and levee system.

1.2 The objective of the Study

The primary objective of the current study is to investigate the moisture variation at the pavement subgrade on Yazoo clay.

To undertake this objective, the current study will focus on 2 major tasks, as presented below.

i. Investigation of change in hydraulic conductivity of Yazoo clay with different wet-dry cycles at the laboratory.
ii. Investigation of the effect of seasonal variation and different rainfall on the saturation at the slopes and underneath the pavement.
iii. Investigation of the effect of seasonal variation and different rainfall on the saturation of levee systems.

Chapter 2: LITERATURE REVIEW

2.1 Yazoo Clay

Yazoo clay soil is highly expansive and extended over central Mississippi, Alabama, and Southern Louisiana (Figure 2.1). Most of the structures are constructed on expansive Yazoo clay in Mississippi. The average composition of the Yazoo clay is 28% smectite (probably montmorillonite), 24% kaolinite, 22% quartz, 15% calcite, 8% illite, 2% feldspar, and 1% gypsum based on recent x-ray diffraction results (Taylor 2005). Surface exposures of Yazoo are weathered to a maximum depth of approximately 45 ft. Below the ground surface. Landris et al. (2012) weathered Yazoo clay has a distinctive yellow-brown color while unweathered Yazoo clay is blue-gray. The expansive clay soil undergoes shrink-swell behavior due to seasonal moisture variation. Due to the high shrink-swell behavior, the shear strength of the soil reduces to fully soften or residual shear strength, which eventually leads to slope failure. These failures of structures and the embankment slope can be expensive to repair.

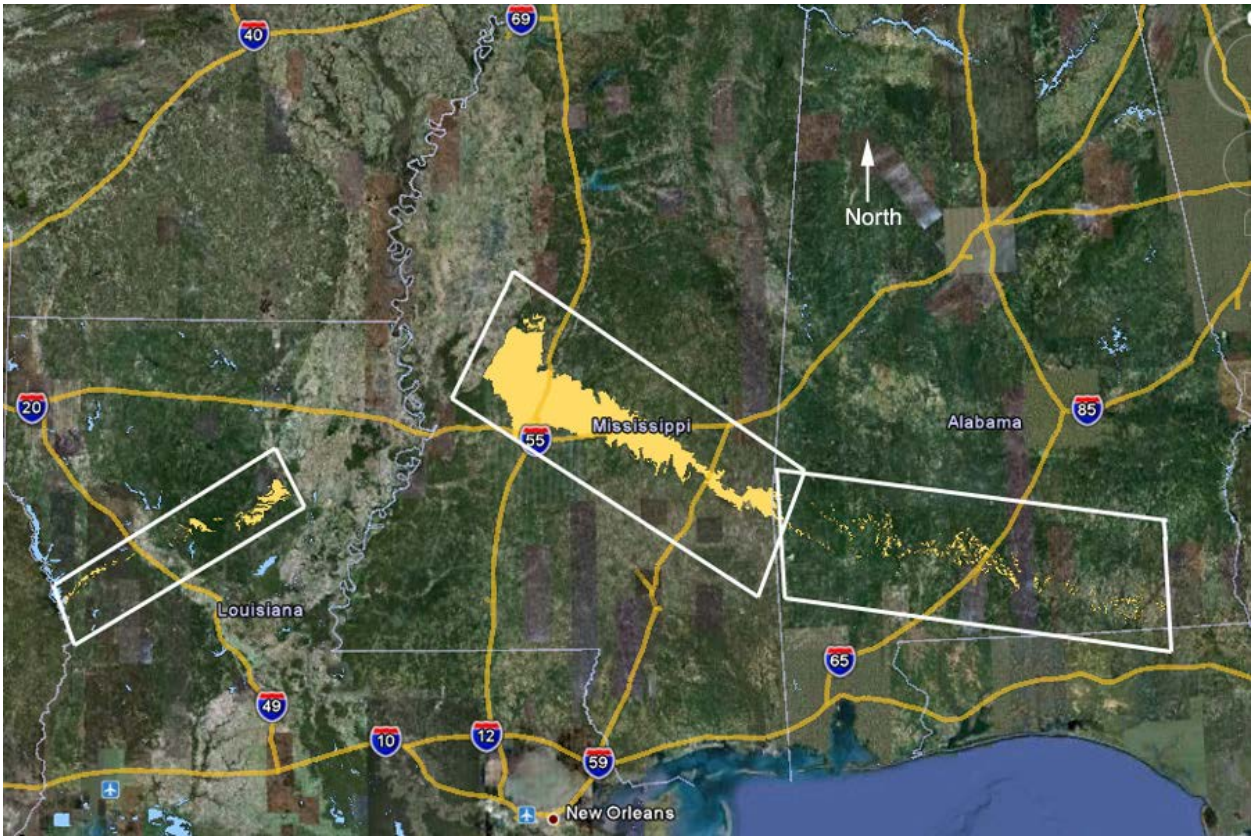

Figure 2.1 Boundary boxes of the Jackson Formation, including Yazoo clay and its geological equivalents, in Mississippi, Alabama, and Louisiana (after USGS 2010)

For compacted clay embankments, the main reason behind the progressive change in shear strength is as a result of weathering, which decreases the drained peak shear strength of compacted clays towards the fully softened shear strength to the residual strength. The concept of fully softened shear strength (FSS) was first proposed by Skempton and Henkel (1964) after investigating the cause of slope failures in cuts within London Brown clays (a stiff, fissured clay). From Skempton and Henkel's research, it was concluded

that fully softened shear (critical) strengths should be used when analyzing slope stability for first-time slides in overconsolidated clays. In 1937 Taylor acknowledged that once a soil reached its peak strength, the resistance often fell to a lower value upon further shear deformation. This idea was reiterated in 1964 when Skempton defined this lower value of strength as the residual strength condition. Skempton (1964) concluded that the residual strength applies to slope stability analyses of natural slopes and excavations in stiff fissured over-consolidated clays as well as slopes in these materials that had experienced previous failures. In 1970 Skempton recognized there was a fully softened shear strength, which lies between the peak strength and residual strength. He concluded that the fully softened shear strength is numerically equal to the peak strength of the soil in its normally consolidated state. Initially, the fully softened shear strength was considered to apply primarily to slope failures in stiff fissured over-consolidated natural clay and shale deposits. However, subsequent research suggested that repeated wetting and drying can also reduce the strength of compacted high plasticity clays and shales to the normally consolidated, or fully softened state.

Following Skempton (1964, 1985), drained residual shear strength measured by laboratory tests has been successfully used for stability analyses of reactivated landslides (e.g., Skempton and Petley 1967; Hutchinson 1969; James 1970; Palladino and Peck 1972; Morgenstern 1977; Terzaghi et al. 1996). Mesri and Shahien (2003) have summarized laboratory and field experience to show that drained residual shear strength from laboratory tests. The residual shear strength is mobilized on the entire slip surface of reactivated landslides in first-time slope failures. Stability analyses by Huvaj-Sarihan (2009) for additional reactivated landslides support these conclusions. Though the determination of soil strength parameters for shallow slope stability analysis is the most critical task as the factor of safety will be significantly reduced (Rogers and Wright 1986). This research work tends to determine the progressive change in the mechanical properties of high plastic Yazoo clay, which is very important for shallow slope stability analysis. Changes in basic soil properties due to weathering can provide valuable insight into the change in soil strength parameters. To simulate the loss of shear strength shallow slope failure condition, direct shear tests in the laboratory were conducted for peak, fully soften, and residual conditions at low normal stresses (< 100kPa).

Expansive Yazoo clay soil is highly susceptible to climate change, and it is dominant in central Mississippi and neighboring states. Yazoo clay undergoes volume change due to wetting or drying under different seasonal variations. These repeated volume changes can give rise to ground movements, which may result in structural damages, resulting in the high cost of repair or reconstruction. During the wetting period, the highly plastic expansive clay soil absorbs water, and it swells. On the other hand, the soil shrinks during the drying period. However, there is limited research on the effect of the different wet and dry cycles on the void ratio of expansive soils. Due to the shrinkage and swelling behavior of the Yazoo clay, the hydraulic conductivity varies over the different seasons and has higher vertical permeability during the dry season. With high vertical permeability, the rainwater can easily percolate in the pavement subgrade and slopes, which accelerates the failure. The current study investigates the change in unsaturated vertical and horizontal permeability and its effect on the maritime and multimodal infrastructures, especially on the pavement, slopes of highway embankment, and levees.

2.2 Engineering Aspects of Yazoo Clay

2.2.1 *Weathered versus Unweathered Clay*

Local geologists and engineers describe Yazoo clay as being either “unweathered” or “weathered.” Unweathered clay has a visually distinct blue color that grades into a gray-blue and gray, or it may have a green to grayish-green color. Silt having a light gray color occurs locally in thin seams and lamina. Cycles

of exposure to air, wetting, and drying tend to cause oxidation and acceleration of clay weathering. Exposure to drying is accompanied by shrinkage and weathering, causing mineralogical changes, which in turn change the structural and strength characteristics of clay. Many types of clay lose their stability due to drying and tend to "slake" during rewetting (Mitchell, 1993). When air-dried Yazoo clay is wetted, it quickly slakes but is affected very little by water if at its natural water content. Detrimental swelling can be expected when Yazoo clay is allowed to dry below the optimum gravimetric water content (~15%) and is then wetted (Redus, 1962). As shown later in this report, Yazoo clay can appreciably swell when inundated from its natural water content state. Boston "blue clay" has a softer consistency, but it's upper (assumedly weathered) component is a layer of hard yellow clay (Mitchell 1993). Yazoo "blue clay" is unweathered but is typically overlain with visually distinguishable (assumedly weathered) hard yellow clay. Yazoo clay exhibits weathering effects similar to other high-plasticity clays, in that drying (desiccation) generally increases strength, decreases compressibility, and increases swell potential. Yazoo clay is remarkably similar to another argillaceous sedimentary expansive soil, London Clay, assumed to originate during the same Eocene era (De Freitas and Mannion 2007). Its weathered upper consistency is soft to firm, with ochre staining due to oxidation of iron compounds. The upper 4 ft (1.21m) or so is the active zone. The lower-depth unweathered clay is blue-gray, firm to very stiff, and highly fissured. London clay is problematic as a shrink-swell material (Kovacevic et al. 2007; Hight et al. 2007; Jones and Terrington 2011), also similar to Yazoo clay. The unweathered Yazoo clay has structural breaks with slickenside (joints and fissures) features. These slickenside breaks are probably due to unloading after pre-consolidation or from shrinkage cracking during drying. Fissures have been found in normally consolidated clays at water contents well above their shrinkage limit (Lee, 2012).

The weathered Yazoo clay is generally found in a zone between the ground surface and the deeper unweathered clay. It has a visually-distinct color ranging from a limonite-stained orange to yellow. Near the surface, its consistency is usually soft and gummy, but it becomes firmer with depth. At the surface, caliche and gypsum crystals are standard weathering features, and the clay may or may not be calcareous. At or near the surface, most bedding features and fossils weather and become unrecognizable, but with depth, these features become gradually distinguishable. Near the surface, the fractured nature of the soft clay allows mixing with the surface material, which can include loess silt, alluvial sands, and gravel. Thus, the near-surface weathered zone can have significantly altered the structural composition. Weathered Yazoo clay is marked by numerous fractures. These fractures allow water to penetrate the otherwise low-permeability clay and enhance weathering at depth (Lee 2012).

Martin's (2007) SEM study examined non-clay components in eight samples. Highly fractured Yazoo clay has surface coatings and vein fillings of secondary calcite, gypsum, manganese oxides, and iron oxides. Bedding planes may contain sand and silt seams or fossil layers. The SEM study observed these features. The Yazoo clay surface generally followed the contour of the ground surface. There was more elevation change in the NW-SE direction than in the N-S direction, and this elevation difference might be a primary indicator of Yazoo clay spatial variability. Figure 2.2 indicates that the weathered clay generally lies above the unweathered clay. Both were documented at just about any depth below the ground surface, and unweathered clay was found above the weathered clay (Lee, 2012).

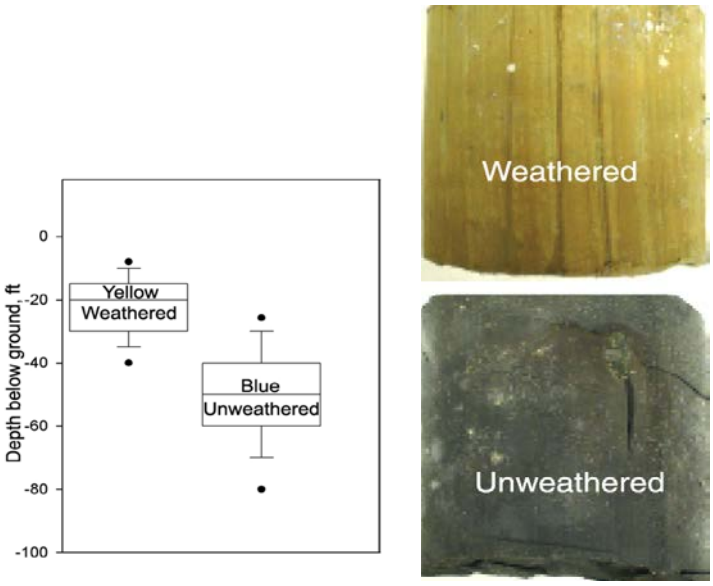

(a) (b)

Figure 2.2 (a) Box plots showing a range of depths for visually-classified samples, (b) Yazoo clay samples illustrating color differences for visual degree-of-weathering discrimination. (Lee (2012))

2.2.2 *Geotechnical Index Properties*

Lee (2012) performed a state study on the properties and characteristics of Yazoo clay soil in Mississippi. During the study, Yazoo clay soil samples from different locations were investigated and presented an average index property value. Table 2.1 lists the mean values for all the Yazoo clay soil data visually separated by sample color from that study. The 'weathered' samples were yellowish, and the 'unweathered' samples had a blue color. Weathered clay was visually identified in samples from the surface to 40 ft (12.19m) depths. Visually-identified unweathered clay was sampled and tested between depths of 25 ft and 80 ft below ground surface (Lee, 2012).

Lee (2012) also analyzed the correlations between geotechnical properties and available mineralogy data. The study indicated that the mineralogy of Yazoo clay includes quartz, clay, calcite, smectite, illite, and kaolinite content percentages. There was little correlation between sample depth (or elevation above mean sea level, as shown in

Figure 2.3) and regional VC. There also appeared to be little correlation between regional VC and visual color identification of weathering as a function of depth (or elevation) (Lee (2012)). Using visual color identification (yellow or blue) as the primary method to discriminate between weathered and unweathered clay may not be a reliable indicator for regional VC. Regression analysis, performed by Lee (2012), indicated almost no correlation between the averaged VC values as a function of depth. Averaged VC values did exhibit an observable pattern when grouped by depth intervals (Lee (2012)).

Table 2.1 Yazoo clay average index property values (Lee (2012))

Parameter	Weathered (yellow)		Unweathered (blue)		All	
	Mean	Stan Dev	Mean	Stan Dev	Mean	Stan Dev
ɣ dry, lbs/cu ft	82	9	82	9	82	9
ɣ wet, lbs/cu ft	112	10	114	9	113	10
Moisture Content %	38	9	39	9	39	9
Field Void Ratio	0.99	0.21	1.03	0.22	1.02	0.22
LL %	94	19	95	16	94	17
Pl %	35	8	37	8	36	8
PI %	59	16	58	13	59	14
VC %	140	39	138	38	138	39
*Clay %	53	21	65	14	60	18
* Calcite %	13	16	18	14	16	15
*Smectite %	45	18	48	13	46	15
*Illite %	16	17	11	10	13	14
*Kaolinite %	39	11	42	8	41	10

*XRD data

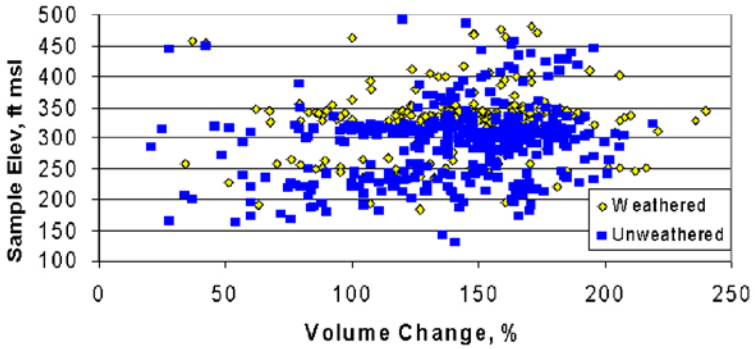

Figure 2.3 Volume change percent (VC%) values for all Yazoo clay data in the 5-county area of central Mississippi, plotted by elevation above mean sea level (MSL) (Lee (2012))

Based on the study performed and summarized by Lee (2012), Figure 2.4 shows that the PL values did not change very much by depth, but the LL (and thus the PI) values varied in concert with the VC% values. Although these data are regional, the following trends were noted:

1 Average VC% and LL values were lowest above -10 ft (3.048m) and around 50 ft (15.24m).
2 Average VC% and LL values were highest around -10 ft (3.048m), -25 ft (7.62m), and 55 ft (16.76m).
3 These regional data indicated the non-uniformity of Atterberg limits and expansive behavior patterns with depth.

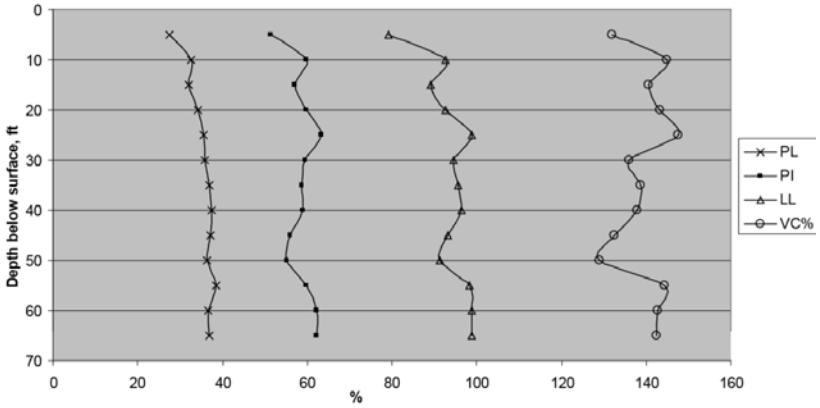

Figure 2.4 Regional weathered plus un-weathered Yazoo clay VC % and Atterberg limit values, averaged by 5-ft (1.524m) depth intervals (Lee (2012))

Lee (2012) indicated that the only significant geotechnical index property correlation was between dry density and natural water content (correlation coefficient R= 0.94). Sample weathering discrimination was irrelevant for this correlation. The high correlation was noted regardless of the degree of weathering. The best-fit non-linear regression equation (Figure 2.5) was:

$$Dry_{density}, pcf = 142.2e^{-0.0143w\%}$$

Where e=natural log base=2.178 and w%=water content percent.

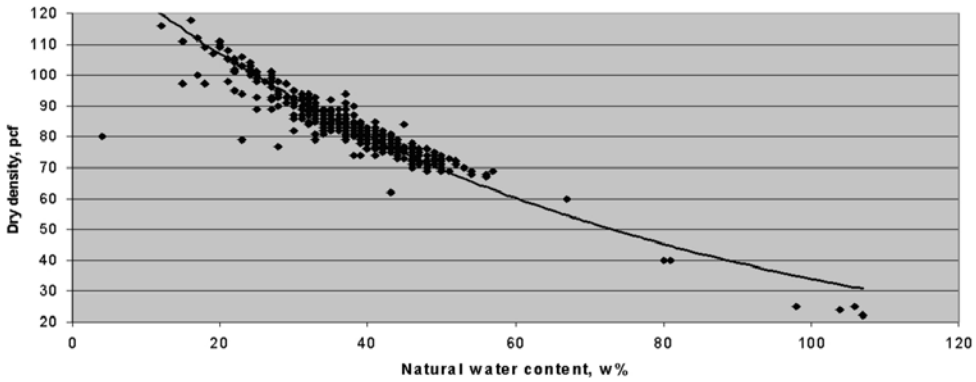

Figure 2.5 Dry density versus natural water content for all Yazoo clay data in the 5-county area of central Mississippi (Lee (2012))

The flow of water in the liquid phase in unsaturated soils is characterized by both hydraulic conductivity and the SWCC. The hydraulic conductivity of unsaturated soil cannot generally be assumed to be constant. Instead, it is a variable which is predominantly a function of the water content or the matric suction of the unsaturated soil. In an unsaturated soil, the hydraulic conductivity is significantly affected by the degree of saturation (or water content) of the soil. Water flows through the pores paces filled with water; therefore, the percentage of voids filled with water is an essential factor.

The hydraulic conductivity function of an unsaturated soil (change in hydraulic conductivity with suction or water content) can be determined using either direct or indirect techniques. Direct measurements of

hydraulic conductivity can be performed either in the laboratory or in the field. The two most common techniques used in the direct measurement of the hydraulic conductivity function of an unsaturated soil are the steady-state method (Klute, 1965) that can be performed in the laboratory using a permeameter, and the transient method, that can be performed in the laboratory (Hamilton et al., 1981) or in the field (Watson,1966; Hillel,1982). More attention is increasingly being directed to the accurate Measurement of unsaturated soil hydraulic properties close to saturation (Leij and van Genuchten, 1999), i.e., moisture conditions that are strongly affected by the soil's structure and macro-pores. Traditional transient laboratory methods, such as the horizontal infiltration method(KluteandDirksen,1986), outflow methods (Gardner,1956; BensonandGribb,1997), and instantaneous profile methods (RichardsandWeeks,1953; Chiu and Shackelford,1998) show relatively little sensitivity to the hydraulic conductivity at near-saturated conditions, and hence, are more suitable for estimating the hydraulic conductivity at medium saturation levels; however, the measurement of unsaturated hydraulic conductivity in the laboratory is time-consuming and costly, as it requires special devices and generally the service of a skilled technical person. Therefore, numerous theoretical (indirect) methods have been proposed by researchers to predict the hydraulic conductivity of unsaturated soils (Fredlund et al., 1994; van Genuchten, 1980; Mualem,1976; Kunze et al., 1968; Brooks and Corey,1964). Most of these predictive methods require saturated hydraulic conductivity and the soil-water characteristic curve (SWCC) as inputs.

Khan et al. (2019) have developed the Soil Water Retention Curve (SWRC) curve for the Yazoo clay soil in Mississippi, shown in Figure 2.6. Nobahar et al., 2019 has developed the SWRC curve based on the filter paper method proposed by Bulut et al., 2001. The Van Genuchten (1980) model is presented in equation 1 and equation 2.

$$\theta = \theta + \theta r + ((\theta_s - \theta r)/[1 + (\alpha h)^n]^m) \quad (1)$$

$$m = 1 - (1/n) \quad (2)$$

Where h is the pressure head, α, m and n are the Van Genuchten fitting parameters, and θs and θr are the saturated and residual water content, respectively.

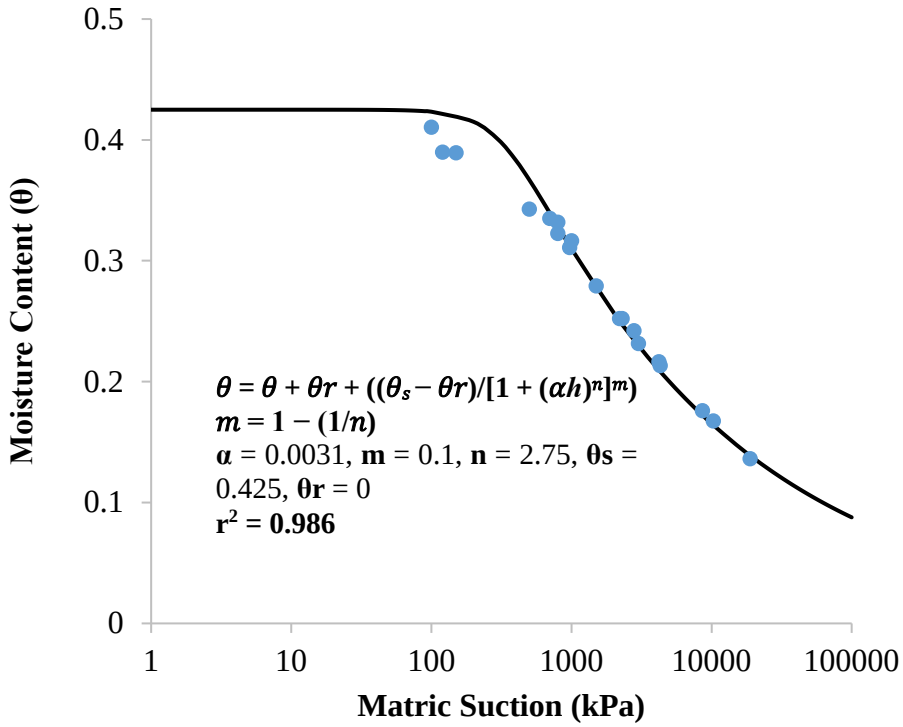

Figure 2.6 Soil water retention curve of Yazoo clay (Nobahar et al. 2019)

2.3 Changes in Factor of Safety of Slopes made by Yazoo Clay

During the previous project supported by MarTREC, Khan et al., 2019 investigated the effect of rainfall and wet-dry cycles on the changes in the factor of safety of the highway slopes. During this study, Khan et al., 2019 have conducted extensive safety analysis using the finite element method by introducing coupled flow deformation analysis. Moreover, the concept of the unsaturated soil is included in the slope stability analysis to investigate the triggering condition of the slope failure in Yazoo clay soil.

Khan et al., 2019 has conducted stability analysis using the unsaturated moisture and matric suction profile of the soil, using fully-coupled flow analysis, considering a total rainfall event of 126.2 mm. The study was conducted using four different cases of weathering of the expansive Yazoo clay soil at different wet-dry cycles. The slip surface for the 126.2 mm rainfall volume of the 3H: 1V slope within four cases is presented in Figure 2.7. During the phi-c reduction analysis conducted by Khan et al., 2019, at the failure strength, the factor of safety of the soil is determined. Besides the determination of the soil strength, the FEM package calculates displacement at the soil body. The displaced area represents the failure area (deformation contour), and the edge of displaced soil is presenting the slip surface of the slope. Based on the FEM results, it can also be observed that the factor of safety changed with different rainfall durations.

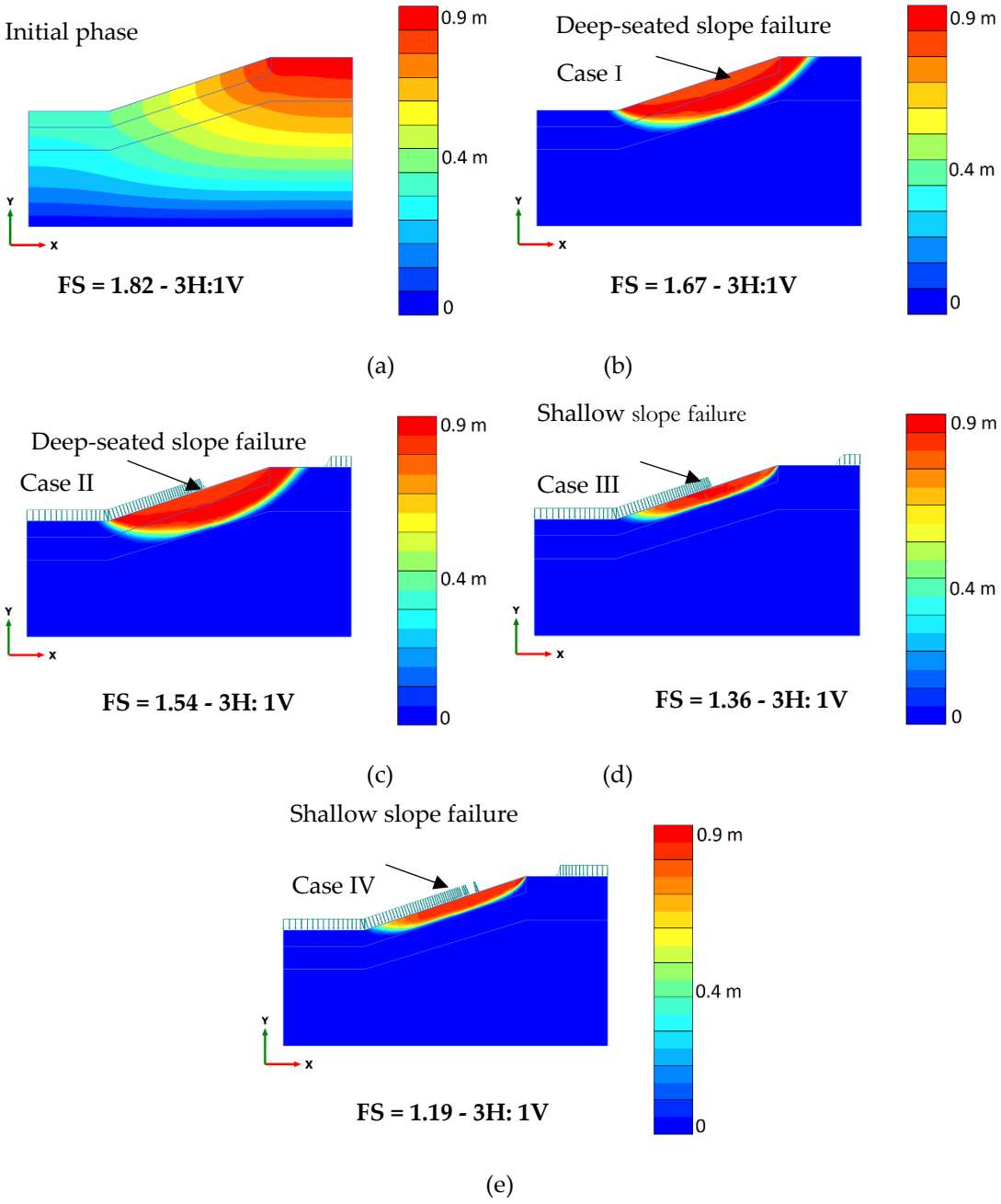

Figure 2.7 Stability analysis results for 126.2 mm rainfall volume for one-day rainfall duration for 3H:1V slope on Yazoo clay (a) before rainfall (b) Case I (c) Case II (d) Case III (e) Case IV (Khan et al., 2019).

Khan et al., 2019 extended the work and investigated the changes in the factor of safety for the 3H: 1V slope with consideration four cases is presented in Figure 2.8, which shows the progressive variation of the factor of safety for Case I to Case IV. During this analysis, Case I represents the just constructed slopes. On the other hand, Case II, Case III and Case IV represent the weathered strength of the slopes subjected to 3, 5 and 7 numbers of wet-dry cycles. The failure surface was observed to be deep-seated in Case I and shallow in Cases II to IV, which is due to the progressive change in the shear strength due to the repeated wet-dry cycles. Khan et al., 2019 indicated that as the rainfall influenced the matric suction value at the topsoil, a

significant change in the factor of safety occurred, leading to shallow slip surface failure. The factor of safety considering the effect of two total rainfall periods of Rv = 126.2 mm (2 hours) and Rv = 271.7 mm (3 days) reduced from 1.7 to 1.2 and 1.68 to 1.02 respectively considering the effect of the 7th wet-dry cycles at the topsoil. Consequently, the factor of safety reached a critical value after the topsoil layer shear strength was replaced with the seven wet and dry cycle's value with higher total rainfall. Khan et al., 2019 investigated that at dry state with 7 wet-dry cycles, the slopes are stable (FS = 1.4). However, the slope will fail at the presence of consistent 3 days of rainfall after 7N of wet-dry cycles.

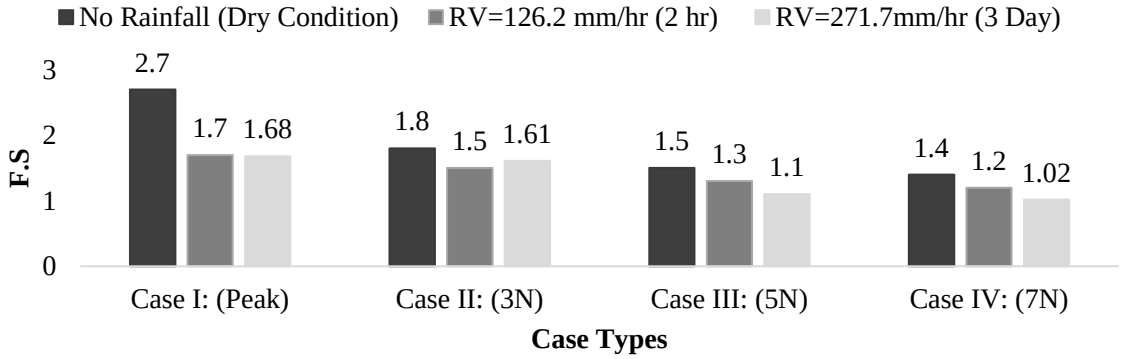

Figure 2.8 Change in the factor of safety (Khan et al., 2019).

2.4 Current Gap in the Literature on Yazoo Clay Behavior

Several researchers, such as Martin (2007), Lee (2012), Khan et al. (2019); Nobahar et al. (2019); Nobahar et al. (2020) has investigated the physical and mechanical characteristics of the Yazoo clay. Moreover, the changes in the shear strength of Yazoo clay and its associated effect on the stability of the highway embankment has been conducted in the literature. It is well understood that the expansive Yazoo clay experienced shrink-swell behavior due to wet-dry cycles. However, how the hydraulic conductivity of Yazoo clay changes during the shrinkage and swelling action, the current literature cannot explain it. The current study is focused on investigating the changes in the hydraulic conductivity behavior of expansive Yazoo clay.

Chapter 3: LABORATORY TESTING OF YAZOO CLAY SOIL

3.1 Introduction

The laboratory testing program was designed to determine properties relating to volume change behaviors of expansive Yazoo clay soils. Yazoo clay soil samples were collected from a highway site and then tested in the laboratory for basic soil properties and investigated the changes in permeability with different wet-dry cycles. The details of the laboratory testing are presented here.

3.2 Sample Collection and Investigation of the Basic Soil Properties

A Highway slope along I20, located on in Jackson Mississippi (presented in Figure 3.1), has been selected for this study. Representative Yazoo clays soil samples were collected from two boreholes, referred to as SI-1 and SI-2, respectively. The collected samples were investigated in the Jackson state university, geotechnical engineering laboratory. The experimental program was mainly comprised of tests to determine basic soil properties, such as Atterberg limit test, and engineering characteristics, including hydraulic conductivity testing in relation to different wet-dry cycles. A summary of the laboratory procedures, equipment used, and results obtained are presented in the following sections. All representative soil samples were subjected to various physical property measurements.

Figure 3.1 Location of the Slope Site for Soil Samples

3.2.1 *Atterberg Limits Test*

Atterberg tests are performed on only that soil fraction, which passes through a No. 40 sieve (0.425 mm). Consistency limits (LL and PL) are significant to understand the stress history and general properties of the soil met with construction. An estimate of the Plasticity Index is necessary to classify the soils, particularly in highly expansive clays. The Atterberg Limit test was performed in the Geotechnical Engineering Laboratory at Jackson State University. The test was conducted according to ASTM D4318. The Atterberg limit test data are presented in Table 3.1. The moisture content of the soil samples for the liquid limit test is presented in Figure 3.2.

Table 3.1 Variation of Atterberg' limit properties with the depth of selected slope

SI-1			
Depth (ft)	**Liquid Limit (%)**	**Plastic Limit (%)**	**Plasticity Index (%)**
4 - 6	31	18.75	12.3
8 - 10	**Gravel**	-	-
14 - 16	115	23.6	91.4
18 - 20	74	30.3	43.7
24 - 26	88	27.55	60.5
28 - 30	54	22.05	32
SI-2			
Depth (ft)	**Liquid Limit (%)**	**Plastic Limit (%)**	**Plasticity Index (%)**
4 - 6	39	21.5	17.5
8 - 10	39.5	19.4	20.1
14 - 16	41.5	18.95	22.6
18 - 20	68	22.6	45.4
24 - 26	63	19.35	43.7
28 - 30	**No Sample**	-	-

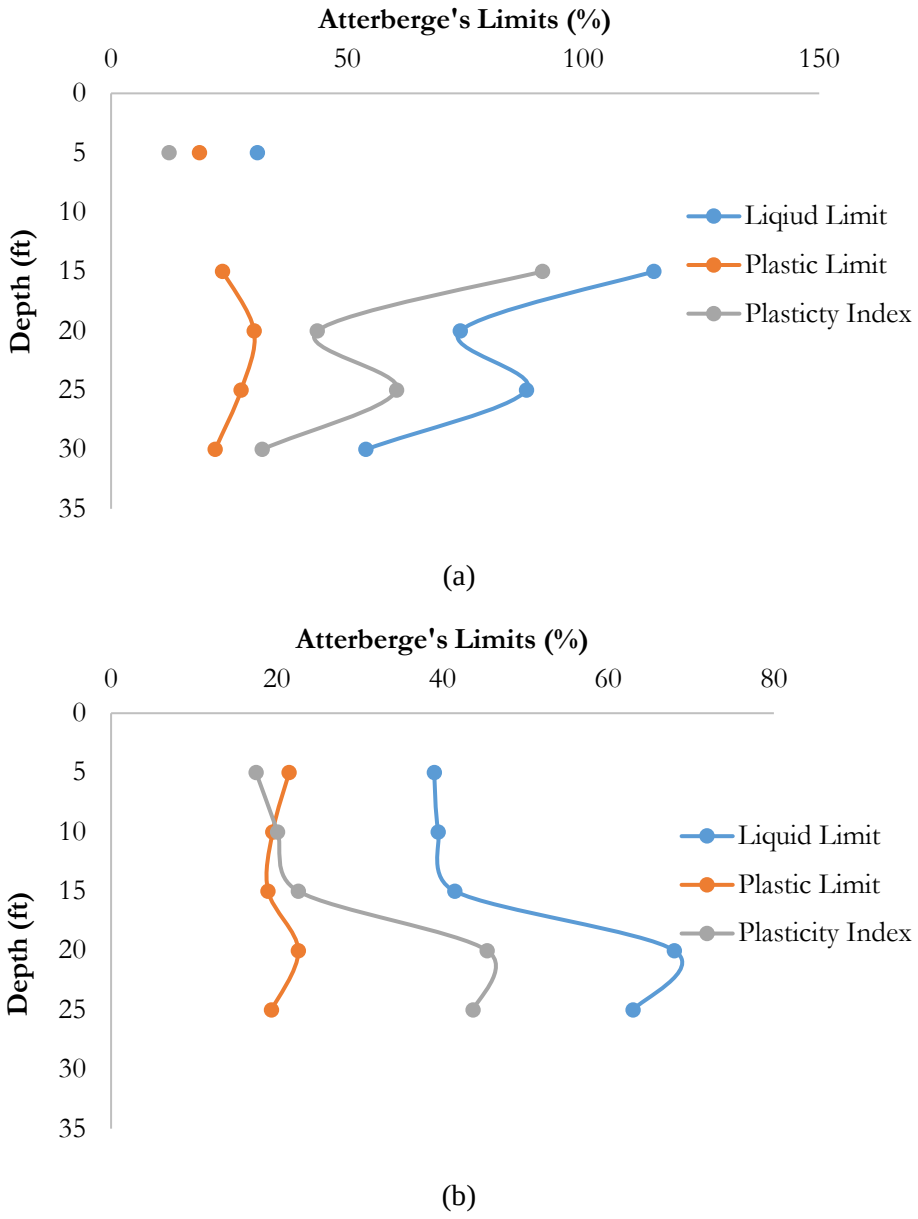

Figure 3.2 Variation of Atterberg Limit Properties of the selected slope made of Yazoo clay with Depth (a) SI-1(failed area) (b) SI-2 (un-failed area)

3.3 Investigation of the Effect of Wet-Dry Cycles on Permeability

Yazoo clay has a very high affinity to the moisture content and causes shrink-swell behavior. During the time of summer, especially when the soil gets dry and loose moisture, Yazoo clay shrinks, which affects permeability behavior. The changes of Permeability at different wet-dry cycles is determined using two technics, a. Using the Mini Disk Infiltrometer and b. Using Moisture Sensors. Besides, the changes in the Soil-Structure at different Wet-Dry Cycles were investigated using SEM Imaging.

3.4 SEM Imaging to Investigate the Changes in the Soil Micro-Structure

The changes in the Microstructure of Yazoo Clay was investigated using Scanning Electron Microscope (SEM). Yazoo clay soil samples were compacted and then exposed to 3, 5, and 7 numbers of wet-dry cycles. After the wet-dry cycles, samples were tested to investigate the microstructure. Figure 3.3 shows the changes of Yazoo clay microstructure and voids after the 3rd, 5th, and 7th number of wet-dry cycles. The ultimate available resolution with SEM is on the order of 0.2 μm (0.66 μft). This order was used during the examination of Yazoo clay because of the sample's high cohesion and very tiny particles compared to silt or sand that can be examined on the order of 0.5 μm (1.64 μft). Conclusively, from the SEM image shown below, the increase in the void ratio will have an influence in the hydraulic permeability.

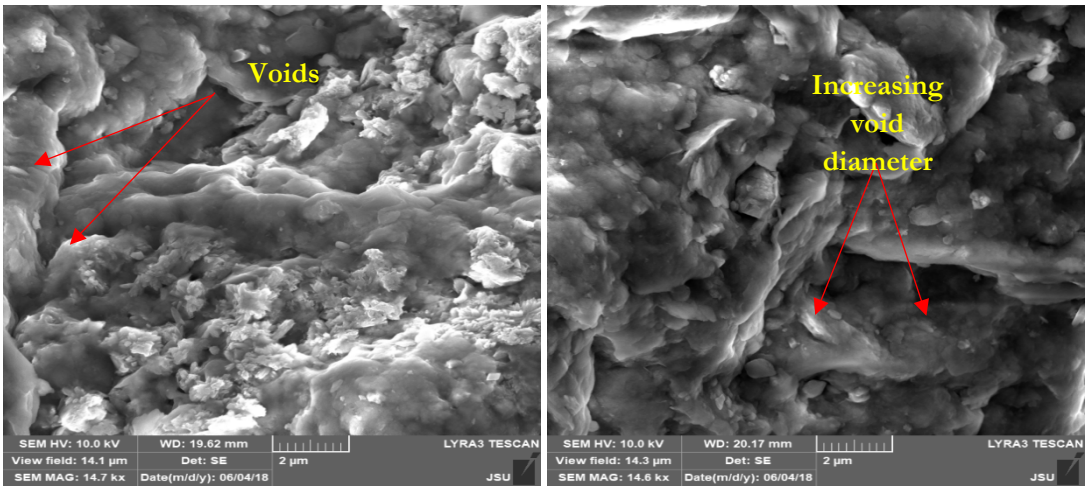

(a) (b)

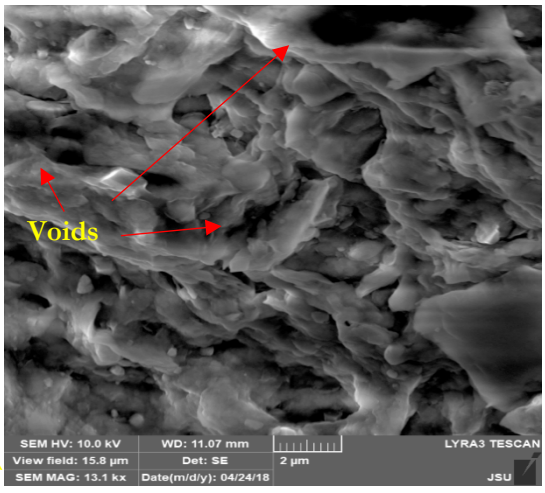

(c)

Figure 3.3 Change in pore space of Yazoo clay using SEM imaging after the sample subjected to (a) 3 wet-dry cycles (b) 5 wet-dry cycles (c) 7 wet-dry cycles.

The study was further extended to examine the chemical composition of the Yazoo clay sample (Table 3.2). As indicated in Table 2.2, the Yazoo clay has a high percentage of the Oxygen (54.14%), Silicon (25.21%) and Aluminum (10.90%), which indicates that the majority mineral of the Yazoo clay is montmorillonite (Barton, 2002)

Table 3.2 Yazoo clay sample chemical composition based on SEM data

Mineral Composition of Yazoo Clay Sample	Weight (%)	Weight % Error (+/-1 Sigma)	Normalized Weight (%)	Normalized Weight % Error (+/- Sigma)	Atom %
Carbon	1.36	±0.11	1.36	±0.11	2.26
Oxygen	54.14	±0.40	54.14	±0.40	67.67
Flourine	0.00	---	0.00	---	0.00
Magnesium	1.22	±0.08	1.22	±0.08	1.00
Alluminum	10.90	±0.13	10.90	±0.13	8.08
Silicon	25.21	±0.18	25.21	±0.18	17.95
Potassium	1.44	±0.08	1.44	±0.08	0.74
Calcium	1.53	±0.09	1.53	±0.09	0.77
Titanum	0.46	±0.05	0.46	±0.05	0.19
Iron	3.74	±0.21	3.74	±0.21	1.34

Permeability of saturated soils k is a function of void ratio e. For unsaturated soils, the coefficient of permeability with respect to water k_w is a function of both void ratio e and water content w.
The application of flow laws to engineering problems, such as the design of earth dams, tailing dams, clay liners for waste management practice, and slopes subjected to rainwater infiltration (Fredlund et al., 1994), requires the quantification of the hydraulic properties of soil. Darcy's law is commonly used to model the flow of water through unsaturated soil (Buckingham, 1907; Richards, 1931; Childs and Collis-George, 1950).

3.5 Unsaturated Hydraulic Conductivity Testing using Mini Disk Infiltrometer

The hydraulic conductivity of the soil is the rate at which water can move through the soil under certain conditions and hydraulic gradients. Water movement through soil typically happens under saturated and unsaturated conditions. Mini Disk Infiltrometer is a tension Infiltrometer where it measures the unsaturated hydraulic conductivity of the medium when it is placed on at different applied tensions. Flow-through an unsaturated soil is more complicated than flow through continuously saturated pore spaces. Macro pores generally filled with air, leaving only the finer pores to accommodate water movement. The hydraulic conductivity of the soil is strongly dependent on the detailed pore geometry, water content, and differences in matric potential. (Rose, 1966; Brady and Weil, 1999)
The Mini Disk Infiltrometer measures the hydraulic conductivity of the medium it is placed upon. It has an adjustable suction (0.5 to 7 cm) to get additional information about the soil by eliminating macropores with an air entry value smaller than the suction of the Infiltrometer. It is done by controlling the infiltration with a small negative pressure or suction. When the water is under tension or suction, it does not enter macro pores such as cracks but goes further into and through the soil as determined by the hydraulic forces in the

soil. Saturated conductivity occurs when all the pores, including the large ones (such as cracks or wormholes), are filled. Infiltrating water under a tension prevents the filling of the macropores and gives a hydraulic conductivity characteristic off the soil matrix, and is less spatially variable. Unsaturated soil hydraulic conductivity is a function of water potential and water content of the soil. Usually, a decrease in conductivity is expected as the soil dries is due primarily to the movement of air into the soil to replace the water. As the air moves in, the pathways for water flow between soil particles become smaller and more tortuous, and flow becomes more difficult compared to the soil in a saturated state.

3.5.1 *Calibrating the Minidisk Infiltrometer*

Since different soil types infiltrate water at different rates, measuring the change of volume vs. time can often be difficult, particularly in a sandy soil where the water infiltrates rapidly. The suction rate is adjusted to better accommodate measuring infiltration for the type of soil you are measuring. For most soils, a suction rate of 2 cm should be adequate. During the current study, the Mini Disk Infiltrometer was calibrated for Yazoo clay. To adjust the suction rate, the suction tube is moved up or down, so the water level in the bubble chamber is even with the desired suction rate marked on the side of the suction tube. If the suction tube is difficult to move, a small amount of vacuum grease is applied on the tube to ease movement. During the calibration process, the starting water volume is recorded. At time zero, the Infiltrometer is placed on the surface, assuring that it makes solid contact with the soil surface. The water volume is recorded at regular time intervals as the water infiltrates.

3.5.2 *Calculating Hydraulic conductivity*

A number of methods are available for determining soil hydraulic conductivity using Mini Disk Infiltrometer. The method proposed by Zhang (1997) works well for measurements of infiltration into dry soil. The method requires measuring cumulative infiltration versus time and fitting the results with the function.

$$I = C_1 t + C_2 \sqrt{t} \tag{3.1}$$

Where are the parameters? C_1 is related to hydraulic conductivity, and C_2 is the soil sportively. The hydraulic conductivity for the soil (k) is then computed from.

$$k = \frac{C_1}{A} \tag{3.2}$$

Where C_1 is the slope of the curve of the cumulative infiltration versus the square root of time, and A is a value relating the van Genuchten parameters for a given soil type to the suction rate and radius of the Infiltrometer disk. The value A is determined from equations 3.3 and 3.4.

$$A = \frac{11.65\left(n^{0.1}-1\right)\exp[2.92(n-1.9)\alpha h_0]}{(\alpha r_0)^{0.91}} \tag{3.3}$$

$$A = \frac{11.65\left(n^{0.1}-1\right)\exp[7.5(n-1.9)\alpha h_0]}{(\alpha r_0)^{0.91}} \tag{3.4}$$

Where n and a are the van Genuchten parameters for the soil, r_o is the disk radius, and ho is the suction at the disk surface. The Mini Disk Infiltrometer infiltrates water at the suction of -0.5 to -6 cm and has a radius of 2.25 cm. The van Genuchten parameters for the 12 texture classes were obtained from Carsel and Parrish (1988) is presented in Table 3.3.

Table 3.3 Van Genuchten parameters for 12 soil texture classes and A values for a 2.25 cm disk radius and suction values from 0.5 to 6 cm.

Texture/Soil Type	Suction, h_o						
	-0.5	-1	-2	-3	-4	-5	-6
	A						
Sand	2.84	2.40	1.73	1.24	0.89	0.64	0.46
Loamy Sand	2.99	2.79	2.43	2.12	1.84	1.61	1.40
Sandy Loam	3.88	3.89	3.91	3.93	3.95	3.98	4.00
Loam	5.46	5.72	6.27	6.87	7.53	8.25	9.05
Silt	7.92	8.18	8.71	9.29	9.90	10.55	11.24
Silt Loam	7.10	7.37	7.93	8.53	9.19	9.89	10.64
Sandy Clay Loam	3.21	3.52	4.24	5.11	6.15	7.41	8.92
Clay Loam	5.86	6.11	6.64	7.23	7.86	8.55	9.30
Silty Clay Loam	7.89	8.09	8.51	8.95	9.41	9.90	10.41
Sandy Clay	3.34	3.57	4.09	4.68	5.36	6.14	7.04
Silty Clay	6.08	6.17	6.36	6.56	6.76	6.97	7.18
Clay	4.00	4.10	4.30	4.51	4.74	4.98	5.22

3.5.3 *Test Methods and Results*

After determining the index properties of the soils, the Yazoo clay soil samples were air-dried, processed via mortar and pestle to reduce the size of the clay clods, and stored in buckets until the material was needed for testing. Once needed, the material was split from the bucket, and water was added to achieve the desired initial moisture content. The prepared soil was then bagged in sealable containers and stored for up a week to allow for moisture equilibration prior to compaction in the mold. The specimens were prepared and compacted inside the box by determining the amount of moist soil needed to achieve the target unit weight of 82-100 lb/ft^3. That amount of soil by mass was divided into three equal parts and compacted into the mold. Each lift of material was compacted in the box until 67% volume filled was occupied in order to achieve a uniform density throughout the box and to allow for a change in the void. A straight edge was compacted into the mold such that the surface of the compacted soil was even. The surface was checked with a straight edge to ensure no voids or high spots were left during the compaction of the sample.

After calibrating and setting up the Infiltrometer, the following steps were used to complete the wetting and drying cycles and determining the hydraulic permeability. The laboratory set up to determine hydraulic permeability using mini-disk permeameter is presented in Figure 3.4.

- The wetting cycle process was simulated by wetting the sample with the infiltrometer, and readings were recorded every 30 secs.
- Once the primary wetting cycle elapses, the drying cycle was started by taking the samples into a constructed drying chamber. During the wetting and drying cycles, the environmental chamber was kept at 120ºF – 125ºF, simulating the maximum measured summer temperature of Mississippi.
- The above steps were repeated until a total of three wetting and drying cycles were achieved. After the drying process was completed, the samples were allowed to cool down before starting the next wetting cycle. The method described previously to dry the specimen has shown to expedite the time required to achieve the first collapse and does not significantly affect the results obtained (Krisdani et al. 2008; Basma et al. 1996). The primary swell or shrinkage for the initial wetting cycle for both soils was achieved within 48 hours from the start of the test.

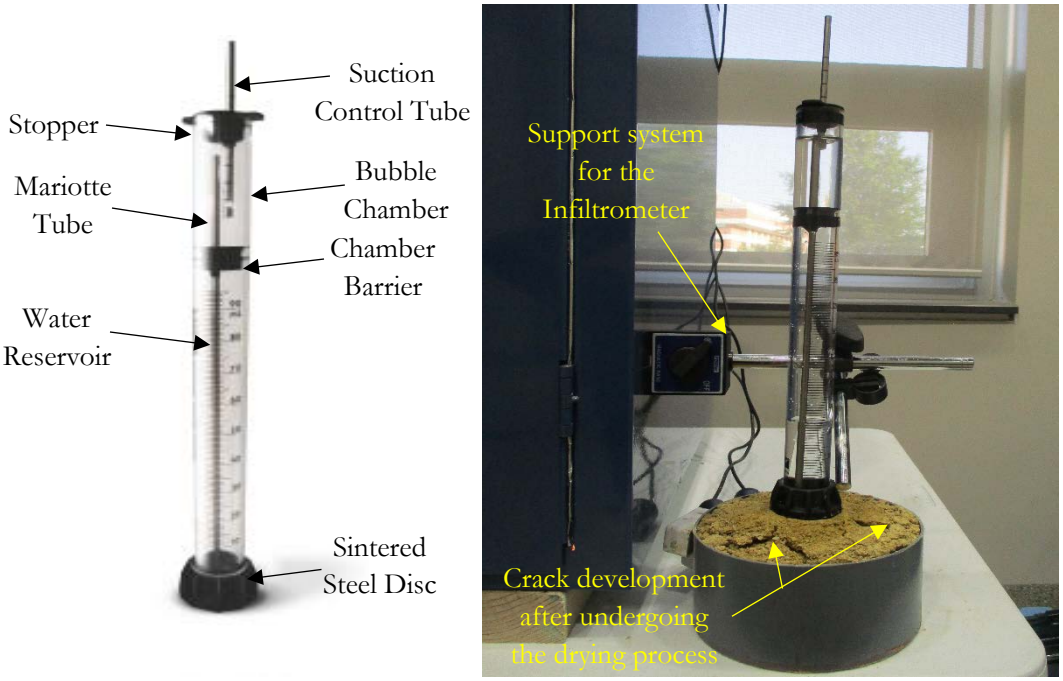

(a) (b)

Figure 3.4 Laboratory hydraulic conductivity set up (a) Mini disk Infiltrometer (b) Testing of the samples using Mini Disk Infiltrometer.

Soil infiltration refers to the soil's ability to allow water movement into and through the soil profile. It allows the soil to temporarily store water, making it available for uptake by plants and soil organisms. Infiltration rates are a measure of how fast water enters the soil. For initial laboratory assessment using the mini-disk infiltrometer, the infiltration curve is presented by plotting the infiltration rate in centimeters over the square root of time it takes soil to absorb each milliliter of water applied to the soil surface. Figure 3.5 shows the change in the infiltration rate over time for different wet-dry cycles (1N, 2N, and 3N of wet-dry cycles). The infiltration rate curve narrows closer to a shorter time interval at the end of the 3N wet-dry cycle for the different initial moisture content presented. This is attributed to the development of cracks on

the surface of the Yazoo clay surfaces as the number of wet-dry cycles increased. Also, studying the effect of initial moisture content on the infiltration rate curve, it can be observed that after the 1N wet-dry cycle, there was a more crack development on the surface of the Yazoo clay sample after the 1N wet-dry cycle for the 35% initial moisture content sample than the samples with lower initial moisture contents. This was very much evident in the significant increase of the infiltration rate for the sample shown by a sharp narrowing of the infiltration rate curve in Figure 3.5 (f). This also confirmed why the mini-disk infiltrometer was not suitable in measuring the hydraulic conductivity of soils with high surface cracks as it leads to a negative Kv reading. Water infiltrating too slowly may lead to ponding on level fields, erosion from surface runoff on sloping fields, or inadequate moisture for crop production. Porous and soils with cracks allow water to infiltrate faster and recharge groundwater aquifers and sustain a base flow in streams. An infiltration rate that is too high can lead to swelling and an increase in voids of soil in the case of expansive soils (Khan et al. 2019).

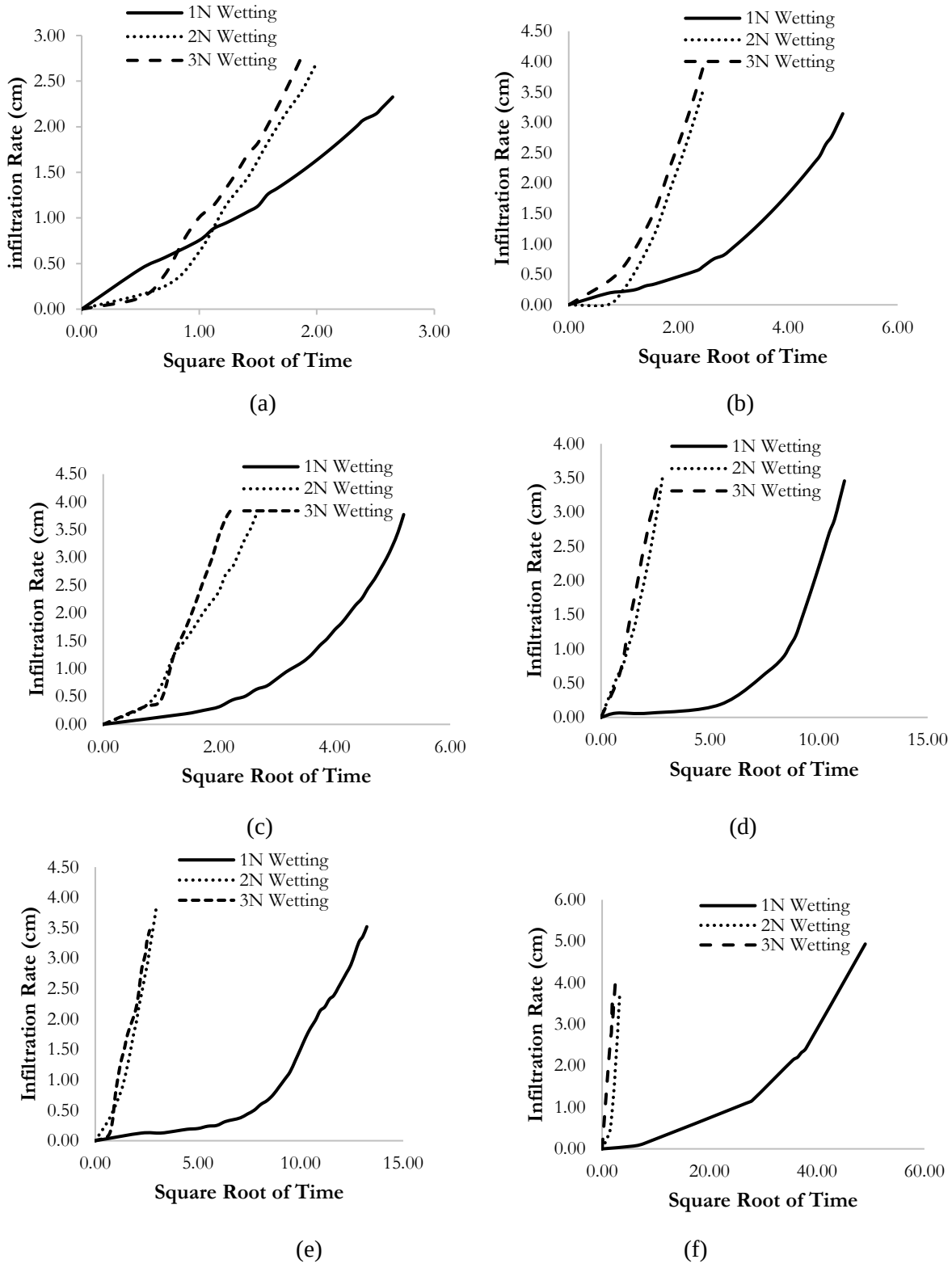

Figure 3.5 Change in infiltration rate over time (a) 10% Volumetric moisture content (b) 15% Volumetric moisture content (c) 20% Volumetric moisture content (d) 25% Volumetric moisture content (e) 35% Volumetric moisture content

The variation of the hydraulic conductivity values with different wet-dry cycles for samples of different initial moisture contents are presented in Figure 3.6. Although there is no noticeable trend considering the effect of initial moisture content, which may be due to the impossible human control of depth and width variation in the development (which occur naturally) on each sample at different wet-dry cycles. But as expected, there was an increment of the K_v values as the number of wet-dry cycles increases. During the drying process, there were vertical and horizontal cracks observed in the soil samples. These cracks became the preferential wetting paths during the wetting phase by promoting swelling and closure of the cracks (Abbaszadeh 2011), which decreased the time required to reach a primary swell or collapse condition. The cracks are due to anisotropic volume change, which leads to the development of tensile stresses in the restrained direction caused by the externally applied net normal stress (Kodikara et al. 1999). Once the tensile stresses exceed the tensile strength of the soil, the soil tends to crack, releasing the strain energy developed in the soil. After the soil cracks, the restraints placed on the soil are partially released, which allows the soil to undergo further volume change more isotopically; however, the soil suction can build up to higher tensile forces thus leading to additional cracking in the sample. Chen (1988) argued that regardless of the initial matric suction (or moisture content) of the material, the dry density seems to govern the swell characteristics of expansive soils. However, the results obtained in this study showed that the initial matric suction (or moisture content) is also an important factor that needs to be considered. When comparing samples subjected to the same w, results showed that the swell potential increased when the matric suction was increased.

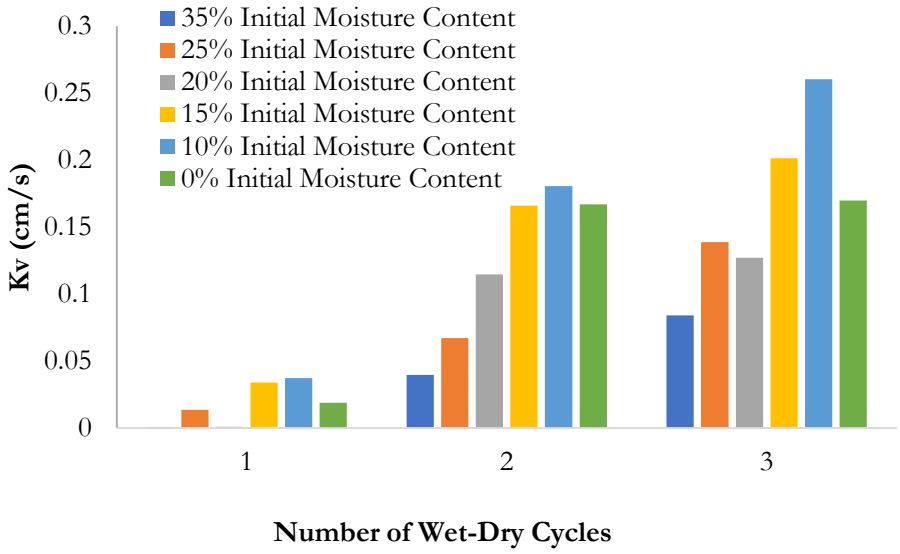

Figure 3.6 Change in Hydraulic conductivity of different initial moisture contents at different wet-dry cycle

3.6 Unsaturated Hydraulic Conductivity Testing using Moisture Sensors

To observe the changes in the permeability variations with the cyclic wet-dry cycles, an instantaneous profile method to measure the permeability was utilized. 3-inch diameter and 6 inches high circular PVC pipe section were utilized to compact Yazoo clay soil samples at different initial moisture content to investigate the changes in the unsaturated vertical permeability. Two moisture and temperature sensor was

installed at 2-inch spacing along with the height of the samples. Similar to the Mini Disk Infiltrometer testing, samples were compacted at optimum moisture content in the test box. Later, each test device at a compacted state will be subjected to 0, 3, and 5, wet-dry cycles, respectively. The samples inside the test devices were wetted to a fully saturated state and then dried by controlling the incandescent bulb attached to the box, to simulate the most extreme case.

After wetting up the moisture sensor, the following steps similar to the procedure, as described for Mini Disk Infiltrometer, were used to complete the wetting and drying cycles. The laboratory set up of using the moisture sensors to determine the changes in the permeability is presented in Figure 3.7.

- A data logger was used to record the volumetric moisture content with time for all moisture sensor devices. The wetting cycle process was simulated by wetting the sample, and the change in moisture content was recorded every 5 mins respectively, with a data logger program from the start of the wetting cycle for at least 24 hours while the sample was allowed to seat for moisture equilibrium.
- Once the primary wetting cycle elapses, the drying cycle was started by taking the samples into a constructed drying chamber. During the drying cycles, the environmental chamber was kept at 120^{o}F – 125^{o}F, simulating the maximum measured summer temperature of Mississippi. The data logger recorded the change in volumetric moisture content for about 24 hours.
- The above steps were repeated until a total of three wetting and drying cycles were achieved. After the drying process was completed, the samples were allowed to cool before starting the next wetting cycle. The method described previously to dry the specimen has shown to expedite the time required to achieve primary collapse and does not significantly affect the results obtained (Krisdani et al. 2008; Basma et al. 1996). The primary swell or collapse for the initial wetting cycle for both soils was achieved within 48 hours from the start of the test.

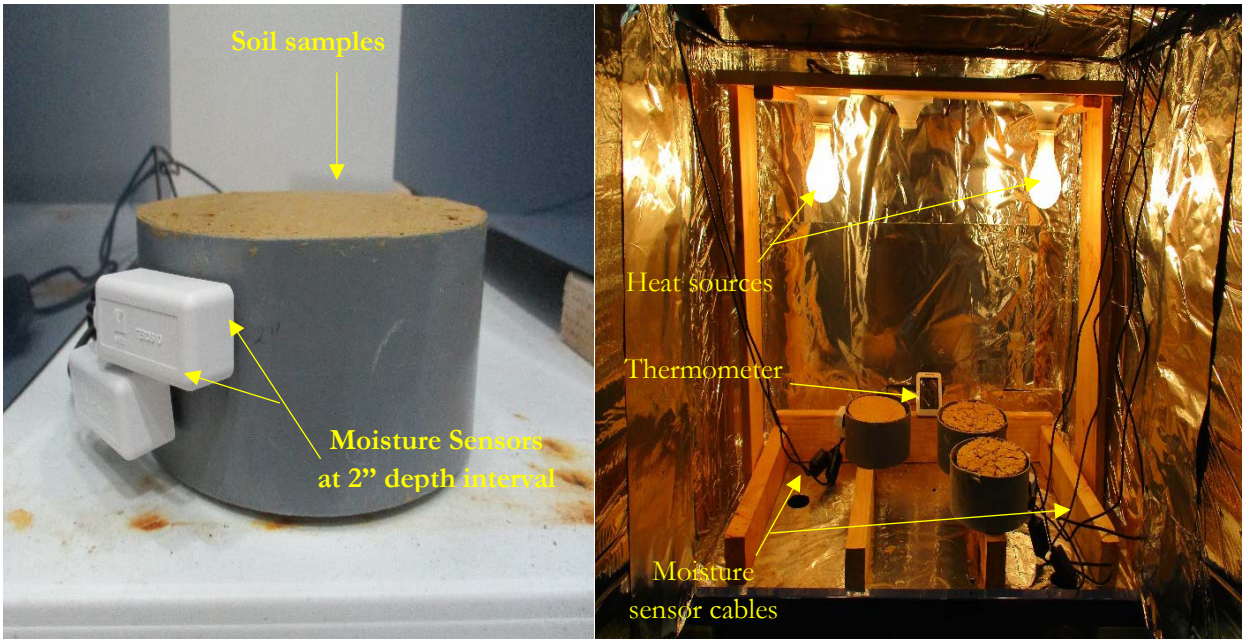

Figure 3.7 Laboratory hydraulic conductivity set up (a) Yazoo clay soil sample with instrumented moisture sensors (b) Drying cycle simulation process with the instrumented samples

3.6.1 *Determination of the hydraulic conductivity using the Teros10 moisture sensor instrumentation*

Variation of volumetric moisture content over time up to the 3N wet-dry cycle is shown in Figure 3.8. Where Figure 3.8 (a) shows the change in volumetric moisture content for 20% and 25% initial moisture contents at different sample depth and Figure 3.8 (b) shows the change in volumetric moisture content for 10%, 15% and 35% initial moisture contents at 4" depth from the surface of the soil sample. Researchers using partial drying, usually dry the expansive soil back to either the initial moisture content of the sample or to in situ moisture content. Those using the full drying technique dry the expansive soil to residual moisture content or at air-dried moisture content. Results have shown that expansive soils subjected to the full dry condition tend to have higher swell potential at lower applied stress with an increase in wetting and drying cycles. Expansive soils subjected to partial drying, on the other hand, tend to have lower swell potential at lower applied stress with an increase in wetting and drying cycles (Basma et al. 1996; Subba Rao and Satyadas 1987; Tripathy et al. 2002). Shrinking or aging phenomena, which result in differential changes in the soil structure, depending on the Wetting and drying history of the sample and can cause different water contents in the soil during drying and wetting at the same suction. The solution of air, or the lease of dissolved air from the soil–water, can also have a differential effect on the suction–water content relationship of the soil during wetting and drying. The results in Figure 3.8 depict that none of the wetting curves reaches full saturation at the end of the wetting paths. The looser the sample, the lower the degree of saturation (Gallage and Uchimura, 2010).

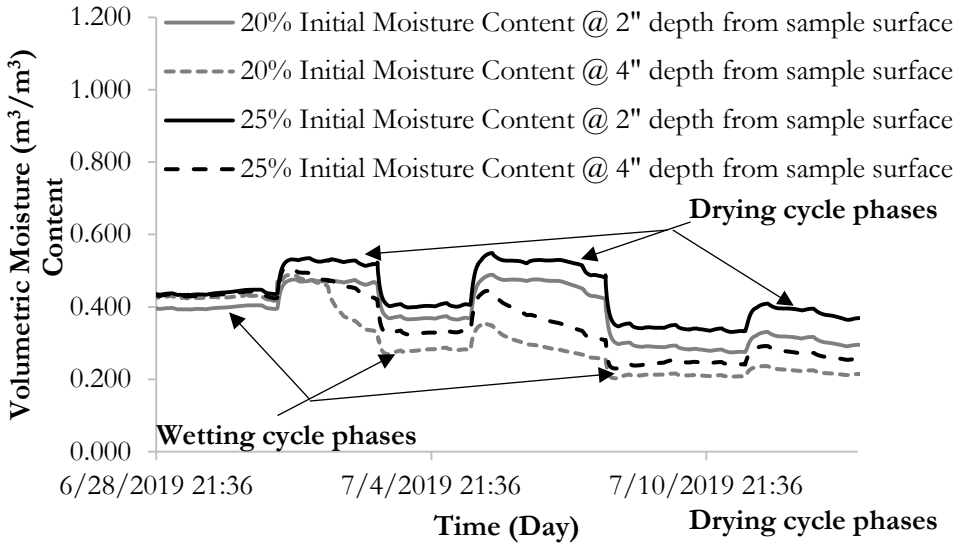

(a)

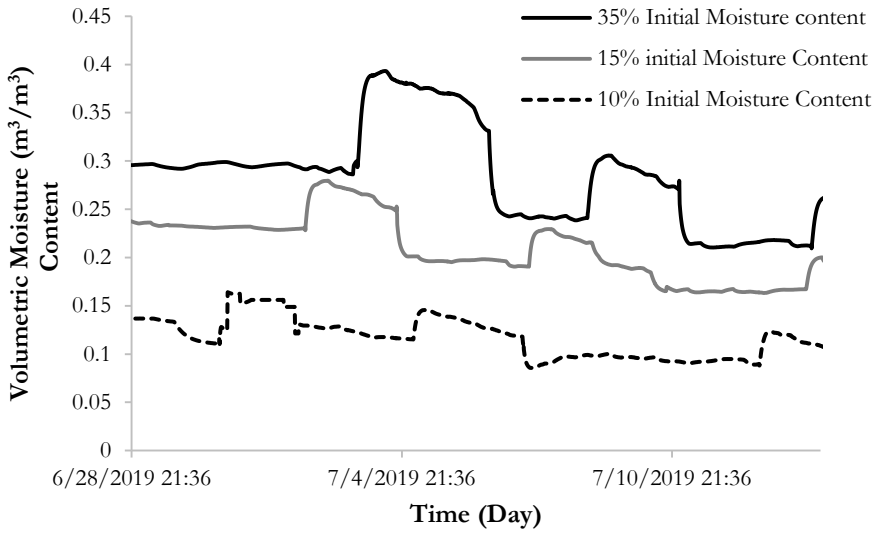

(b)

Figure 3.8 Variation of volumetric moisture content overtime at 3N wet-dry cycle (a) change in volumetric moisture content for 20% and 25% initial moisture contents at different sample depth (b) change in volumetric moisture content for 10%, 15% and 35% initial moisture contents

During this study, data from the instrumentation was at every 5 min interval. Sensors at 2 in and 4 in sample depth were installed for the 20% and 25 % initial moisture content samples shown in Figure 3.8. The sensors registered instantaneous responses to water infiltration. The peak soil moisture content at different wet-dry cycles is presented in Table 3.4 and Table 3.5. The values at which the moisture content readings stabilized were considered the equilibrium moisture contents for the remaining depths. Sensors at varying depths experienced individual peaks in response to each water infiltration event. Moisture contents rose from 1% to 15% in amplitude and were likely limited to the temporary. Since temporal variations occurring within a short time period can induce volumetric deformation in expansive clay, the temporary

rises in moisture content are significant to consider. The largest increases were seen during periods of the 1N wet-dry cycle. The drying path prevented the moisture from rebounding to the initial levels, thereby decreasing as the number of wet-dry cycles increases. The 25% initial moisture content sensor at 2 in depth from the surface of the sample experienced more significant rises in moisture content than the sensor at 4-inch depth from the sample surface, a result that could be attributed to the sensor's proximity to the ground surface. Also, as expected, the 20% initial moisture sensor at 4-inch depth experienced the lowest moisture reading, and this can be a result of the low initial moisture content and also the depth of the sensor.

As observed in both Table 3.4 and Table 3.5, regardless of the initial moisture content, the hydraulic permeability of the Yazoo clay dropped with the increasing number of the wet-dry cycles. With the increase in the wet-dry cycles, the propagation of the desiccation cracks increases, as presented in Figure 3.9. This increment in the desiccation cracks certainly influenced the increment in the hydraulic permeability of Yazoo clay.

Table 3.4 Variation of VMC and hydraulic conductivity in Response to water infiltration and number of wet-dry cycles respectively (20% initial moisture content)

Sensor Depth (Inch)	*1N*			*2N*			*3N*		
	Peak Sensor Reading	*Time (hr)*	*Kv (cm/sec)*	*Peak Sensor Reading*	*Time (hr)*	*Kv (cm/sec)*	*Peak Sensor Reading*	*Time (hr)*	*Kv (cm/sec)*
2	0.432	21:45	$1.47E^{-4}$	0.37	06:50	$1.41E^{-3}$	0.298	06:30	$1.69E^{-2}$
4	0.405	03:30		0.334	17:50		0.247	09:40	

Table 3.5 Variation of VMC and hydraulic conductivity in Response to water infiltration and number of wet-dry cycles respectively (25% initial moisture content)

Sensor Depth (Inch)	*1N*			*2N*			*3N*		
	Peak Sensor Reading	*Time (hr)*	*Kv (cm/sec)*	*Peak Sensor Reading*	*Time (hr)*	*Kv (cm/sec)*	*Peak Sensor Reading*	*Time (hr)*	*Kv (cm/sec)*
2	0.448	03:30	$8.65E^{-5}$	0.408	06:20	$1.22E^{-4}$	0.349	06:40	$4.7E^{-4}$
4	0.442	20:00		0.334	17:50		0.247	09:40	

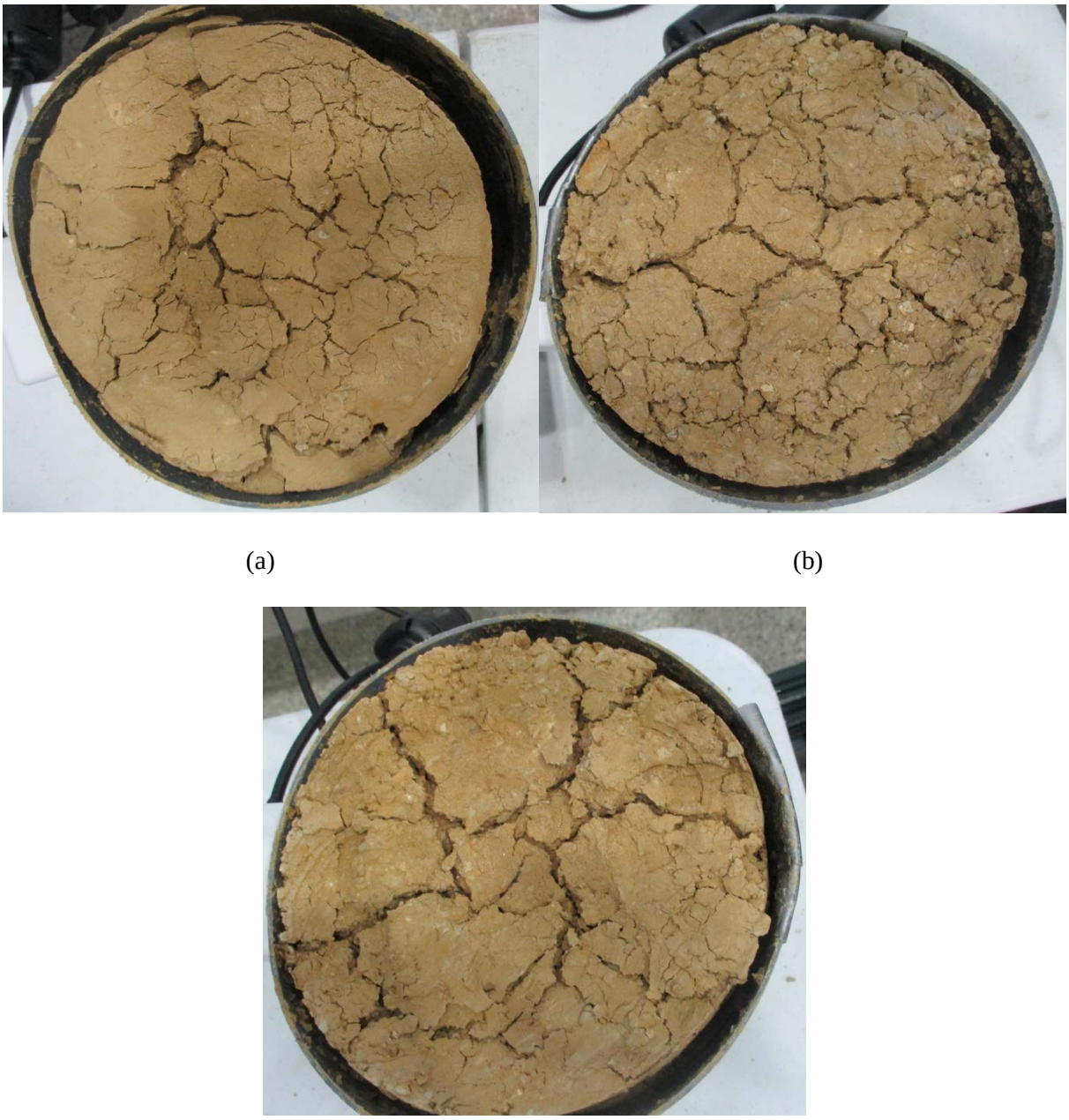

(a) (b)

(c)

Figure 3.9 Desiccation cracks in Soil Samples, a. 1 Wet-Dry Cycles, b. 3 Wet-dry Cycles, and c. 5 wet-dry cycles

3.7 Comparison of the Hydraulic Conductivity

Comparing the two methods, the differences in values of hydraulic conductivity can be attributed, resulting in the suction characteristics. As stated in the methodology of using the mini-disk infiltrometer, a suction value of 0.5 cm was suggested for expansive clay soils, but our knowledge of the difference in behavior of expansive soils should be considered as expansive soils differ in liquid limit and plasticity index which gives the reason while adopting a suction value of an unknown property of expansive soil into another can

affect the result. As can be seen in the two method results, the mini-disk infiltrometer gave a high value of hydraulic conductivity than the calculated values using the automated moisture sensors. Hence, using a higher suction value will have a definite effect on the result, correlates to a higher intensity and thus greater permeability through the soil. Conversely, lower intensity correlates to lower permeability. Also, the mini-disk infiltrometer is more challenging especially when dealing with a very high plastic clay such as the Yazoo clay in that as the soil sample undergo different wet-dry cycles, more desiccation cracks are observed on the surface which in turn affects the balance of the mini-disk infiltrometer and also reducing the mini-disk suction base to soil surface contact area which is needed to establish balanced steady reading. This is the most challenging factor in adopting this method for highly plastic clay soil. Furthermore, the human error factor should not be ignored as this method is done manually unlike the moisture sensor method which is plugged into the data logger and readings are automatically recorded on a set interval. Based on the above observations with the two methods, it is evident that the method two gives more accurate hydraulic conductivity results.

The samples for this study were collected from a highway slope site to investigate the changes in hydraulic conductivity. It should be noted that regardless of the location of the samples, the laboratory test results are applicable to levees constructed by expansive Yazoo clay soil. During this study, the hydraulic conductivity results are utilized to investigate the flow behavior in highway embankment as well as in levees.

Chapter 4: Finite Element Analysis to Investigate Flow Behavior

4.1 Impact of Rainfall

Most highway fill slopes in the Mississippi areas are constructed using in-situ high plasticity clay soil, which is highly expansive. These fill slopes have recurring shallow failures a few years after construction, causing a significant maintenance problem for the Mississippi Department of Transportation (MDOT). Shallow slope failures generally do not constitute a hazard to human life or cause significant damage; however, the highly plastic clay soil developed desiccation cracks. This may have significantly increased the permeability along the vertical direction of topsoil at the active zone. (Khan et al. (2017)). In some cases, the infiltration of rainwater results in a reduction in soil shear strength and matric suction, which leads to a reduction in slope stability. The slope stability is reduced by both rainfall intensity and duration. (Hossain et al., 2013). Prolong drought creates significant shrinkage cracks, which provides a vertical preferential path during rainfall. The suction observed to decrease significantly with higher intensity and longer duration of rainfall. (Khan et al. (2017)). In a case study, Yalcin (2007) showed that the rainfall also increases the water content in clays that leads to a reduction in the stability of natural slopes. As a result, the rainfall causes a decrease in shear strength by either reducing soil cohesion or through potential slip surfaces, and then this directly relates to extreme rainfall events.

Rahimi et al. (2010) conducted a study on rainfall-induced slope failure due to antecedent rainfall for high and low conductivity residual soils of Singapore. The authors applied three antecedent rainfall patterns to soil slopes and conducted a transient seepage analysis to investigate the effect of rainfall on the stability of the slope. Results from the study indicated that antecedent rainfall affected the stability of both high-conductivity and low-conductivity soil slopes, with the stability of the low-conductivity soil slopes being more significantly affected. Also, the stability of the slope was controlled by the amount of rainfall that infiltrated within the unsaturated zone of the slope.

NOAA collects the rainfall data all over the US and develops the precipitation pattern of any locality based on the historical data (NOAA Atlas 2014). During this study, the PDS based intensity duration and frequency (IDF) curve of precipitation, based on NOAA Atlas 2014 of Jackson, Mississippi, was collected and adopted for Flow analysis. Based on the PDS curve of Jackson, MS with 100 year return period, different volumes of rainfall 6.14 into 12.8 in for rainfall durations from 2-hrs to 3 days are selected to conduct flow analysis. The rainfall Duration and total rainfall volume are presented in Table 4.1.

Table 4.1 Selected Precipitation pattern from NOAA precipitation data for FEM analysis

Rainfall Duration	Rainfall Volume (in)
2-hrs	6.14
6-hrs	8.63
12-hrs	9.94
24-hrs	11.1
3 days	12.8

The upper bound range of NOAA precipitation estimates was selected and categorized into three categories; High-intensity short duration rainfall (2-hrs duration of 6.14-inch rainfall volume), Medium intensity rainfall (12 hrs. duration of 9.94-inch rainfall volume) and Low-intensity long-duration rainfall (3-day

duration of 12.8 inches of rainfall volume) by the course of this study. The hydraulic function for the selected rainfall intensities is shown in Figure 4.1.

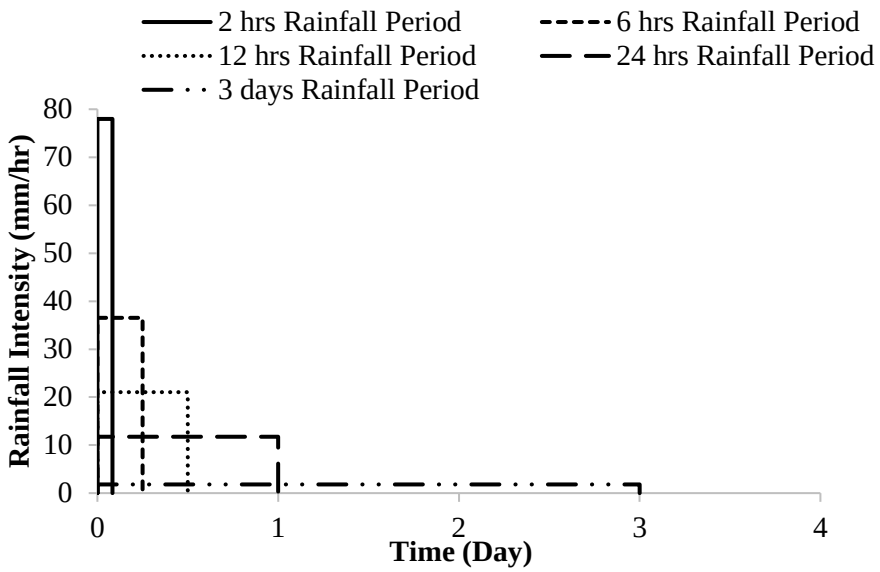

Figure 4.1 Different rainfall intensities for FEM modeling

4.2 Development of Finite Element Model

During this study, the FEM program PLAXIS 2D was used to conduct the flow analysis. A 15-node triangular element was used, which provides a fourth-order interpolation for displacements, and the numerical integration involves twelve Gauss points. The Van Genuchten model is considered as the hydraulic model. In this study, precipitation of different intensities was applied to the soil model to assess the flow behavior during and after rainfall. The analysis was carried out at five rainfall intensities shown in Figure 4.1. The rainfall intensities were selected based on 100-year periods of Mississippi rainfall data.

Laboratory testing indicated that the slope has highly plastic Yazoo clay soil, which causes shrink-swell behavior as it undergoes different wet-dry cycles (Khan et al. 2019). With the shrink-swell behavior, the hydraulic conductivity of the soil samples varies as a different season. Therefore, during this study, different hydraulic conductivity values were applied for the topsoil layer considering three different wet-dry cycles in the active zone. The current study considered the depth of the active zone as 12 ft. below the active zone; the vertical hydraulic conductivity of the soil does not change much. Therefore, below the active zone, both the horizontal and vertical permeability are considered as equal. The schematics of the FEM flow analysis are presented in Figure 4.2.

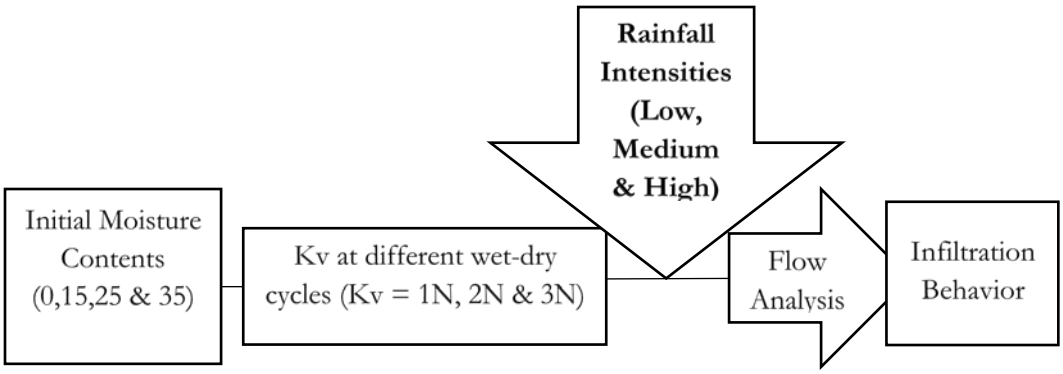

Figure 4.2 Schematics of FEM flow analysis process

4.3 Flow Analysis of Highway Pavement

4.3.1 *Model Development*

To investigate the effect of changes in hydraulic conductivity with different wet-dry cycles on the highway embankment and overlaying pavement, different hydraulic conductivity values were considered in the Flow Analysis. For each case presented, precipitation with different intensities was applied to the soil model to assess the infiltration behavior during rainfall. The flow through the topsoil was determined for each of the intensities assuming rainfall durations lasted 30 min, 60 min, 2 hours, 6 hours, 12 hours, 1 day, 3 days, and 7 days. The representative soil model is presented in Figure 4.3. The boundary condition, as outlined in the mentioned figure, shows the infiltration of the topsoil, which can simulate realistic water ponding at the topsoil layer.

During the dry period, the highly plastic clay soil developed desiccation cracks, which might have significantly increased permeability vertically at the active zone. However, due to the desiccation crack, the permeability in the horizontal direction might not have any effect and could have remained unchanged (Khan et al. 2017, Khan et al. 2018). The Yazoo clay usually has significant cracks that have been observed in the laboratory as well as in the field. The diameter of the cracks varies from 0.12 inch (3 mm - laboratory) to 0.3 in (8 mm - field), where the boundary plays a significant role in defining the size of the cracks. A high vertical permeability value of k_v at different wet-dry cycles was used for the part mentioned above for each of the slopes to simulate the effect of the desiccation crack in the top layer. However, the horizontal permeability remains unchanged, and the value of permeability was selected as $k_h = 3.06*10^{-6}$ cm/sec. In other clay layers, the permeability for both the horizontal and vertical directions was selected as $3.06*10^{-6}$ cm/sec respectively. The water table was placed at 14 ft (4.27 m) below the surface layer from field observation which defines the initial unsaturated condition. In the flow analysis, the left and right boundaries were selected as the closed boundaries, and the top of the slope was selected as rainfall infiltration. The soil parameters for flow analysis are presented in Table 4.2.

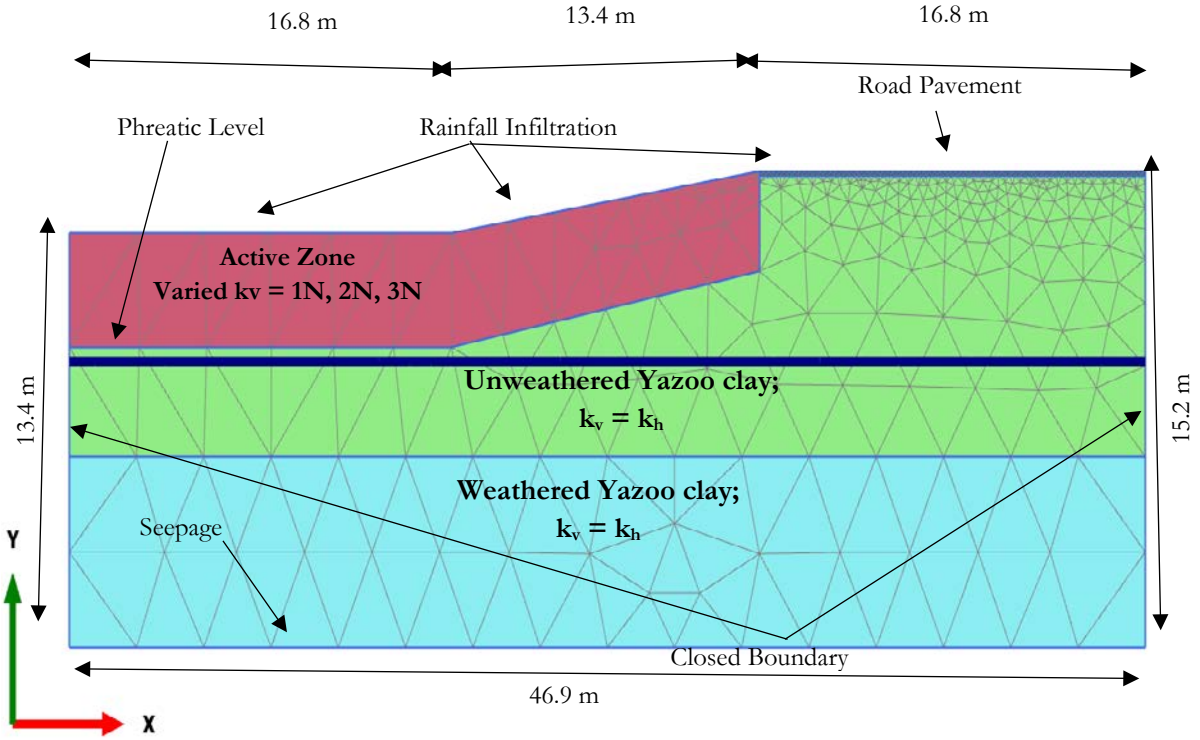

Figure 4.3 Illustration of FEM soil model

Table 4.2 Soil parameters for FEM analysis of highway embankment

Parameter	Symbol	Unit	Soil 2 (Weathered YC)	Soil 3 (Unweathered YC)
Vertical Permeability	k_v	(cm/sec)	$3.06 * 10^{-6}$	$3.06 * 10^{-6}$
Horizontal Permeability	k_h	(cm/sec)	$3.06 * 10^{-6}$	$3.06 * 10^{-6}$
Soil 1 (Active zone) vertical permeability conditions				
Initial Moisture Content (%)	**Calculated Hydraulic conductivity (k) at different wet-dry cycles (N) (cm/sec)**			
	1N		**2N**	**3N**
0	$2.3E^{-2}$		$1.64E^{-1}$	$1.56E^{-1}$
15	$4.85E^{-2}$		$7.82E^{-2}$	$2.06E^{-1}$
25	$9.1E^{-3}$		$8.50E^{-3}$	$3.59E^{-1}$
35	$7.25E^{-4}$		$1.17E^{-1}$	$4.03E^{-1}$
* The soil 1 horizontal permeability at different conditions = $3.06 * 10^{-6}$ (cm/sec).				

4.3.2 *Flow Analyses Results*

The variations of suction at the slope with 3H: 1V ratio for the initial phase (prior to rainfall), 30 min, 2 hrs., 6 hrs., 12 hrs., and 3-day rainfall intensities are presented in Figure 4.4, Figure 4.5, Figure 4.6, and Figure 4.7, which represents the changes in matric suction for hydraulic conductivity with 1 wet-dry cycles

and 35% initial moisture content at the topsoil layer. FEM analysis results for other cases are presented in Appendix A. Based on the flow analysis using FEM method in Plaxis; it is observed that the suction immediately dropped at the toe of the slope after rainfall and continued to drop as rainfall continues, representing the accumulation of water at the corresponding depth. It is also observed that the reduction in suction is continued for a few hours, even after the rainfall due to percolation and redistribution of rainwater within the slope. The effect of rainfall stays there for a few days, and then the suction begins to increase and almost regained its original profile for the top part. A similar trend of infiltration and changes in the suction profile for other cases (Appendix A).

It should be noted that during the FEM analysis, the infiltration boundary was used at the topsoil, which allowed ponding of water to simulate realistic behavior. The ponding status is established when the rainfall intensity is equal to the infiltration capacity. From FEM analysis results, it can be seen that ponding occurrence exists in almost all surficial soil for the toe part of the slope with different rainfall intensities. However, for 12-hr and 3-day rainfall intensity, ponding condition can be found hardly at the slope, due to the low intensities. In particular, ponding has affected the matric suction according to the mentioned rainfall intensities. In other words, ponding occurrence decreases the amount of suction at the topsoil at the toe.

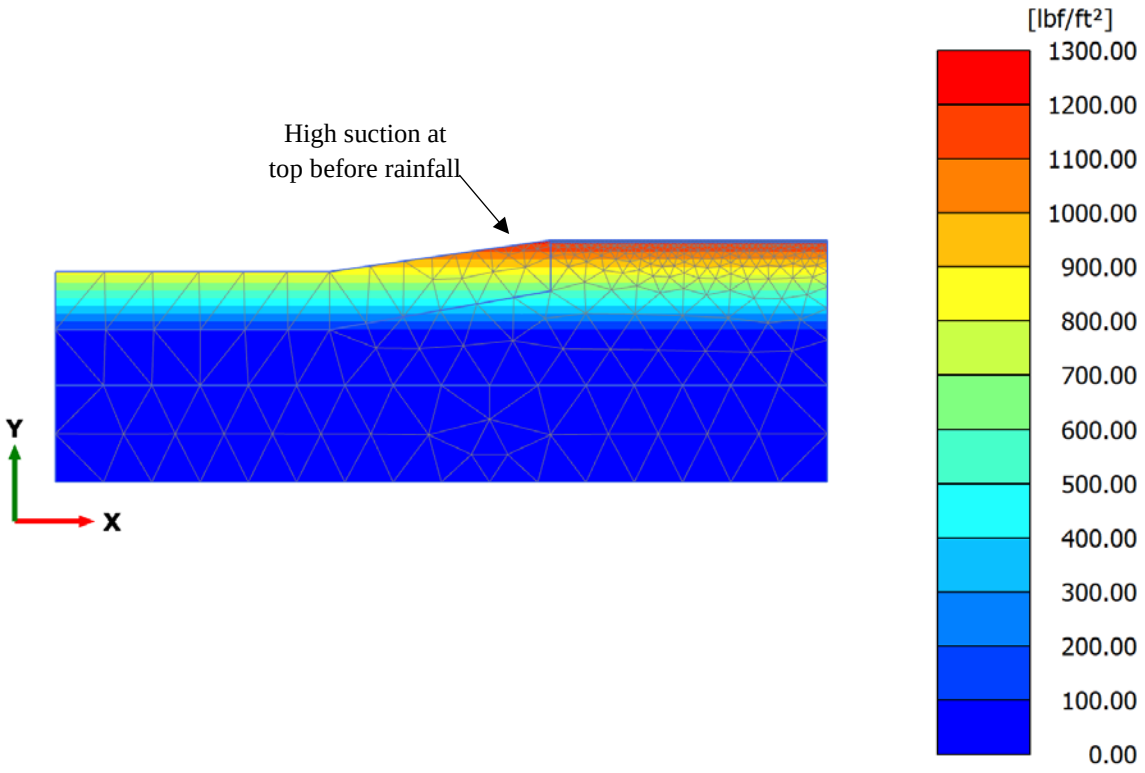

Figure 4.4 Prior to rainfall

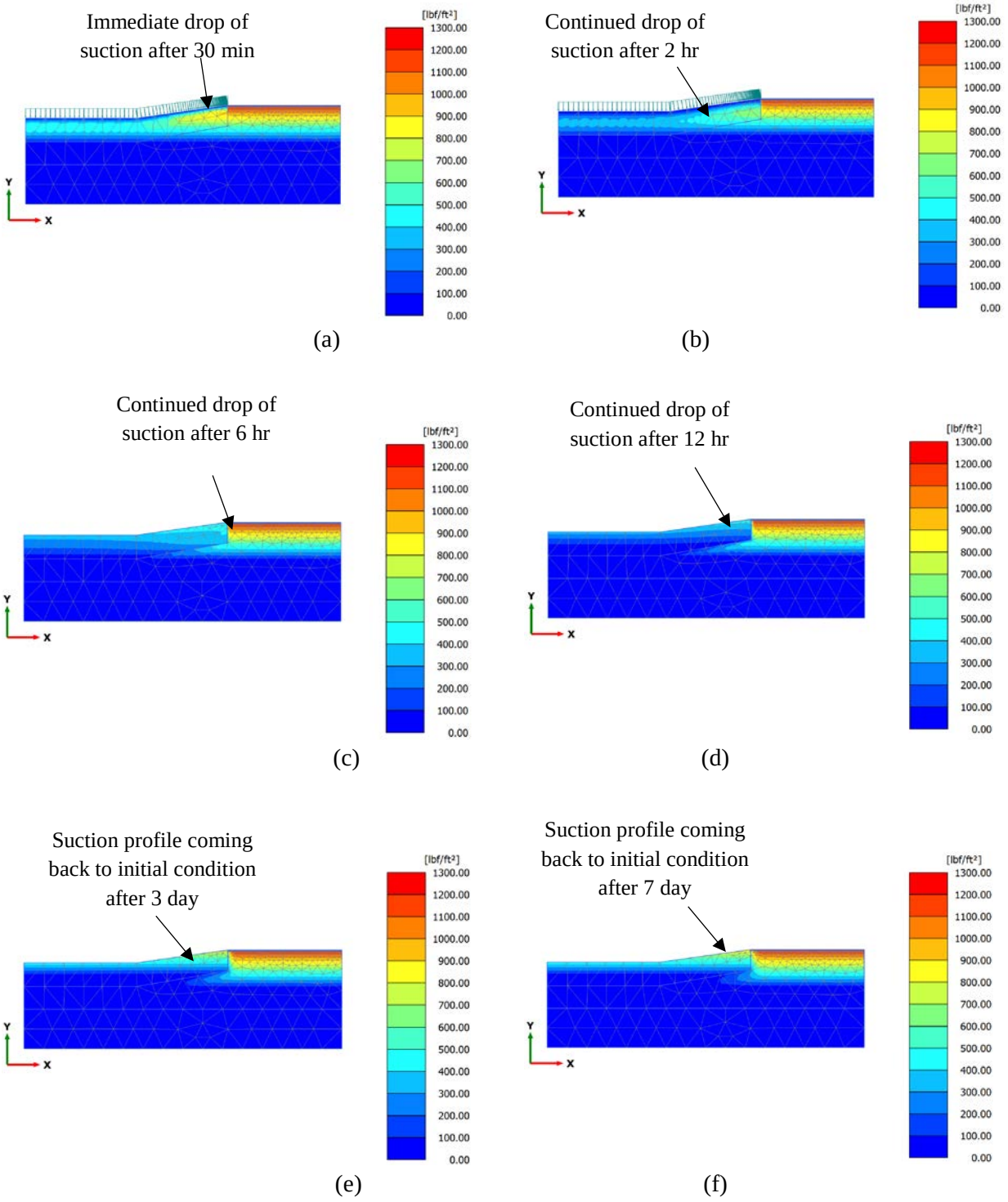

Figure 4.5 Suction variation of 1N wet-dry cycle for 35% initial moisture content at high intensity 2 hrs. rainfall period (a) After 30 mins (b) After 2 hrs. (c) After 6 hrs. (d) After 12 hrs. (e) after 3 days (f) after 7 days

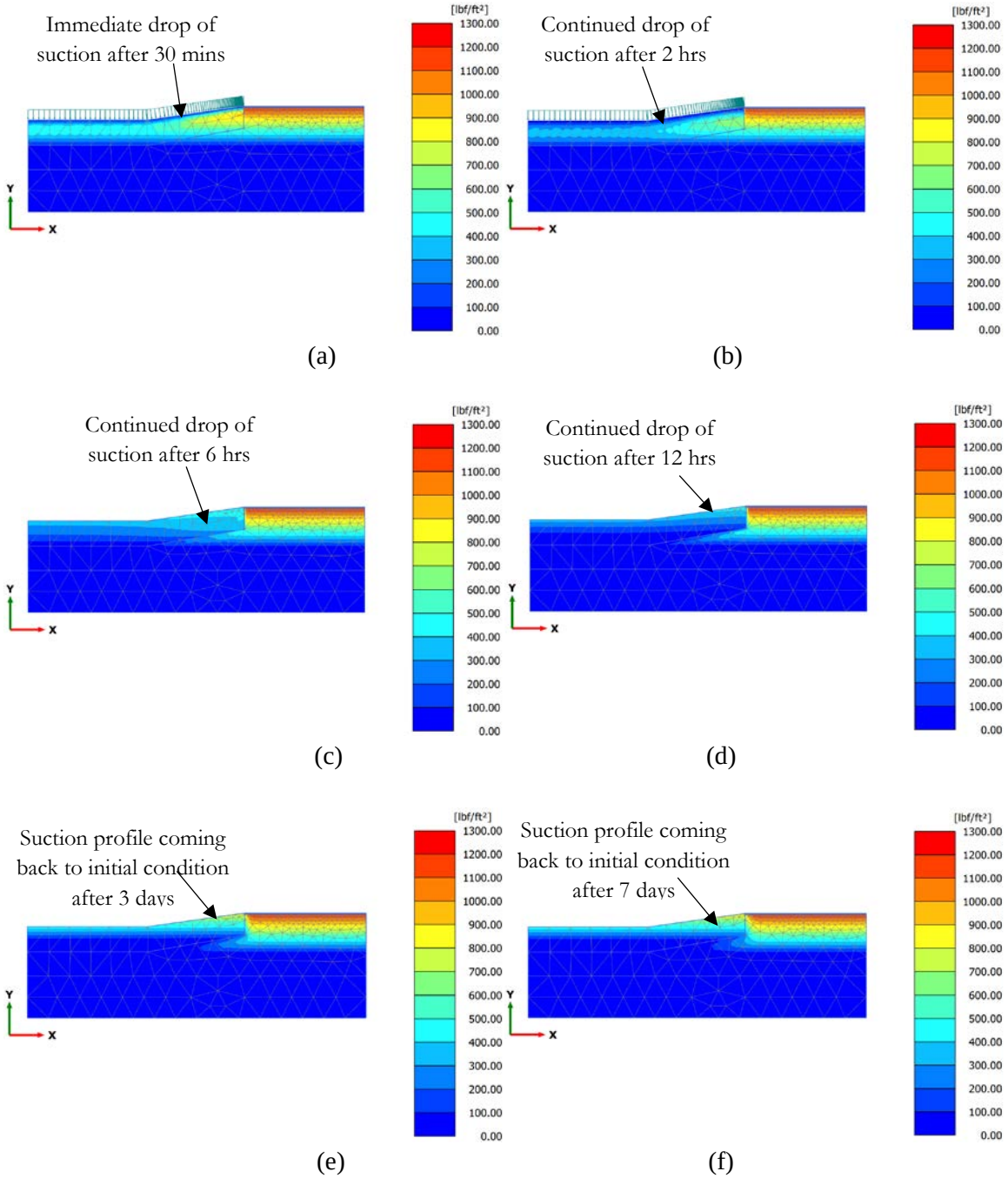

Figure 4.6 Suction variation of 1N wet-dry cycle for 35% initial moisture content at high intensity 12 hrs rainfall period (a) After 30 mins (b) After 2 hrs (c) After 6 hrs (d) After 12 hrs (e) after 3 days (f) after 7 days

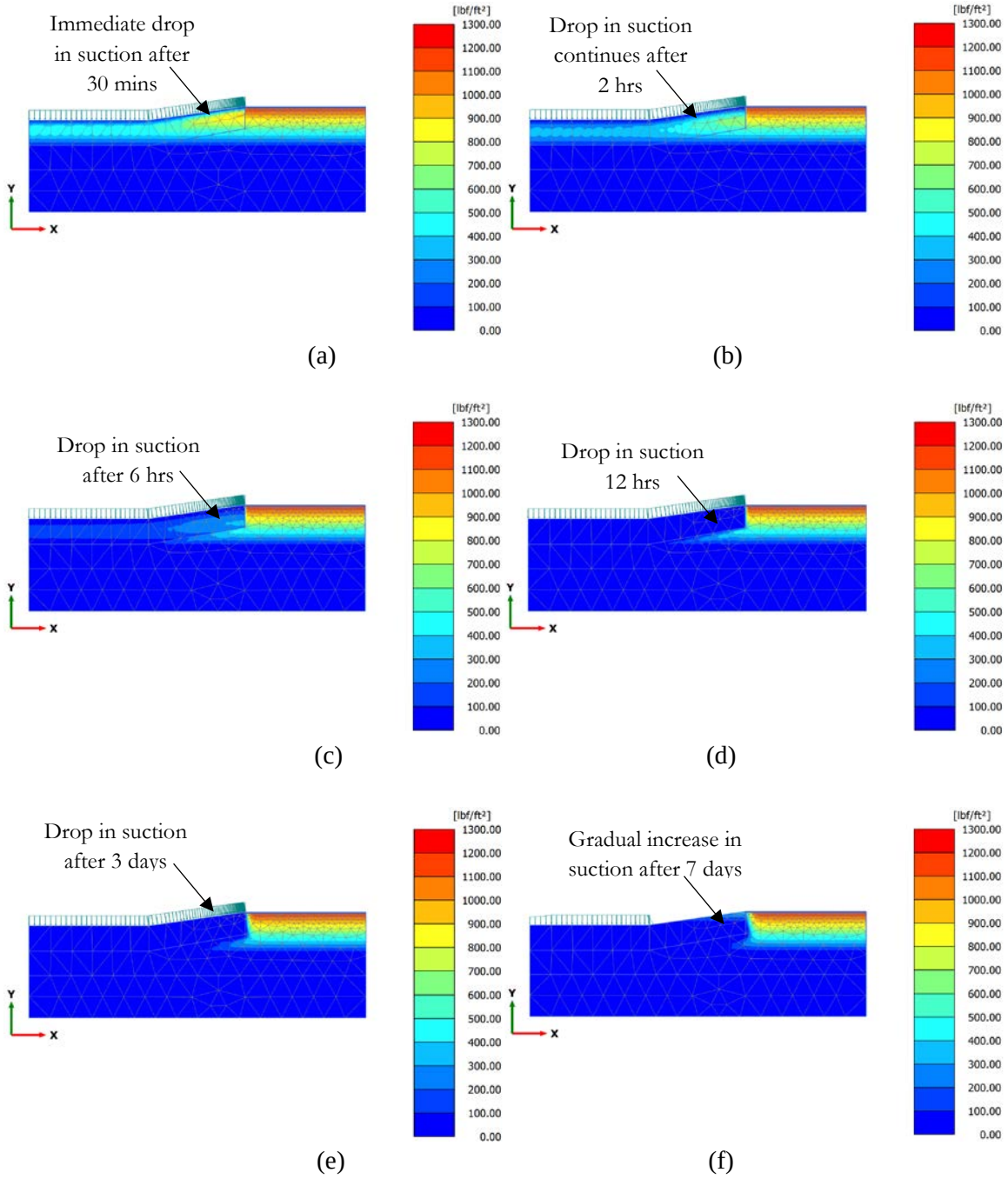

Figure 4.7 Suction variation of 1N wet-dry cycle for 35% initial moisture content at high intensity 3-days rainfall period (a) After 30 mins (b) After 2 hrs (c) After 6 hrs (d) After 12 hrs (e) after 3 days (f) after 7 days

The change in suction was observed with 2 hr, 12 hr, and 3 days of rainfall duration at two different slope locations (middle and crest) and 5 ft (1.52 m) into the road pavement. Discussed below is FEM analysis for 1N suction variation with 35% initial moisture content. Other FEM analysis results are presented in Appendix A and B. Based on Figure 4.8, the change in suction was significant in all rainfall intensities. The

matric suction value prior to rainfall infiltration is about 1200 lb/ft^2 (57.45kPa) (for the selected 3H:1V slope.

Considering the effect of the high-intensity rainfall at different locations of the slope (Figure 4.8a), the matric suction remained unchanged at the 5 ft. (1.52 m) into the pavement point with a value of 54 kPa for a long duration of the post rainfall analysis. This is due to pore pressure build-up as a result of the entrapped rainwater beneath the concrete pavement. There was a noticeable sharp drop of suction from 57.45 kPa to 35 kPa after 6 hr. which jumped back up with a continued a minimal consistent increment up to 41.6 kPa after 7 days at the crest of the slope while the suction value at the middle of the slope had rebounded to about 25 kPa after 7 days having dropped below 10 kPa by 6 hr. post rainfall. This shows about 5%, 28%, and 58% drop in suction at 5 ft. (1.52 m) into the pavement, crest, and middle of the slope respectively after 7 days of 77.98 mm/hr. rainfall intensity. Hence, the most pronounced effect is in the middle of the slope and gradually effecting the pavement over time. Similarly, Figure 4.8(b) shows the effect of the medium intensity rainfall at the three slope locations. A similar trend was also observed but with a much more significant drop in the suction of about 7%, 49% and 79% drop in suction at 5 ft. (1.52 m) into the pavement, crest and middle of the slope respectively after 7-day post rainfall. The suction dropped to a minimum zero value after 21 hr. post rainfall which was observed and lasted for 3 hr. before a noticeable increase was seen, finally, as expected, the suction dropped to a zero value for about 6 days in the middle of the slope with the low-intensity long-duration rainfall. It was by the 7-day post rainfall period that the suction started increasing to about 11.88 kPa The suction at the crest of the slope did not experience sharp drop noticed in Figure 4.8(a) and Figure 4.8(b) but rather the suction gradually dropped to its lowest value of 9.58 kPa after 4 days before gradually increasing up to 19.52 kPa on the 7-day post rainfall. On the other hand, at 5 ft. into the pavement, the suction dropped to 51. 74 kPa from the initial 57.45 kPa.

The almost linear value of suction observed in Figure 4.8(c) indicates that the percolated water could not drain out from the slope due to the very low permeability and SWCC of the highly plastic Yazoo clay soil. Hossain (2012) also observed that the infiltration of rainwater depends on the initial matric suction of the soil. The suction was observed to increase with higher intensity, and it continues with slight changes. This is consistent with the observation made in the literature. Moreover, the change in suction was more significant in the middle of the slope when compared to the crest and 5 ft. (1.52 m) into the pavement. The gradual decrease in suction on the pavement will affect the stability of the pavement and hence, may result in pavement failure over time. It is important to note that the presented trend below is similar to the cases analyzed in this project and are all presented in Appendix B.

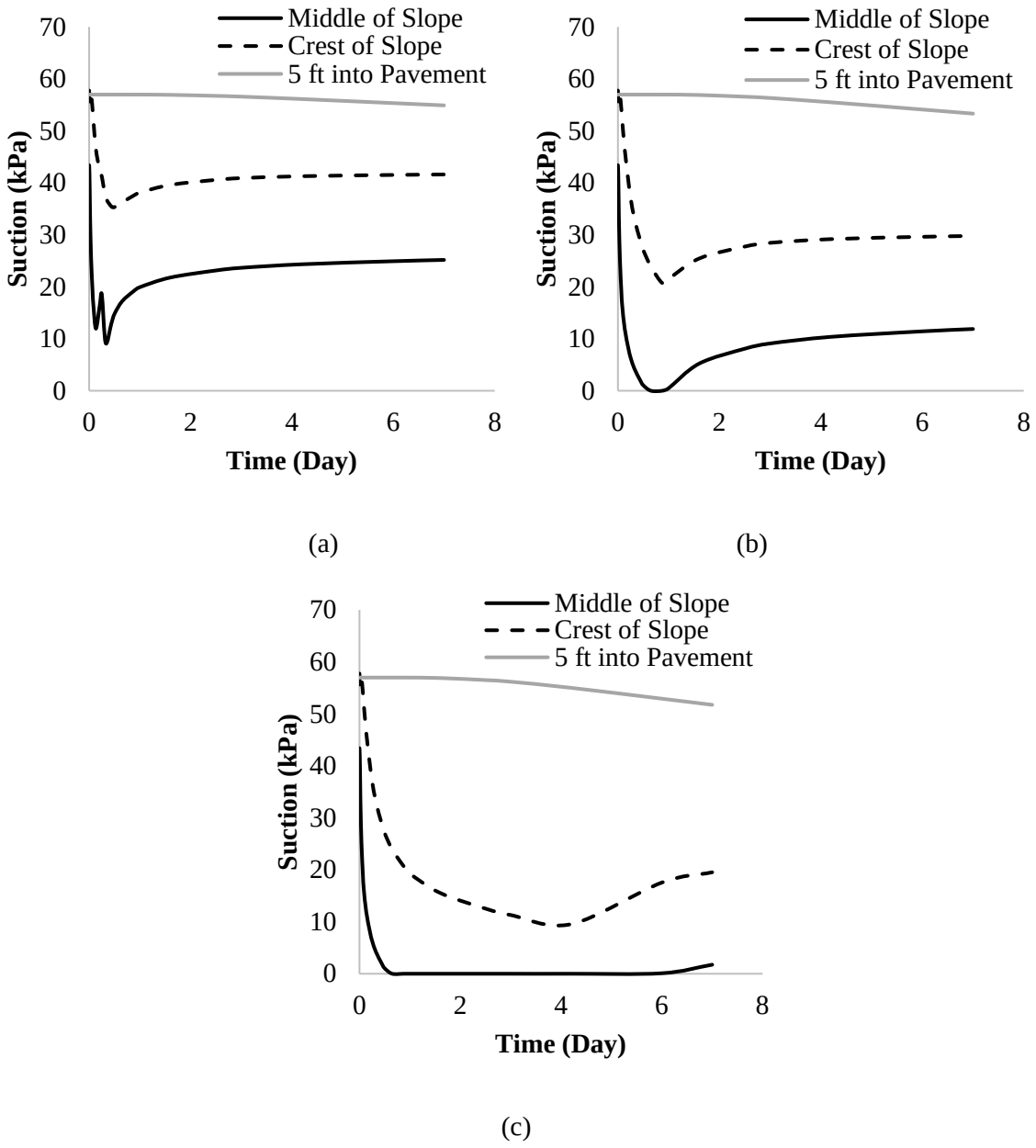

Figure 4.8 1N Suction Variation with 35% initial moisture content (a) Low-intensity rainfall (b) Medium intensity rainfall (c) High-intensity rainfall

4.4 Flow Analysis of a Levee Section

The East Jackson Levee System, located within Rankin County, Mississippi, was federally constructed in 1968 along the left descending bank of the Pearl River and provides risk reduction to the towns of Pearl, Flowood, and Richland. The levee system is approximately 13.5 feet tall and has an approximate length of 11.4 miles. The East Jackson, Flood Control Project, provides benefits to more than 10,000 people that work and live behind the levee, with more than $972 million in land and property value. The layout of the levee system is presented in Figure 4.9. The side slope of the levee faces shallow slope failures, which takes

place due to the infiltration of rainwater. As a result, the levee owner needs to spend millions of dollars on repairing the sloughing and shallow slope failure.

A section of the levee is selected for the flow analysis. The levee has 2.5H: 1V embankment on both sides. As stated earlier in chapter 3, no soil sample was collected from the levee system as the geography of the region depicts similar Yazoo clay soil properties. The same soil property results from the laboratory experiments conducted on the collected soil samples from the highway slope are adopted for the selected levee system. The foundation soil and levee fill materials are considered as the unweathered and weathered Yazoo clay. The soil model and boundary condition for flow analysis are presented in Figure 4.10. The flow analysis was conducted at different rainfall conditions, as presented in Figure 4.1 and varied hydraulic conductivity at the weathered Yazoo clay. The hydraulic conductivities of the levee section for flow analysis are presented in Table 4.3.

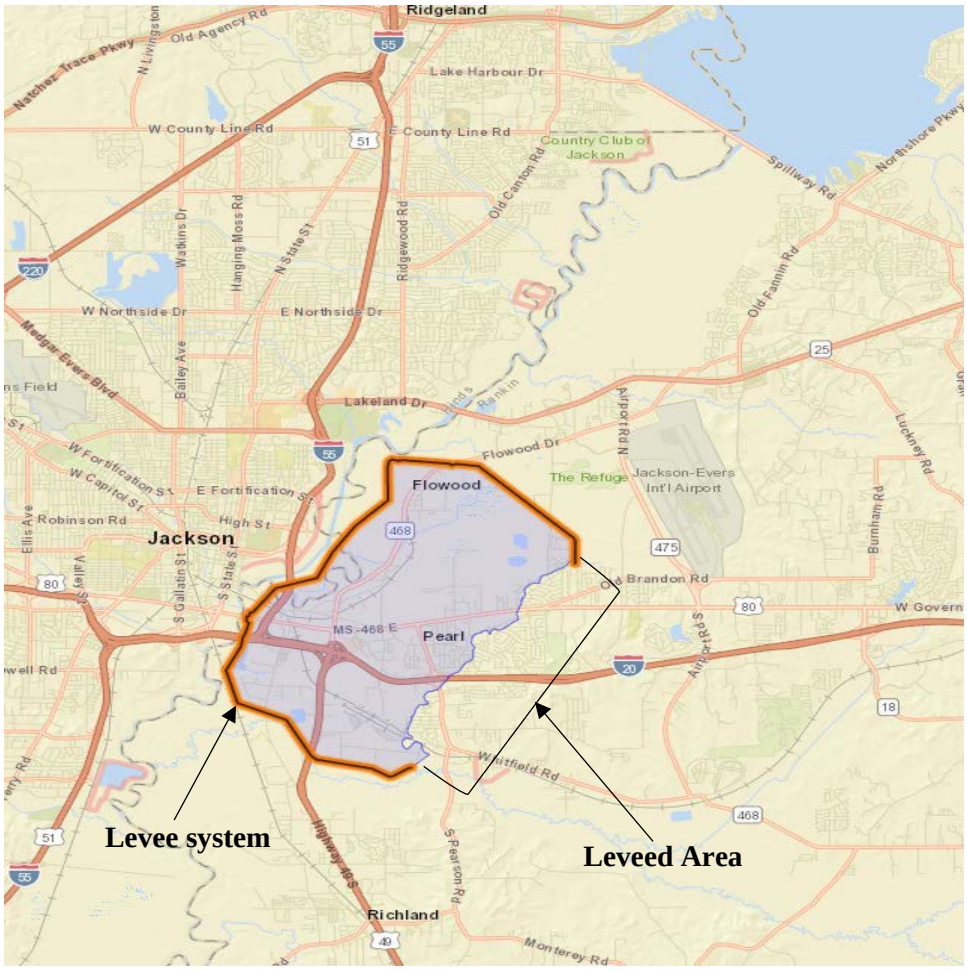

Figure 4.9 East Jackson Levee system

4.4.1 *Variation of suction effect on Levee top without pavement*

The variations of suction at the levee slope with 2.5H: 1V ratio for the initial phase (prior to rainfall), 30 min, 2 hr, 6 hr, 12 hr, and 3-day rainfall intensities are presented in Figure 4.11, Figure 4.12, Figure 4.13, and Figure 4.14. The mentioned figures presented the suction variation with 1 wet-dry cycles with 35%

initial moisture content for the topsoil layer. Other cases presented in Appendix C. Similar to the flow variations for highway slopes as discussed in the previous section, the suction immediately dropped at the toe of the slope after rainfall and continued to drop during the high and medium rainfall volumes. It can be seen that the suction at the top of the levee decreased to a minimum after 12-hr post rainfall but started increasing from the 3-day post rainfall. This increment continued until the 7th –day. For low intensity, long-duration rainfall, the case differs as the levee experienced a zero suction on the 3-day post rainfall, and a gradual increment was noticed on the 7-day post rainfall. This trend of the suction profile is similar for other cases, as presented in Appendix C.

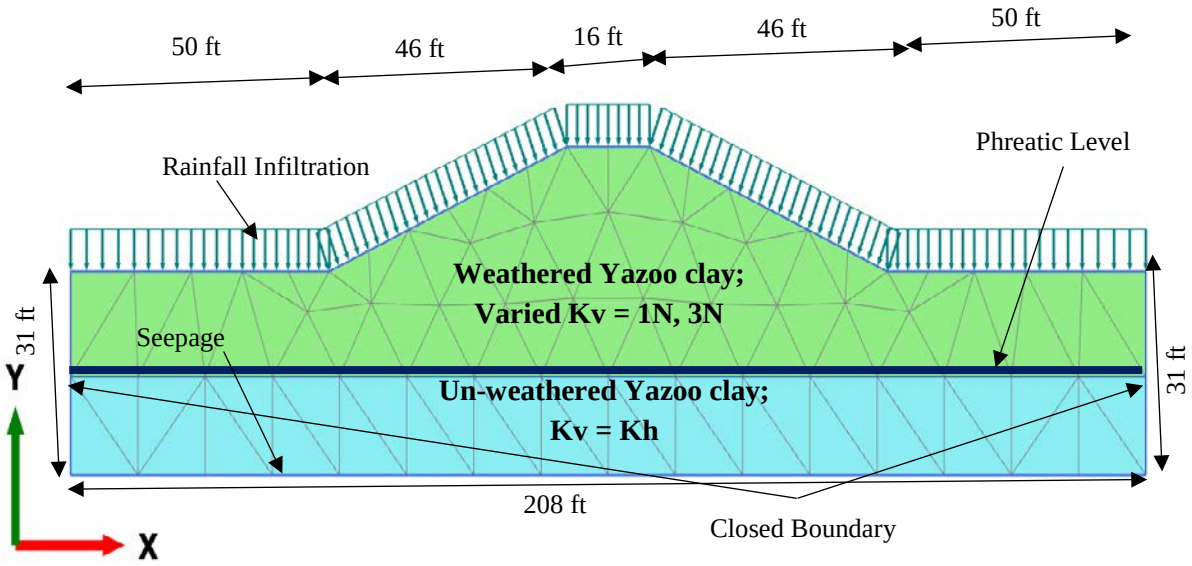

Figure 4.10 Levee Geometry and boundary condition

Table 4.3 Soil Properties for Flow Analysis of the Levee System

Parameter	**Symbol**	**Unit**	**Weathered Yazoo Clay**	**Unweathered Yazoo Clay**
Vertical Permeability	k_v	(cm/sec)	Presented in Part A	$3.06 * 10^{-6}$
Horizontal Permeability	k_h	(cm/sec)	$3.06 * 10^{-6}$	$3.06 * 10^{-6}$

Part A: Vertical permeability conditions of Weathered Yazoo Clay			
Initial Moisture Content (%)	**Calculated Hydraulic conductivity (k) at different wet-dry cycles (N) (cm/sec)**		
	1N	**2N**	**3N**
0	$2.3E^{-2}$	$1.64E^{-1}$	$1.56E^{-1}$
15	$4.85E^{-2}$	$7.82E^{-2}$	$2.06E^{-1}$
25	$9.1E^{-3}$	$8.50E^{-3}$	$3.59E^{-1}$
35	$7.25E^{-4}$	$1.17E^{-1}$	$4.03E^{-1}$

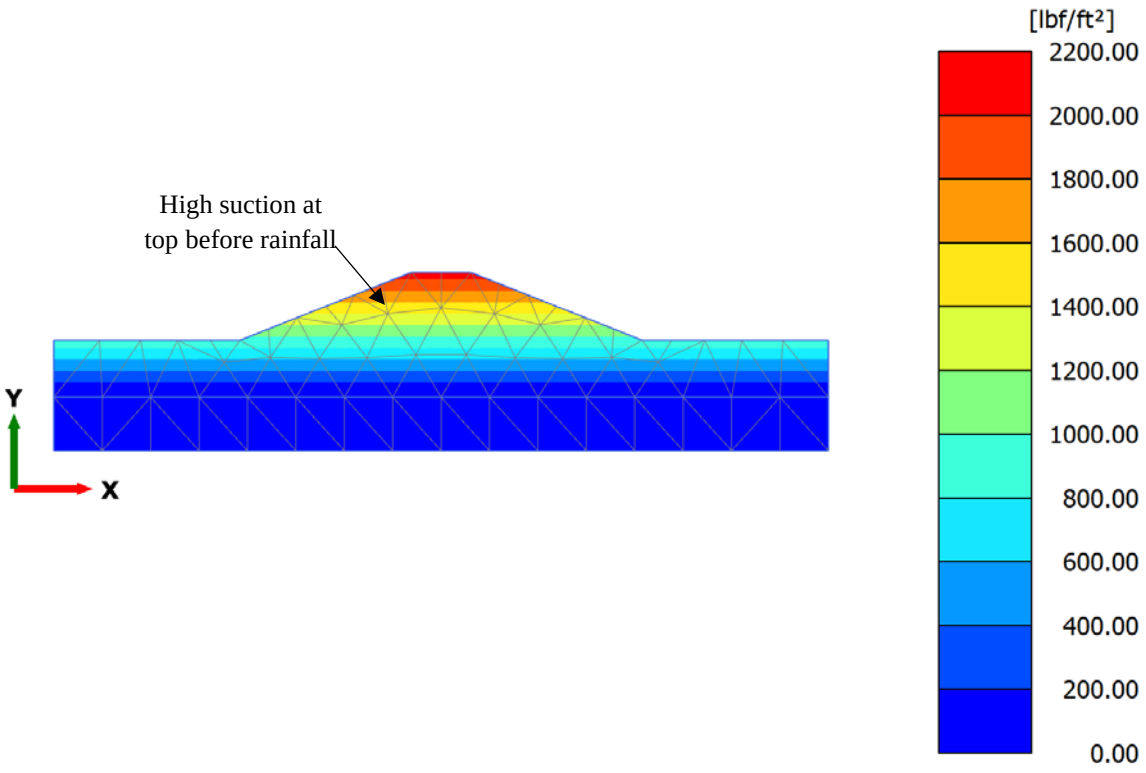

Figure 4.11 Levee suction dissipation prior to rainfall

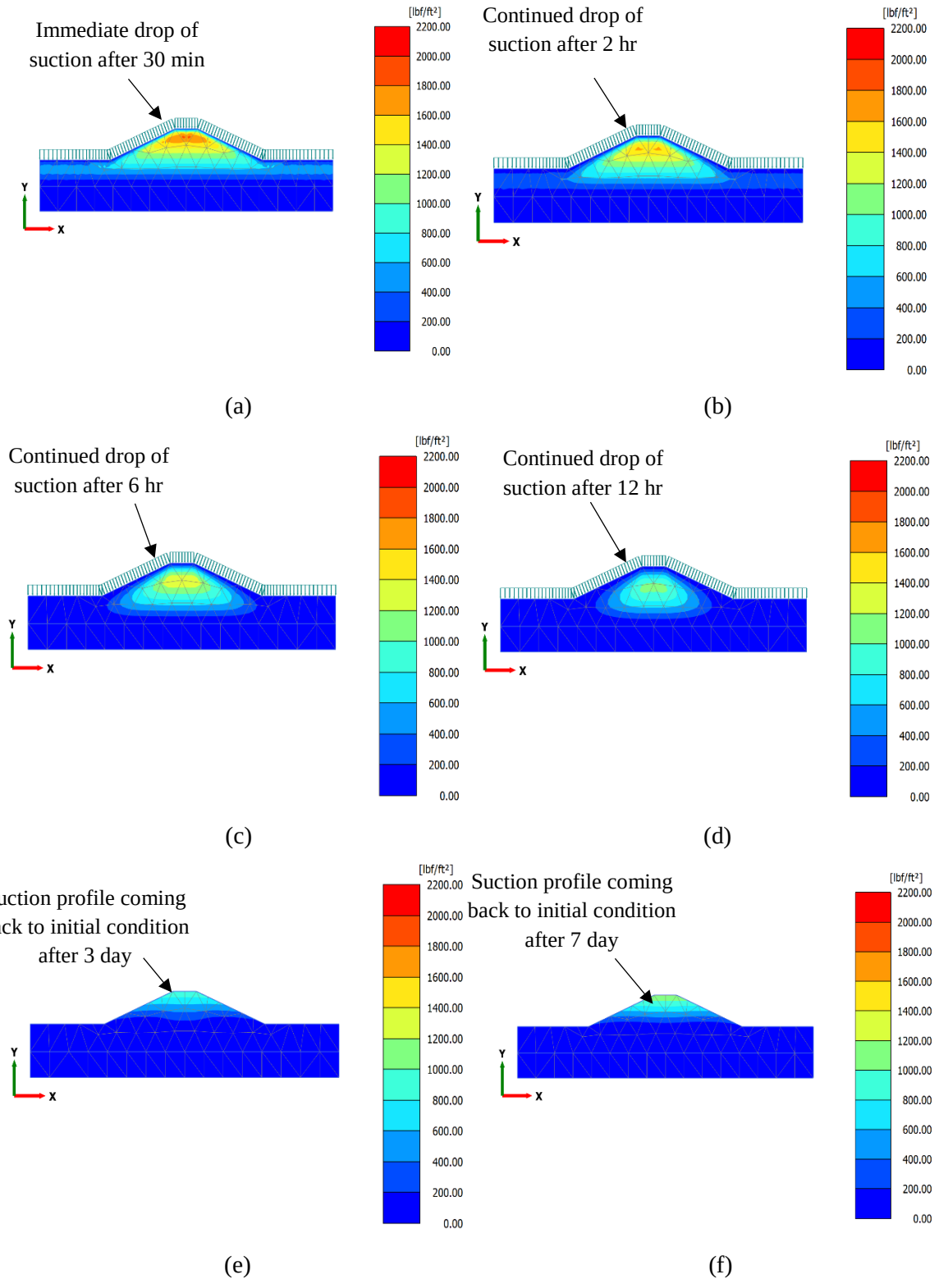

Figure 4.12 Suction variation of 1N wet-dry cycle for 35% initial moisture content at high intensity 2 hr. rainfall period (a) After 30 min (b) After 2 hr. (c) After 6 hr. (d) After 12 hr. (e) after 3 day (f) after 7 day

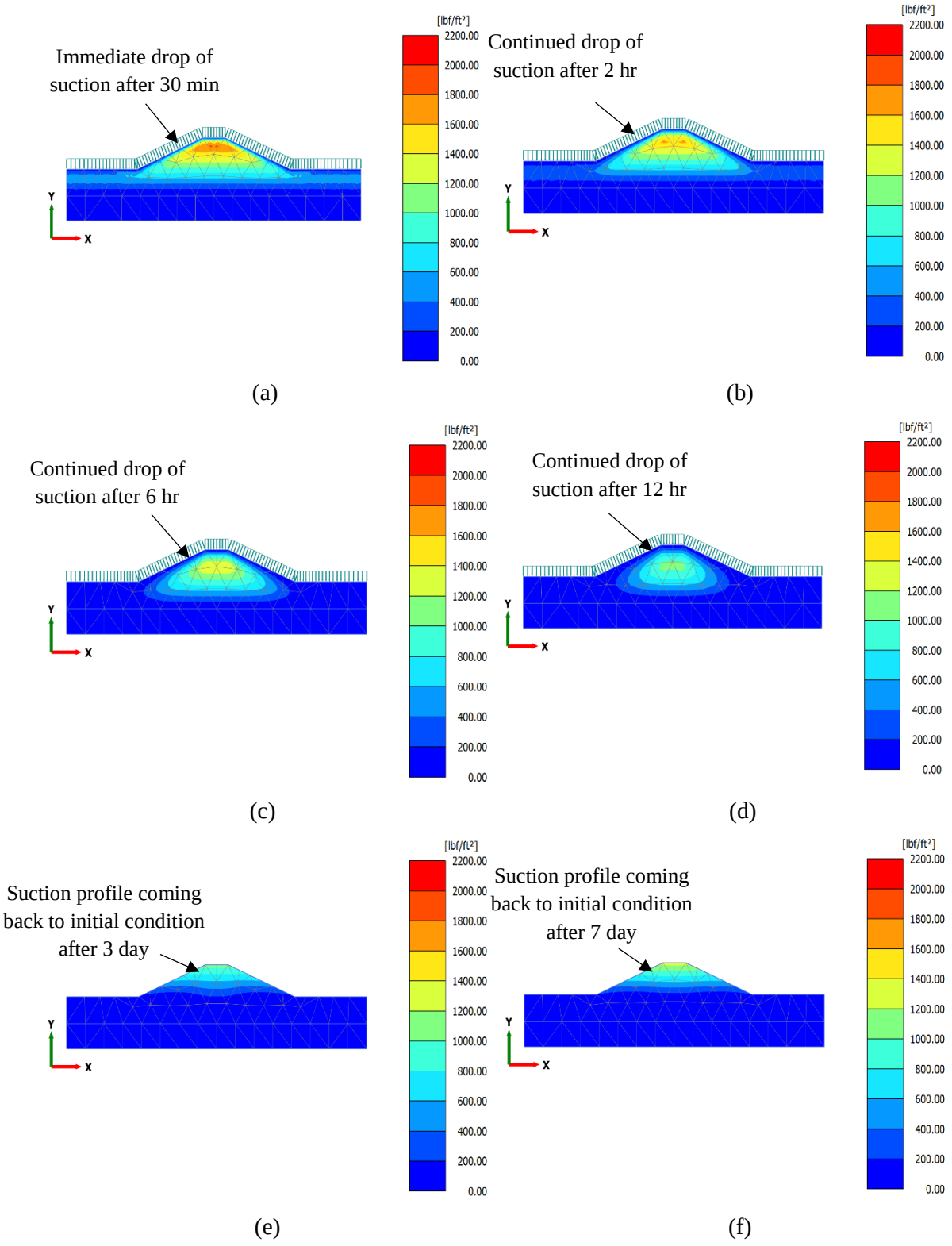

Figure 4.13 Suction variation of 1N wet-dry cycle for 35% initial moisture content at medium intensity 12 hr. rainfall period (a) After 30 min (b) After 2 hr. (c) After 6 hr. (d) After 12 hr. (e) after 3 day(f) after 7 day

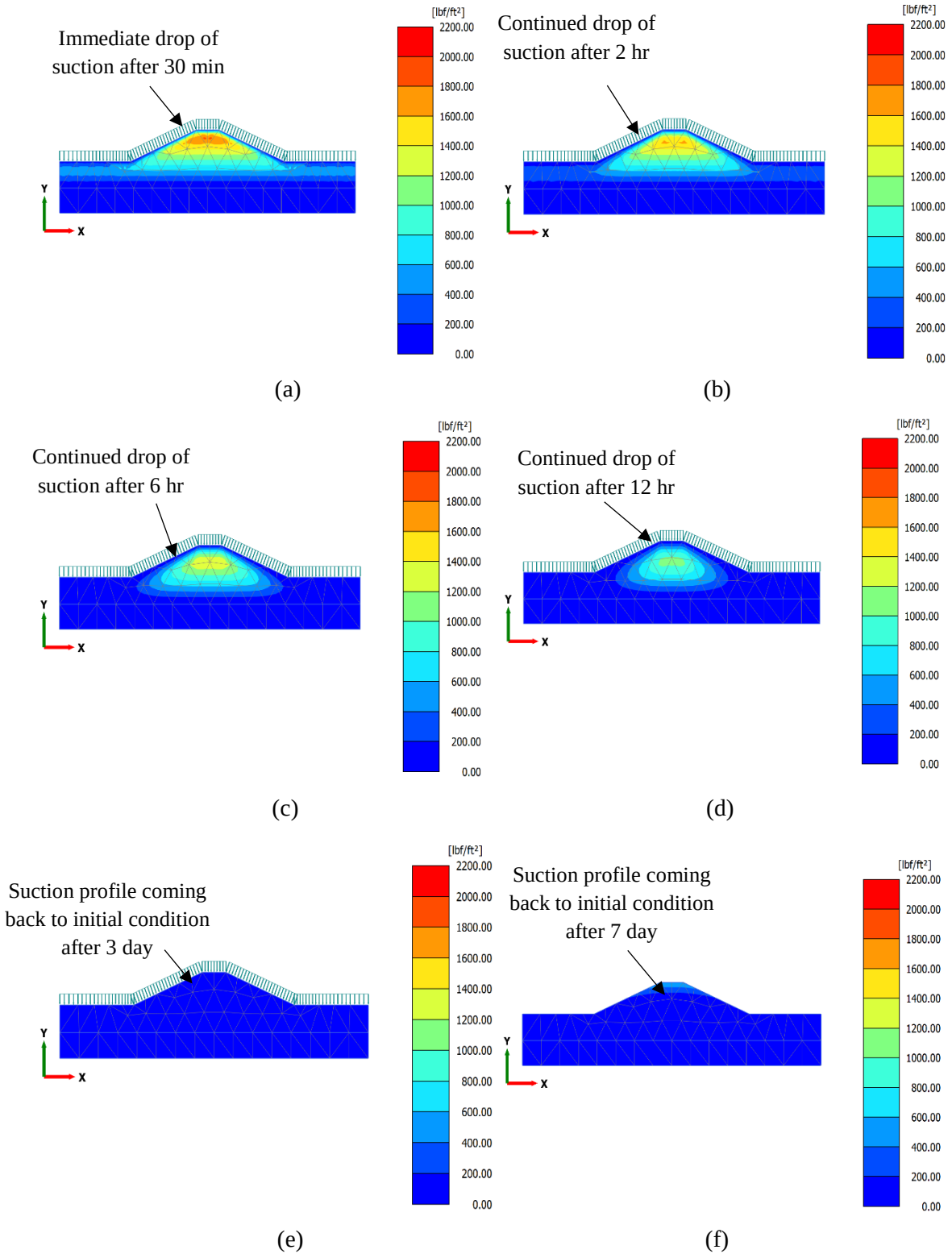

Figure 4.14 Suction variation of 1N wet-dry cycle for 35% initial moisture content at low-intensity 3-day rainfall period (a) After 30 min (b) After 2 hr. (c) After 6 hr. (d) After 12 hr. (e) after 3 day (f) after 7 day

The variation of suction at the top, crest, and middle of the levee at different rainfall intensities are presented in Figure 4.15. It should be noted that the suction variation presented in Figure 4.15 represents the conditions with the hydraulic conductivity with 1 wet-dry cycles with 35% initial moisture content. Based on this plot shows, noticeable change in the suction at the levee top, crest, and middle of the levee system are observed. Considering the effect of the high-intensity rainfall at different locations of the levee, as Figure 4.15 (a), the matric suction experienced a 45% drop after 7-day post rainfall at the levee top from its initial 2200 psf prior to rainfall. Also, the suction at the crest and middle of the levee experienced a similar profile having dropped by 72%. The three locations reached a minimum value after 24-hrs post rainfall before increasing gradually to 1200 psf and 600 psf respectively. A similar trend can be seen in Figure 4.15(b) for the medium intensity rainfall though the percentage suction drop after 7-day post rainfall infiltration where about 42%, 70%, and 70% at the levee top and crest and middle, respectively. Interestingly, for 3-day rainfall volume, a long zero matric suction was experienced up to 4 days before an increment was noticed. Figure 4.15(c) showed about 74%, 93% and 98% drop in suction at the levee top, middle and crest, respectively. More suction variations at the levee section with different hydraulic conductivity values with 1, 2 and 3 wet-dry cycles are highlighted in Appendix D.

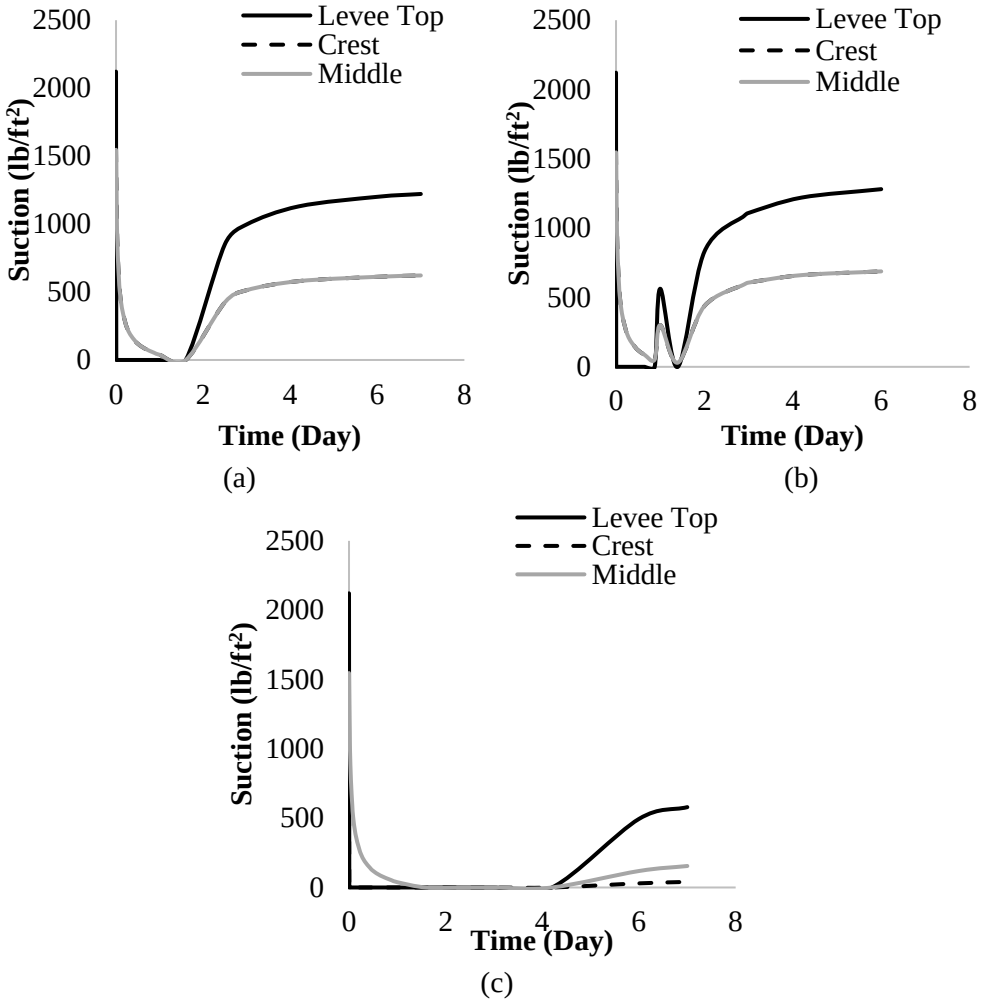

Figure 4.15 1N Suction Variation with 35% initial moisture content (a) High intensity rainfall (b) Medium intensity rainfall (c) Low intensity rainfall

Chapter 5: IMPACTS, BENEFITS OF IMPLEMENTATION & CONCLUSION

5.1 Relevance to the needs of Mississippi

The existence of Yazoo clay soil in Mississippi frequently causes distress in the highway pavement and failures in highway slopes, embankments, levees, which are critical components of the maritime waterway and multimodal transportation infrastructure. Each year, fixing pavement and slopes along highway embankment and levees require a significant maintenance budget. Through this study, understanding of the changes in the hydraulic conductivity in the Yazoo clay will improve the design practice to implement useful pavement subgrade and slope stabilization techniques, which will enhance the effective use of the maintenance budget.

5.2 Implementation of Results

Expansive soils cover more than 25% of the total area of the United States and are responsible for premature shallow slope failure of highway fill slopes, levee, dam, and embankments. According to Federal Highway Administration (FHWA), expansive soils are a very significant problem in many parts of the United States and are responsible for the application of premature maintenance and rehabilitation activities on many miles of roadway and maritime infrastructures each year. The understanding of the changes in the hydraulic conductivity in Yazoo clay and its effect on the saturation behavior indicated the development of the critical condition under sustained rainfall in the levee and highway embankment in Mississippi. This study data will help improve the design practice for Expansive Yazoo Clay, which will help to manage their maintenance budget better to restrict/repair pavement distress and slope failure.

5.3 Conclusions and Recommendations

The hydraulic conductivity of Yazoo clay varies over the different seasons and has higher vertical permeability during the dry season. With high vertical permeability, the rainwater can easily percolate in the pavement subgrade and highway embankments and levee slopes, which accelerates the failure. The current study investigates the change in unsaturated vertical and horizontal permeability and its effect on the maritime and multimodal infrastructures, especially on the pavement and slopes of highway embankment and levees. Based on the results of the hydraulic conductivity testing and the laboratory and numerical analysis on the highway slopes and levee embankment, the following conclusions are advanced:

i. Mini-disk infiltrometer and instantaneous profile method were used to determine the variation of hydraulic conductivity of Yazoo clay at different wet-dry cycles. The mini-disk infiltrometer works well to measure the permeability of Yazoo clay when there are no shrinkage cracks. An increment of the vertical permeability was observed with the increase of the wet-dry cycles. Data from the instrumentation in the instantaneous profile method was utilized to investigate the changes in the moisture content to determine hydraulic conductivity. The hydraulic conductivity of Yazoo clay is very low at a fully compacted phase (~10^{-6} cm/s). However, with an increment in the wet-dry cycles, the hydraulic conductivity of Yazoo clay increases (~10^{-4} cm/s) after the sample is exposed to 3 numbers of wet-dry cycles. Moreover, the largest increases were seen during periods of the 1N wet-dry cycle.
ii. The flow analysis was conducted on the highway and levee embankment, considering the changes in hydraulic conductivity with the presence of rainfall volume from 30 mins to 3 days. It is observed that the soil gets saturated and suction dropped both at the highway and levee slopes with the presence of the rainfall, as the hydraulic conductivity increases with the number of wet-dry cycles. No significant

changes underneath the centerline of pavement are observed. However, near the shoulder of the pavement and at the crest of highway slopes, significant moisture variation is observed. On the other hand, in the case of levee slopes, the level of saturation due to the presence of rainfall is prominent, compared to the saturation behavior observed in the highway pavement and slopes. Considering the effect of the high-intensity rainfall at different locations of the levee, the matric suction experienced a 45% drop after 7-day post rainfall at the levee top from its initial phase. Also, the suction at the crest and middle of the levee slope experienced a similar trend and having dropped by 72%. Due to the moisture intrusion and drop in the matric suction, the slopes in the highway pavement and levee experience significant distress.

iii. Even though the changes in the hydraulic conductivity of Yazoo clay defines the infiltration behavior, which mostly controls the slope failure and pavement distress, the consideration of the climatic loads and associated hydraulic conductivity changes are ignored in the design phase of the highway embankment and levees. By inclusion of the climatic variation, and evaluating the performance, the design life and resilience of the structures can be significantly increased. It is highly recommended to include the variation of the hydraulic conductivity for the design of Maritime and Multimodal Transportation Infrastructures on Yazoo clay. Moreover, a climate-adaptive design is recommended for the repair design of the highway and levee slopes that experience failure due to the weathering action of highly plastic Yazoo clay.

REFERENCES

- Abbaszadeh, M. (2011). “The effect of cracks on unsaturated flow and volume change properties of expansive clays and impacts on foundation performance.” Ph.D. dissertation, Arizona State Univ., Tempe, AZ.
- ASTM (1994). “Standard Test Method for Liquid Limit, Plastic Limit, and Plasticity Index of Soils.” ASTM Designation: D4318-93, *American Society for Testing and Materials*, West Conshohocken, Pa.
- ASTM (2005). “Designation D 4318-05, Standard Test Methods for Liquid Limit, Plastic Limit, and Plasticity Index of Soils.” *American Society for Testing and Materials*, Philadelphia.
- Basma, A. A. (1993). “Prediction of expansion degree for natural compacted clays.” ASTM Geotech. Test. J., 16(4), 542–549.
- Basma, A.A., Al-Homoud, A.S., Malkawi, A.I.H., and AlBashabsheh, M.A. (1996). “Swelling shrinkage behavior of natural expansive clays.” *Applied Clay Science*, vol.11, no.2–4, pp.211–227.
- Brady, N.C. and R.R. Weil. (1999). "The Nature and Properties of Soils." Prentice-Hall, Upper Saddle River, New Jersey.
- Bulut, R., Lytton, R.L, Wray, W.K. (2001). “Soil Suction Measurements by Filter paper.” *Expansive Clay Soils and Vegetative Influence on Shallow Foundations*, 243-261.
- Carsel, R. F., and R. S. Parrish. (1988). "Developing joint probability distributions of soil water retention characteristics" Water Resource Res. 24: 755-769.
- Chen, F. H. (1988). “Foundations on expansive soils.” *Elsevier Science Publishers*, B. V.
- De Freitas, M.H., and Mannion, W.G. (2007). “A biostratigraphy for the London Clay in London.” *Geotechnique*, 57(1), pp. 91 – 99.
- Douglas, S. C., and Dunlap, G. T. (2000). “Light commercial construction on Yazoo clay.” *Proc., 2nd Forensic Congress, ASCE*, Reston, Va., 607–616. Edition. PTI Manual, Phoenix, Arizona.
- Fredlund, D.G., and Rahardjo, H. (1993). “Soil mechanics for unsaturated soils.” John Wiley and Sons, Inc., New York of soils.
- Fredlund, D.G. (2006). “Unsaturated soil mechanics in engineering practice.” Journal of geotechnical and geoenvironmental engineering 132 (3), 286-321.
- Genuchten, V. (1980). “A closed-formed equation for predicting the hydraulic conductivity of unsaturated soils.” *Soil Sci*.
- Griffiths, D. V., Lane, P. A. (1999). “Slope stability analysis by finite elements.’’ *Geo-technique*, 49 (3).
- Hamilton, J. M., Daniel, D. E., and Olson, R. E. (1981). “Measurement of Hydraulic Conductivity of Partially Saturated Soils,” Permeability and Groundwater Contaminant Transport, ASTM STP 746 T. F. Zimmie and C. O. Riggs, Eds., ASTM, pp. 182196.

- Hight, D.W., Gasparre, A., Nishimura, S., Minh, N.A., Jardine, R.J., and Coop, M.R. (2007). "Characteristics of the London Clay from Terminal 5 site at Heathrow Airport." *Geotechnique* 57(1), pp. 3 – 18.

- Hossain, M. S., Hossain, J., Lozano, N., Khan, M.S., Kibria, G. (2012). "Investigation of geohazard potential of highway embankment slopes on expansive clay by using geophysical method." *Geocongress*, American Society of Civil Engineers, Oakland, CA.

- Hossain, J., Hossain, M.S., and Hoyos, L. R. (2013). "Effect of Rainfall on Stability of Unsaturated Earth Slopes Constructed on Expansive Clay." *Geo-Congress, 2013, ASCE*, Vol. 1, pp. 417-425.

- Hutchinson, J. N. (1969). "A Reconsideration of the Coastal Landslides at Folkestone Warren, Kent." *Géotechnique*, volume 19, Issue 1, pp. 6-38.

- Huvaj-Sarihan, N. (2009)." Movement of Reactivated Landslides." thesis, presented to University of Illinois at Urbana-Champaign, in partial fulfillment of the requirements for the degree of Doctor of Philosophy.

- James, P. M. (1970). "Time effects and progressive failure in clay slopes." Ph.D. thesis, Univ. of London, London.

- Johnson, L. D. (1973). "Properties of expansive clay soils, Jackson field test section study." *U.S. Army Engineer Waterways Experiment Station*, Vicksburg, Mississippi, Report 1, Misc. Paper S-73-28.

- Jones, L.D., and Terrington, R. (2011). "Modelling volume change potential in the London Clay." *Quarterly Journal of Engineering Geology and Hydrogeology*, Vol 44, pp. 109 – 122.

- Khan, M. S., and Hossain, M. S. (2015). "Effect of Shrinkage and Swelling Behavior of High Plastic Clay on the Performance of a Highway Slope Reinforced with Recycled Plastic Pin." *Proc. 94th Annual Meeting of Transportation Research Board*, Washington, D.C.

- Khan, M. S., Hossain, S., Ahmed, A., & Faysal, M. (2017). "Investigation of shallow slope failure on expansive clay in Texas." *Engineering Geology*, 219, 118-129.

- Khan, M. S., Ivoke, J., Nobahar, M., and Kibria, G. (2018). "Effect of Wet-Dry Cycles on the Void Ratio of Expansive Yazoo Clay Soil." *Geo-Congress, ASCE*, Pages 1-10 (Under Review).

- Kodikara, J., Barbour, S. L., and Fredlund, D. G. (1999). "Changes in clay structure and behavior due to wetting and drying." Proc., 8th Australia New Zealand Conf. on Geomechanics: Consolidating Knowledge, Australian Geomechanics Society, St. Ives, NSW, Australia, 179–186.
- Krisdani, H., Harianto, R., and Leong, E. C. (2008). "Effects of different drying rates on shrinkage characteristics of a residual soil and soil mixtures." Eng. Geol., 102(1–2), 31–37.
- Sadik Khan, John Ivoke, and Masoud Nobahar (2019). "Coupled Effect of Wet-Dry Cycles and Rainfall on Highway slope made of Yazoo Clay." Geosciences, Open Access Journal by MDPI, ISSN 2076-3263, Manuscript ID 504447, April 28th, 9(8), 341. https://www.mdpi.com/2076-3263/9/8/341

- Kovacevic, N., Hight, D.W., and Potts, D.M. (2007). "Predicting the stand-up time of temporary London Clay slopes at Terminal 5, Heathrow Airport." *Geotechnique*, 57(1), pp. 63 – 74.
- Lee Jr, L. T. (2012). "State Study 151 and 236: Yazoo Clay Investigation." MDOT State Study 236, US Army Corps of Engineers.
- Martin, R. V. (2007). "Sample, describe, and map Yazoo Clay." *Unpublished Report of Mississippi Dept. of Transportation*, MDoT Study 151, Jackson, MS.
- Mesri, G., and Shahien, M. (2003). "Residual shear strength mobilized in first-time slope."
- Mitchell, J. K. (1993). Fundamentals of soil behavior. 2nd. Edition. John Wiley and Sons, Inc., New York.
- Morgenstern, N. R. (1977). "Slopes and excavations." *9th Int. Conf. Soil Mech. and Found. Engineering*, 12(State of the Art), 567–581.
- National Oceanic and Atmospheric Administration Daily Climate Report. (2014), <**http://w2.weather.gov/climate/index.php?wfo=BGM> (**Jun. 5, 2018)
- Neaves, C. (2005). "Montmorillonite / Bentonite clay."
- Nelson, J. D., and Miller, D. J. (1992). Expansive soils: Problem and practice in foundation and pavement engineering. John Wiley and Sons, Inc., New York.
- Nobahar M., Khan M.S., Ivoke J., Amini F. (2019). "Impact of Rainfall Variation on Slope made of Expansive Yazoo Clay Soil in Mississippi." Transportation Infrastructure Geotechnology, Springer US, Online ISSN 2196-7210, July 27th. https://link.springer.com/article/10.1007/s40515-019-00083-w
- Palladino, D. J., and Peck, R. B. (1972). "Slope failures in an overconsolidated clay." *Géotechnique*, 22, 563–595.
- Rahimi, A.; Rahardjo, H.; Leong, E.-C. (2010). "Effect of antecedent rainfall patterns on rainfall-induced slope failure." *J. Geotech. Geoenviron. Eng.*, 137, 483–491.
- Redus, J. F. (1962). "Experiences with expansive clay in Jackson, Miss.," Moisture, Density, Swelling and Swell Pressure Relationships." *Highway Research Board Bulletin* No. 313, pp 40 - 46.
- Rogers, L.E., and Wright, S. G. (1986). "The effect of Wetting and Drying on the Long-Term Shear Strength Parameters for Compacted Beaumont Clay." *Research Rep. 436-2F, Center for Transportation Research*, the University of Texas at Austin, 1986.
- Rose, C.W. (1966). "Agricultural Physics." Permagon Pres. Ltd.
- Skempton, A. W. (1964). "Long-term stability of clay slopes." *Géotechnique*, 14(2), 77 –102.

- Skempton, A. W., and Petley, D. J. (1967). "The strength along structural discontinuities in stiff clays." *Proc., Geotechnical Conf. on Shear Strength of Natural Soils and Rocks, Vol. 2, Norwegian Geotechnical Institute*, Oslo, Norway,29–46.

- Skempton, A. W. (1970). "First-time slides in over-consolidated clays." *Géotechnique*, 20(3), 320–324.

- Skempton, A.W. (1985). "Residual strength of clays in landslides, folded strata, and the laboratory." *Géotechnique*, 35(1), 3-18.

- Subba Rao, K. S., and Satyadas, G. C. (1987). "Swelling potential with cycles of swelling and partial shrinkage." Proc., 6th Int. Conf. on Expansive Soils, New Delhi, India, 137–142.
- Taylor, A.C. (2005). "Mineralogy and engineering properties of the Yazoo clay formation." Jackson Group, master's Thesis, Mississippi State University.

- Terzaghi, K., Peck, R. B., and Mesri, G. (1996). Soil Mechanics in Engineering Practice, 3rd Ed., Wiley, New York, 549.

- Tripathy, S., Subba K. S., Rao, and Fredlund, D. G. (2002). "Water content-void ratio swell-shrink paths of compacted expansive soils." *Can. Geotech. Jour*., vol. 39, pp. 938-959.

- Yalcin, A. (2007). "The Effects of Clay on Landslides: A Case Study." *Applied Clay Science*, Number 77-85.

- Zhang, R. (1997). "Determination of soil sorptivity and hydraulic conductivity from the disk infiltrometer." Soil Sci. Soc. Am. J. 61:1024-1030.

APPENDIX A: FIGURES OF SUCTION VARIATION

1N wet-dry cycle

0% Initial Moisture Content

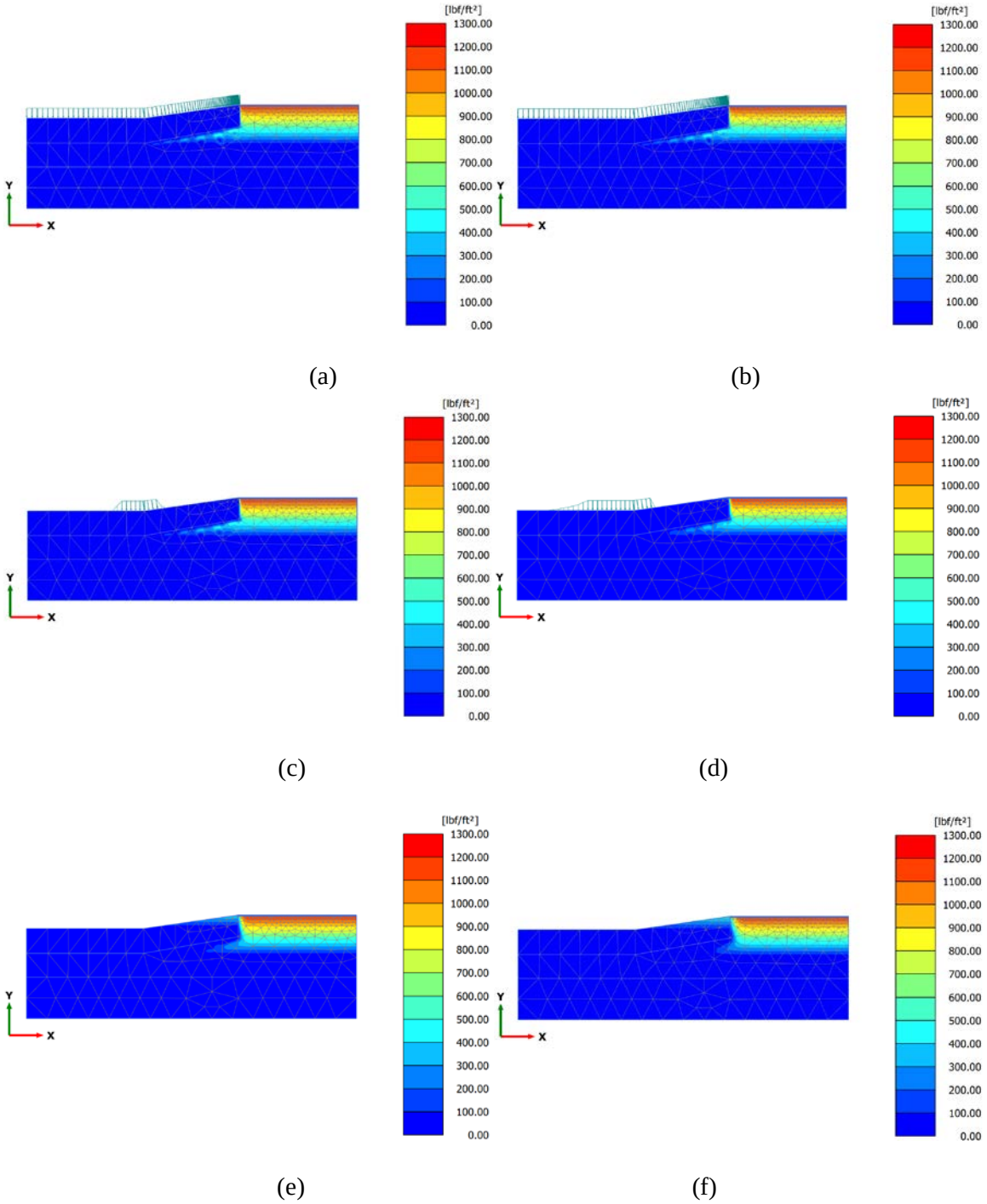

Figure A1 Suction variation of 1N wet-dry cycle for 0% initial moisture content at low intensity 2 hrs rainfall period (a) After 30 mins (b) After 2 hrs (c) After 6 hrs (c) After 12 hrs (d) after 3 days (e) after 7 days

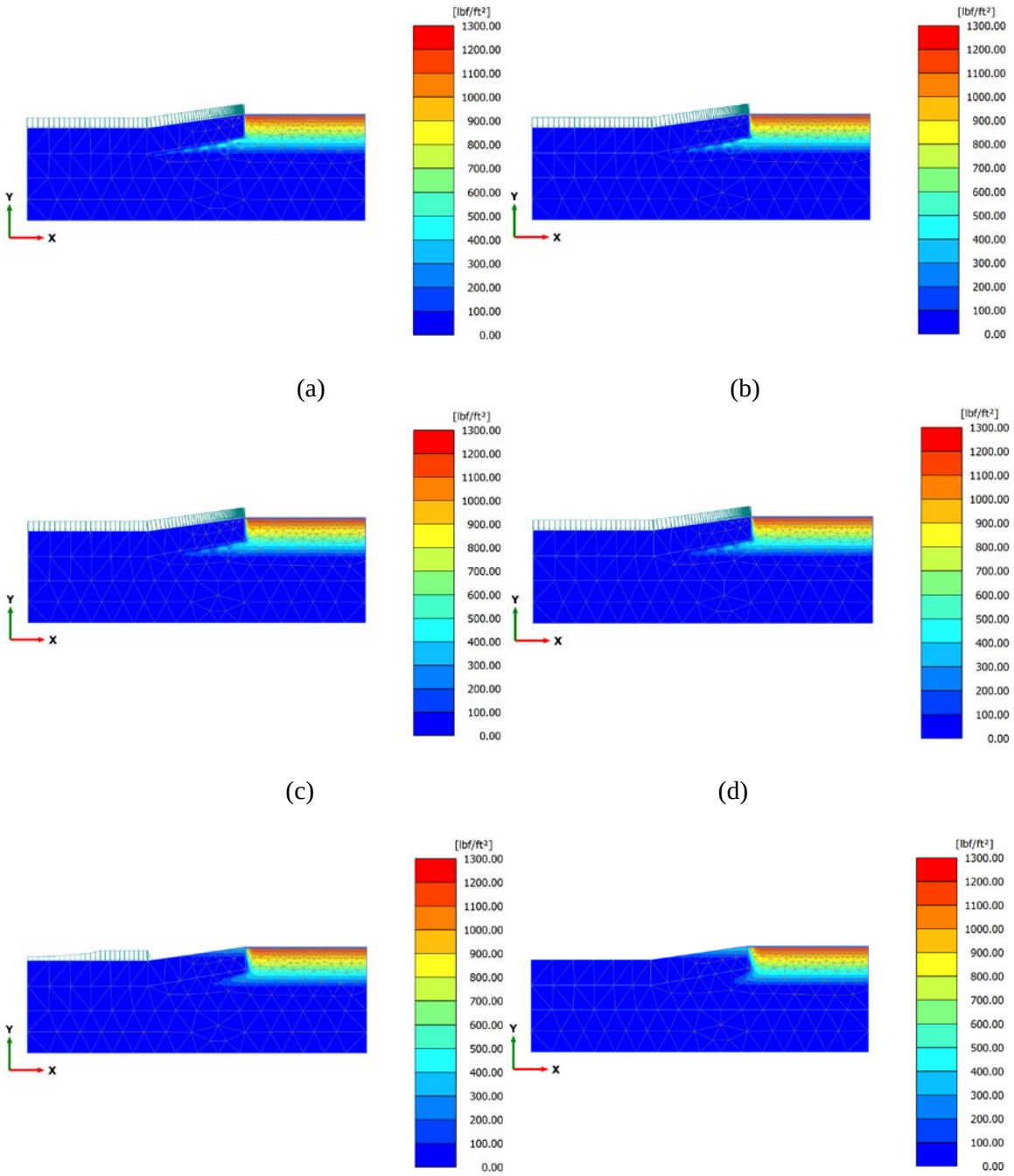

Figure A2 Suction variation of 1N wet-dry cycle for 0% initial moisture content at medium intensity 12 hrs rainfall period (a) After 30 mins (b) After 2 hrs (c) After 6 hrs (d) After 12 hrs (e) after 3 days (f) after 7 days

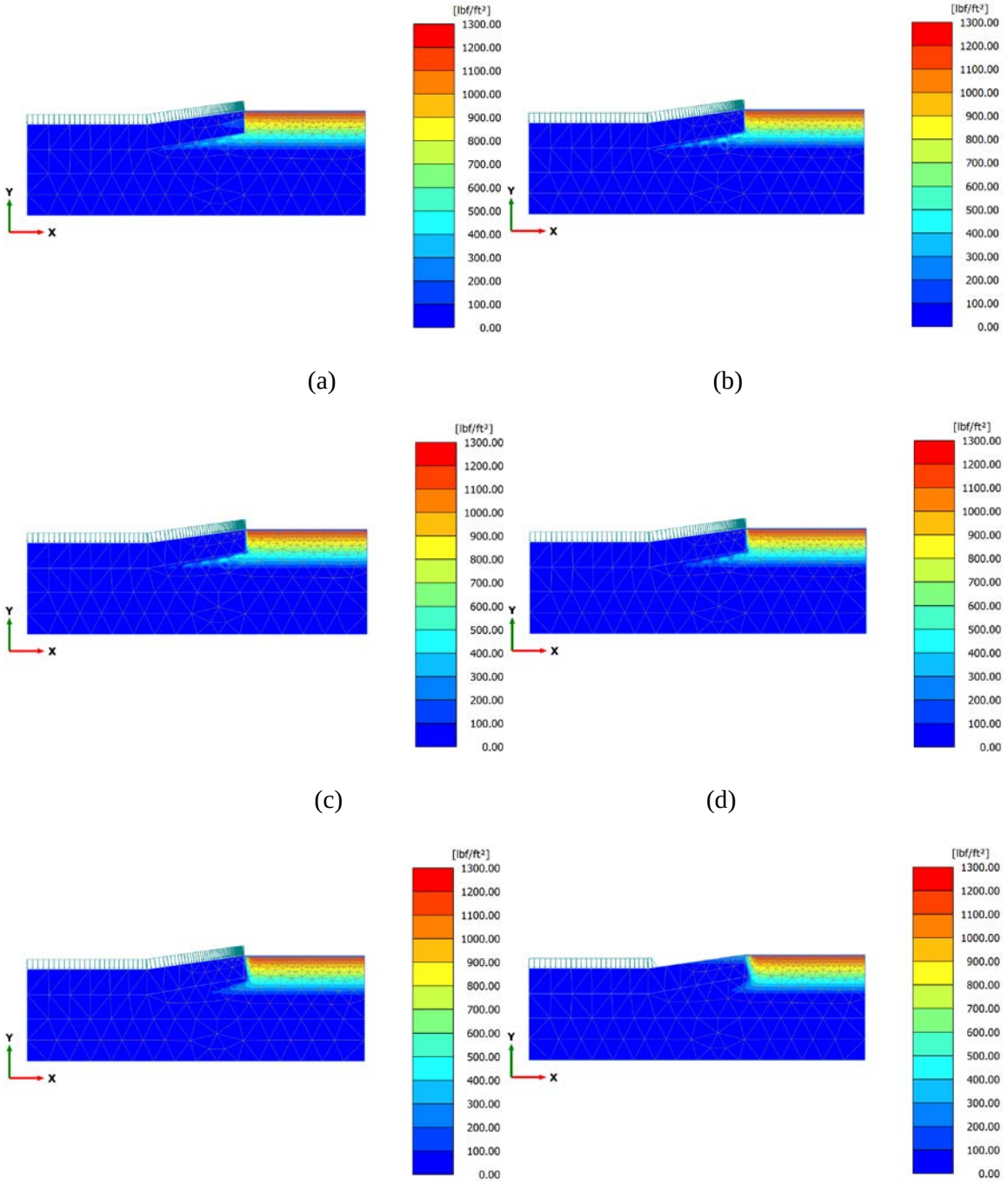

Figure A3 Suction variation of 1N wet-dry cycle for 0% initial moisture content at high intensity 3-day rainfall period (a) After 30 mins (b) After 2 hrs (c) After 6 hrs (d) After 12 hrs (e) after 3 days (f) after 7 days

15% Initial Moisture Content

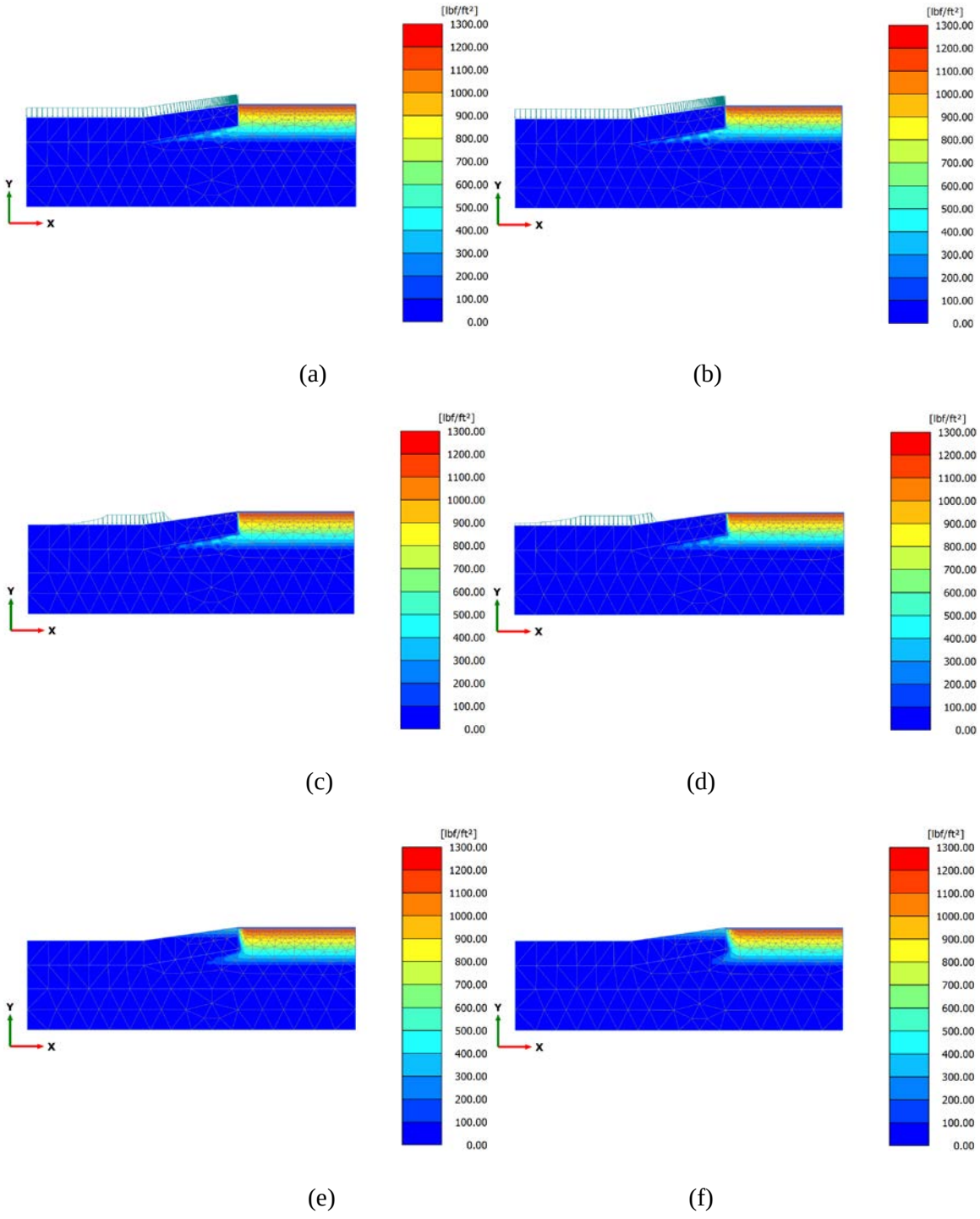

Figure A4 Suction variation of 1N wet-dry cycle for 15% initial moisture content at high intensity 2 hrs rainfall period (a) After 30 mins (b) After 2 hrs (c) After 6 hrs (d) After 12 hrs (e) after 3 days (f) after 7 days

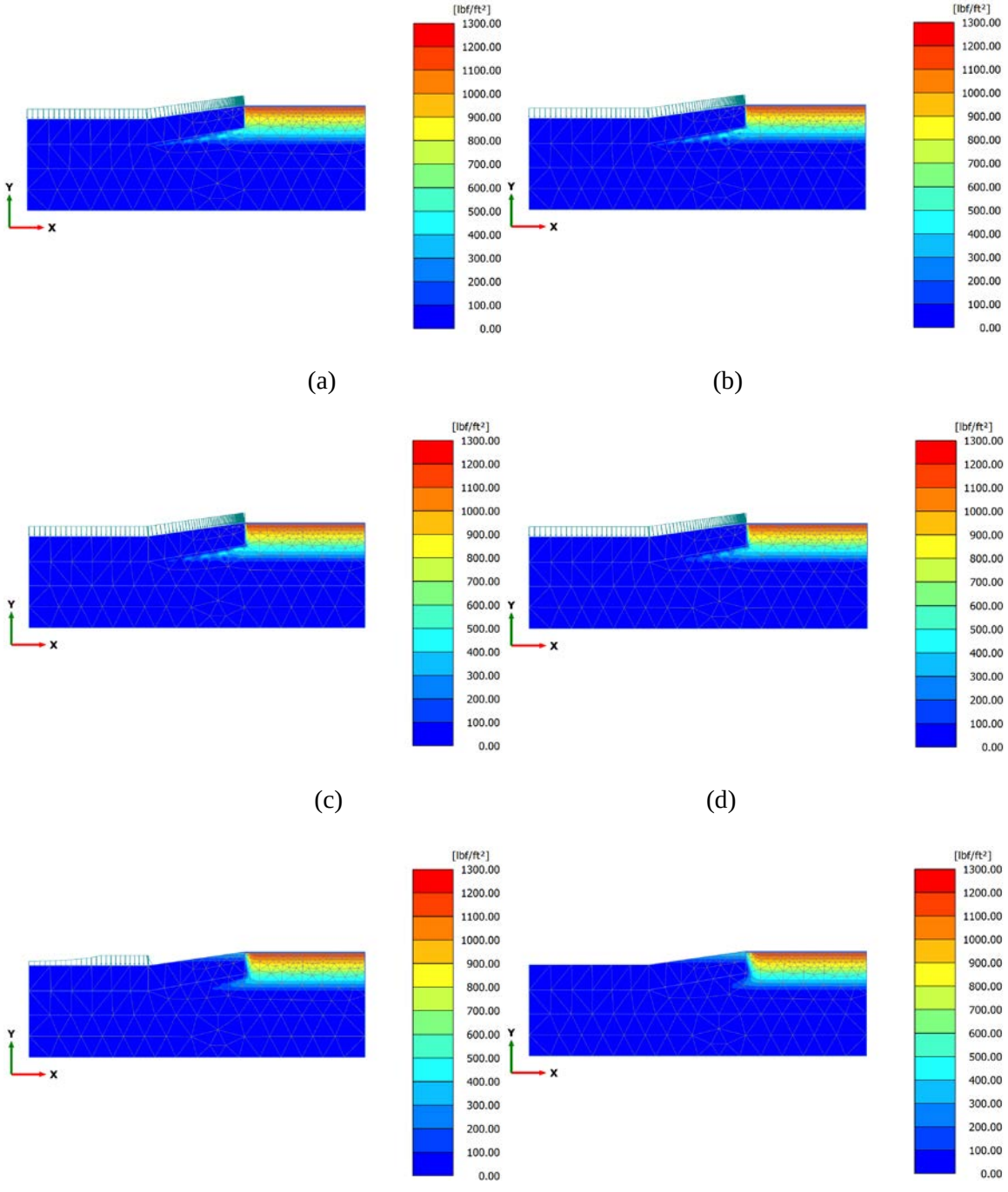

Figure A5 Suction variation of 1N wet-dry cycle for 15% initial moisture content at high intensity 12 hrs rainfall period (a) After 30 mins (b) After 2 hrs (c) After 6 hrs (d) After 12 hrs (e) after 3 days (f) after 7 days

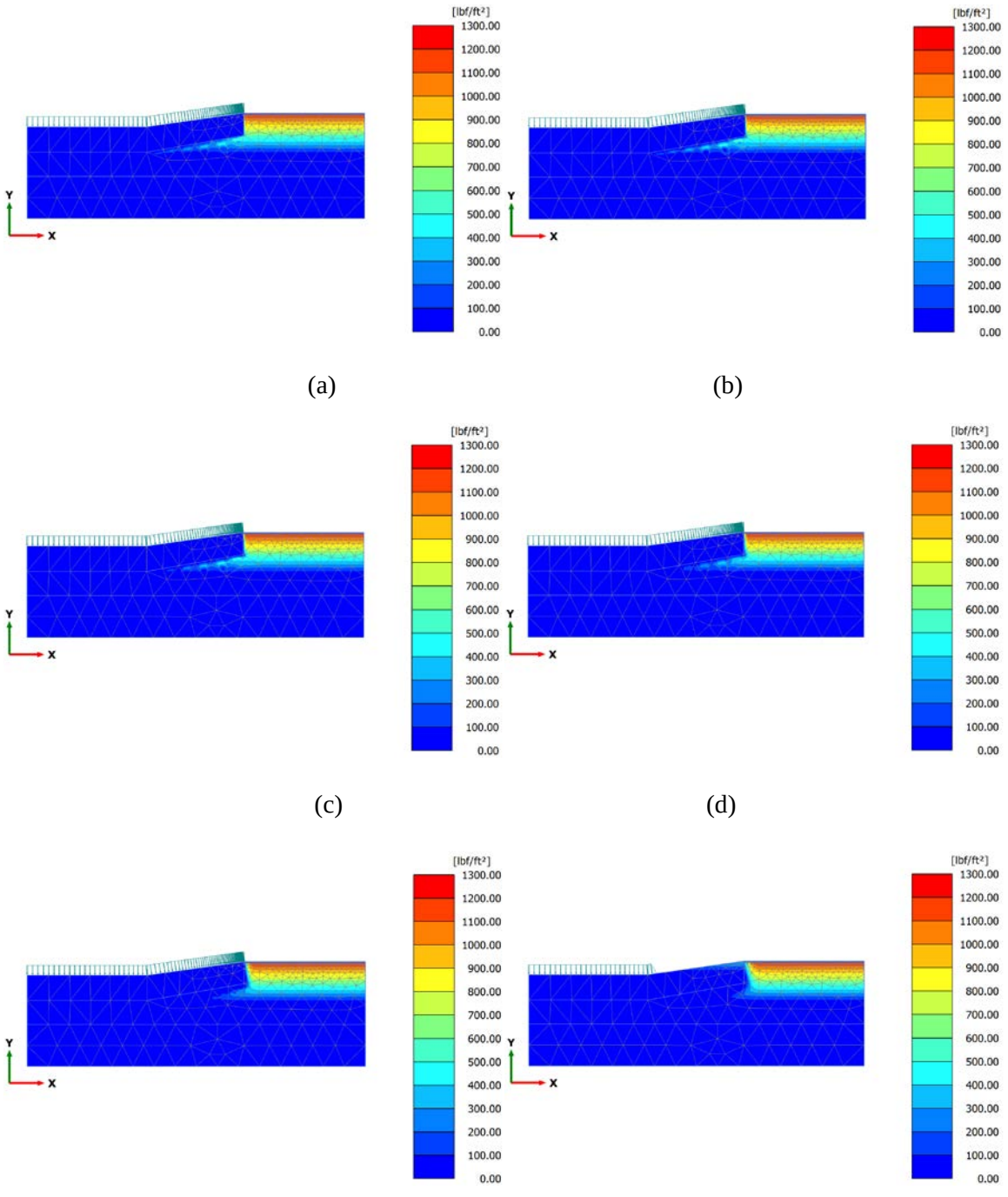

Figure A6 Suction variation of 1N wet-dry cycle for 15% initial moisture content at high intensity 3-day rainfall period (a) After 30 mins (b) After 2 hrs (c) After 6 hrs (d) After 12 hrs (e) after 3 days (f) after 7 days

25% Initial Moisture Content

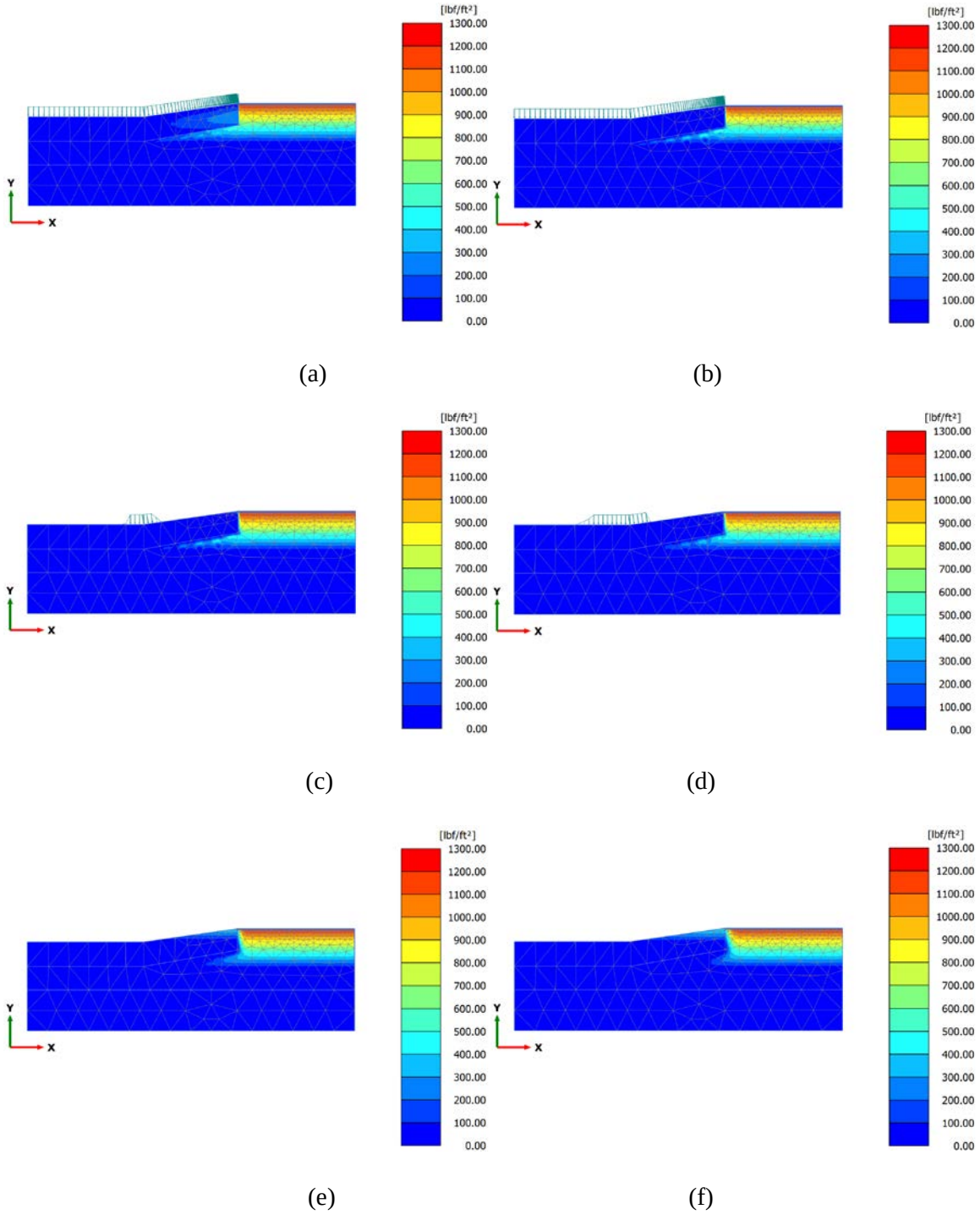

Figure A7 Suction variation of 1N wet-dry cycle for 25% initial moisture content at high intensity 2 hrs rainfall period (a) After 30 mins (b) After 2 hrs (c) After 6 hrs (d) After 12 hrs (e) after 3 days (f) after 7 days

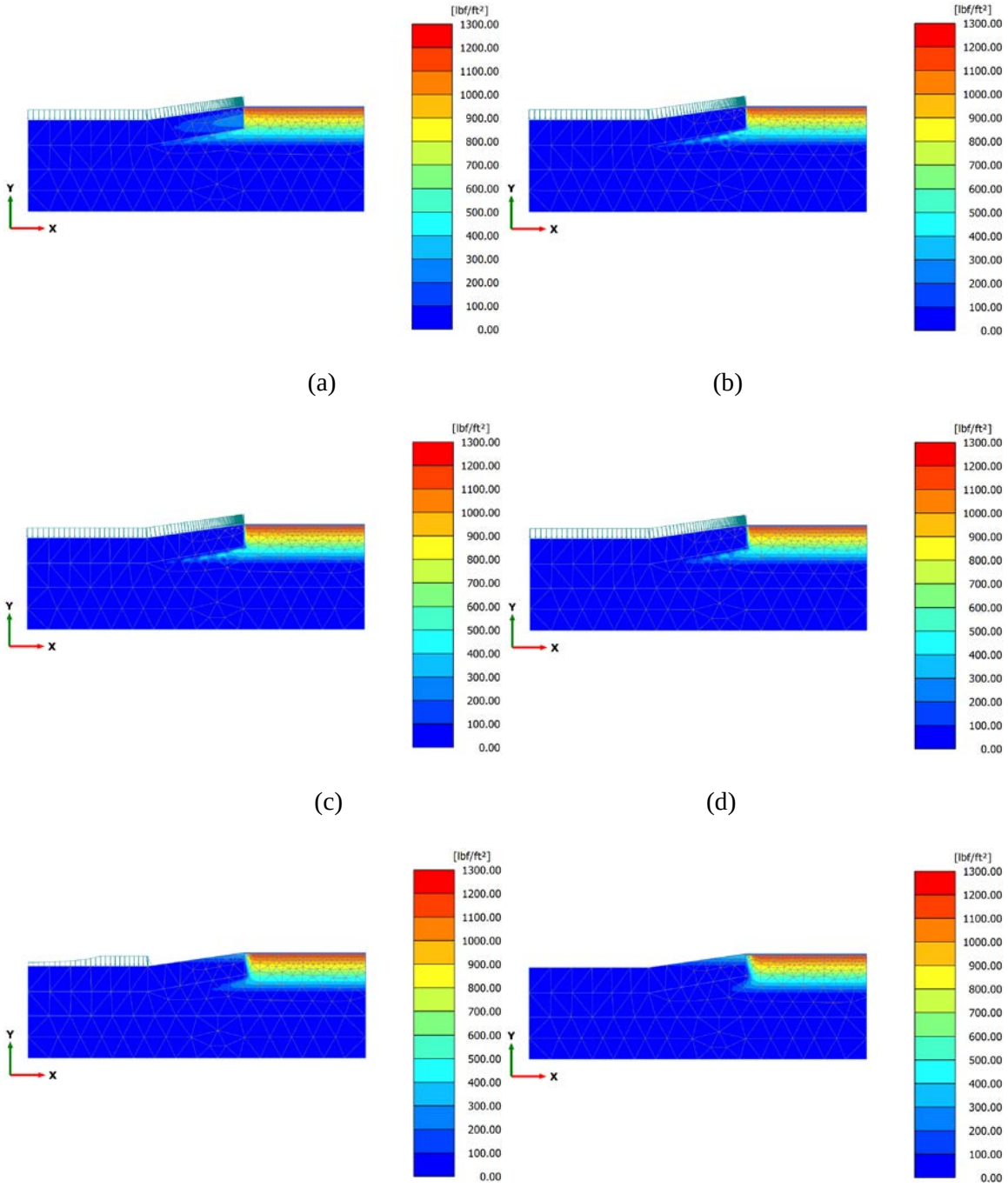

Figure A8 Suction variation of 1N wet-dry cycle for 25% initial moisture content at high intensity 12 hrs rainfall period (a) After 30 mins (b) After 2 hrs (c) After 6 hrs (d) After 12 hrs (e) after 3 days (f) after 7 days

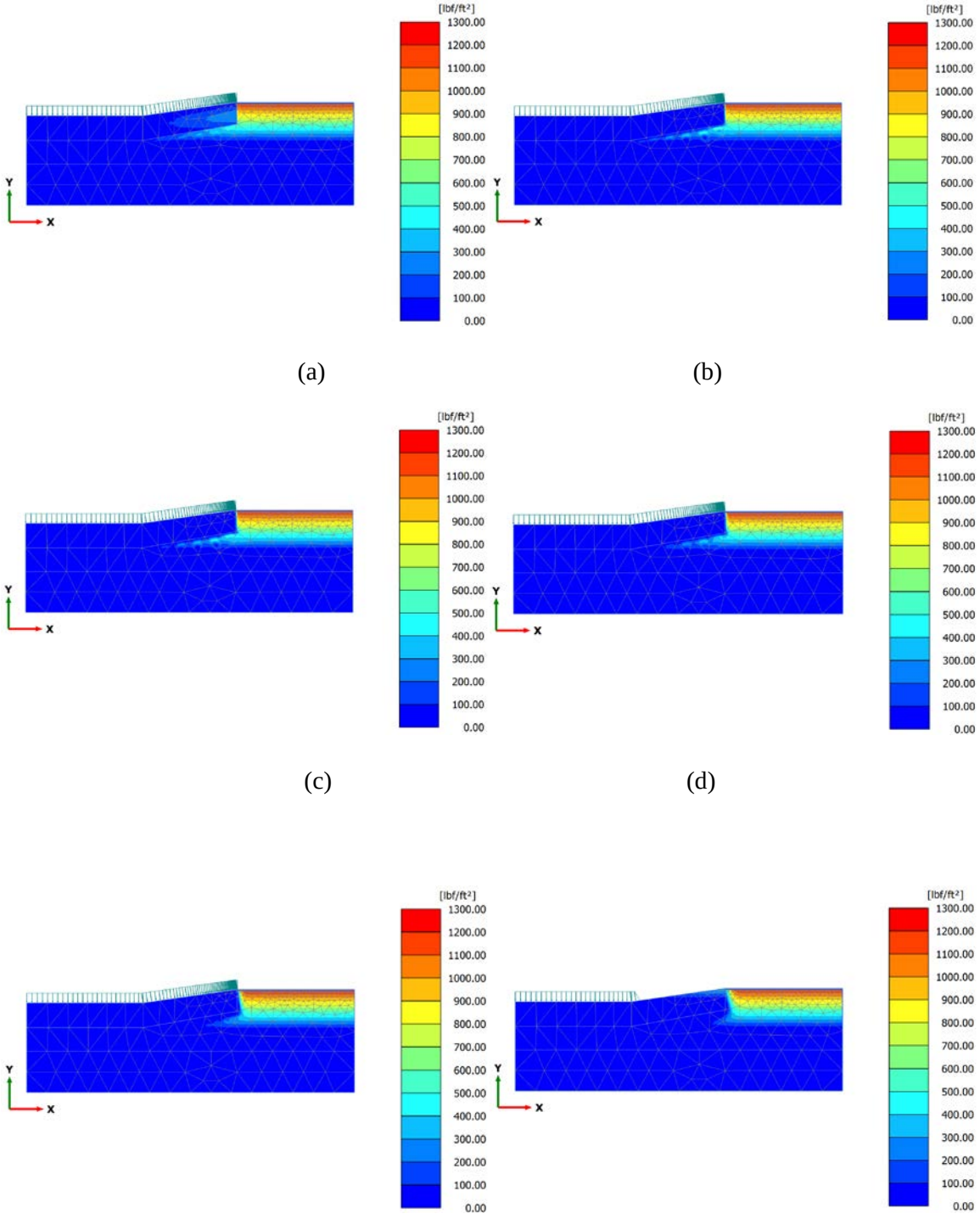

Figure A9 Suction variation of 1N wet-dry cycle for 25% initial moisture content at high intensity 3-days rainfall period (a) After 30 mins (b) After 2 hrs (c) After 6 hrs (d) After 12 hrs € after 3 days (f) after 7 days

2N wet-dry cycle

0% Initial Moisture Content

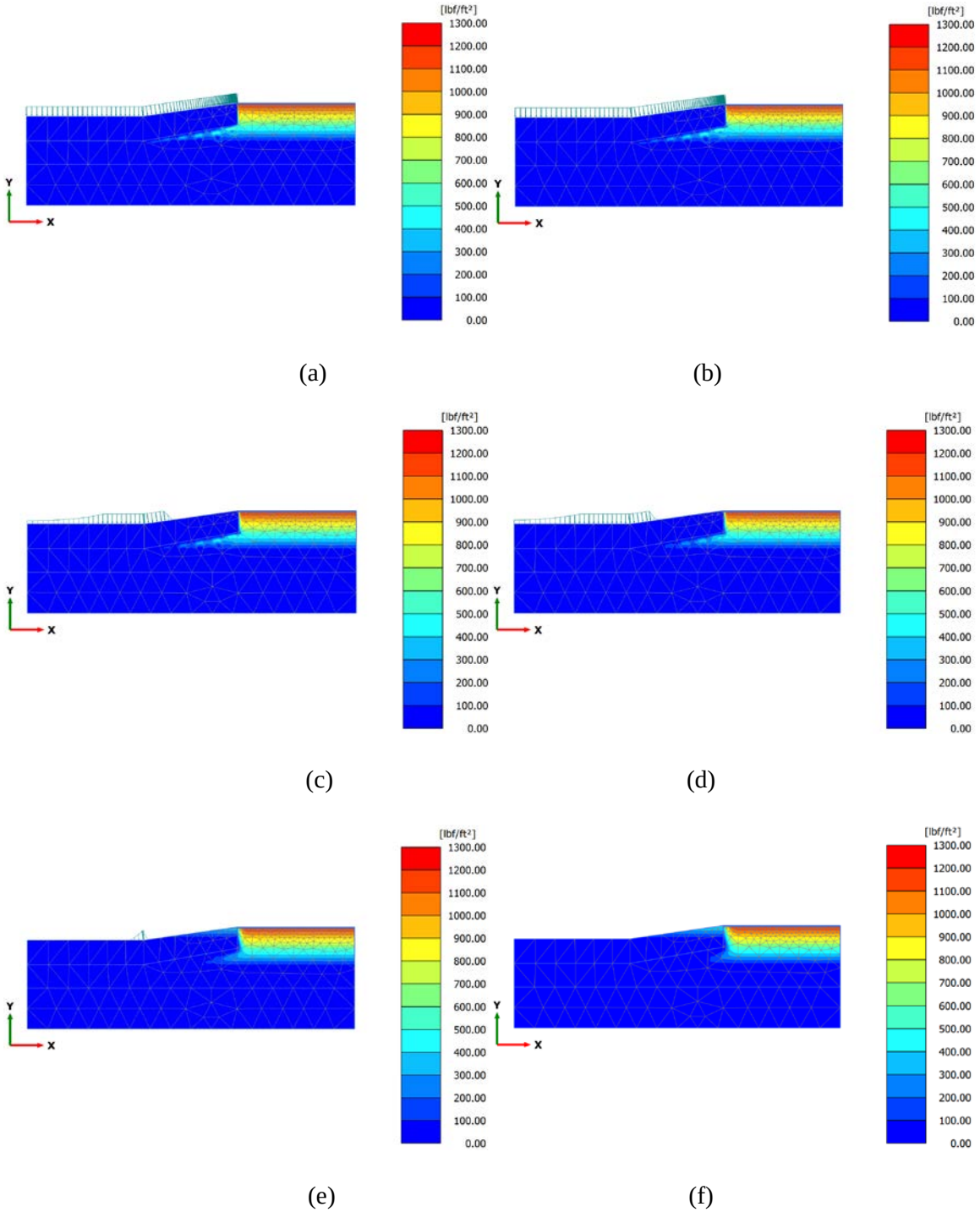

Figure A10 Suction variation of 2N wet-dry cycle for 0% initial moisture content at high intensity 2 hrs rainfall period (a) After 30 mins (b) After 2 hrs (c) After 6 hrs (d) After 12 hrs (e) after 3 days (f) after 7 days

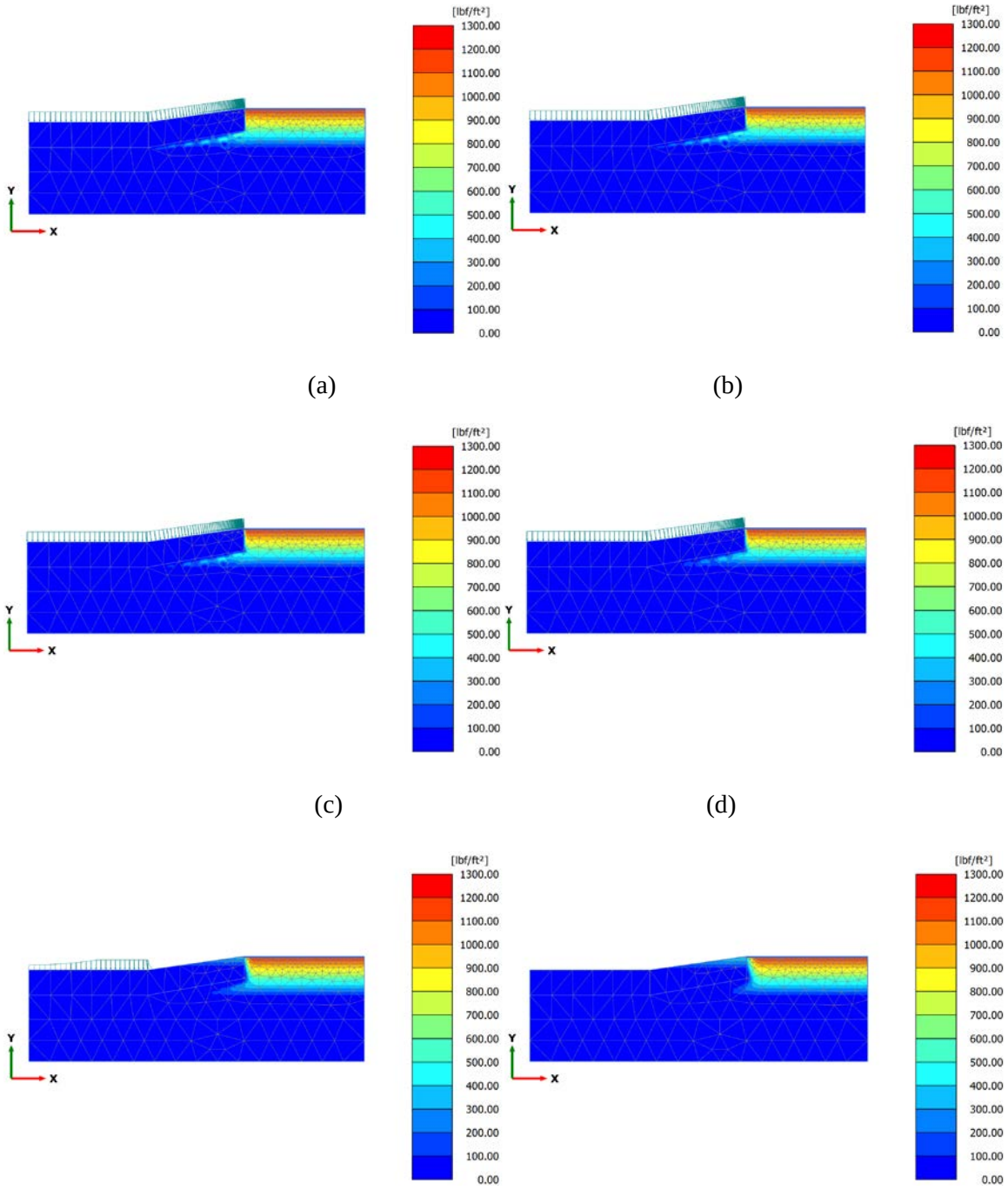

Figure A11 Suction variation of 2N wet-dry cycle for 0% initial moisture content at high intensity 12 hrs rainfall period (a) After 30 mins (b) After 2 hrs (c) After 6 hrs (d) After 12 hrs (e) after 3 days (f) after 7 days

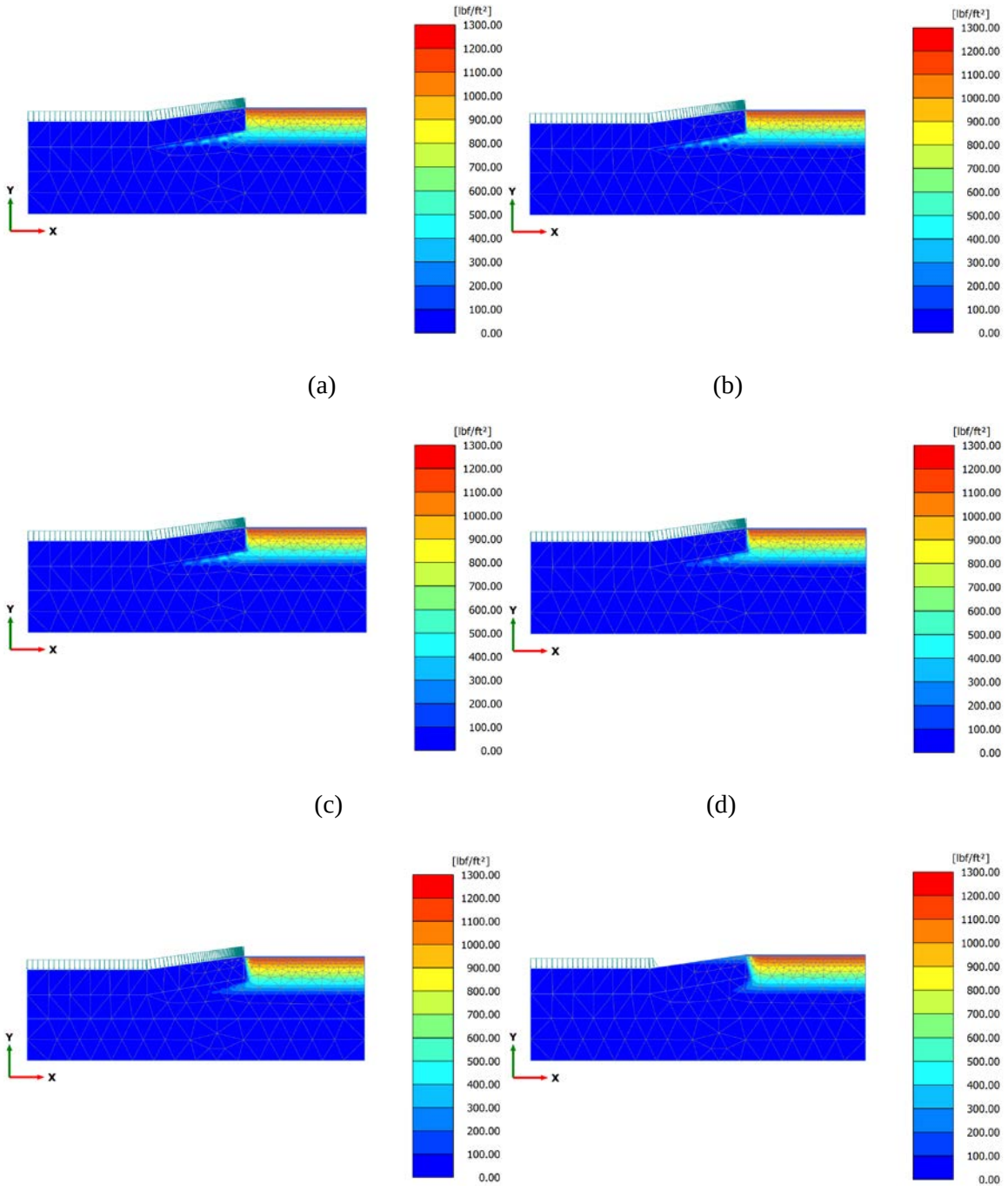

Figure A12 Suction variation of 2N wet-dry cycle for 0% initial moisture content at high intensity 3-day rainfall period (a) After 30 mins (b) After 2 hrs (c) After 6 hrs (d) After 12 hrs (e) after 3 days (f) after 7 days

(15% Initial Moisture Content)

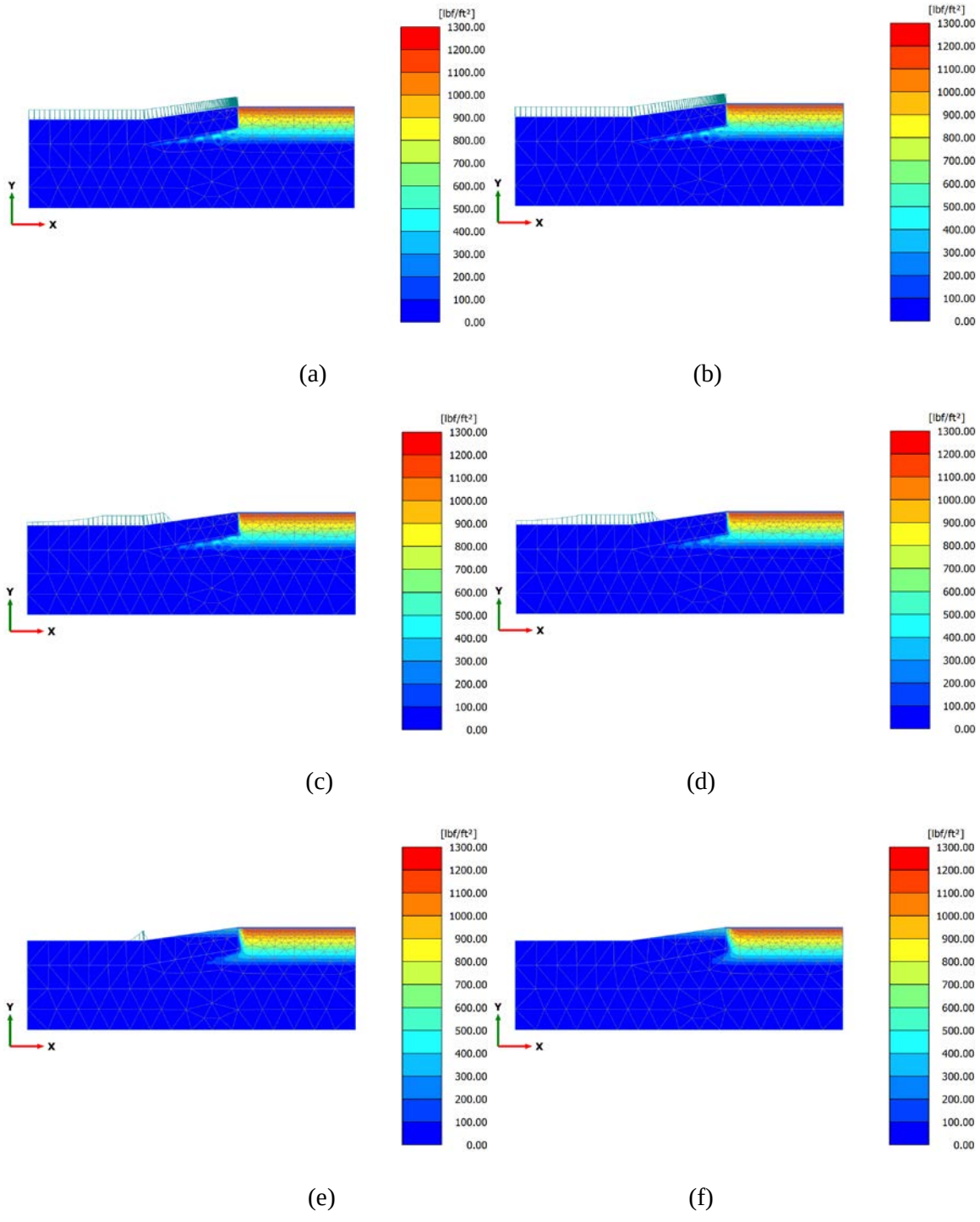

Figure A13 Suction variation of 2N wet-dry cycle for 15% initial moisture content at high intensity 2 hrs rainfall period (a) After 30 mins (b) After 2 hrs (c) After 6 hrs (d) After 12 hrs (e) after 3 days (f) after 7 days

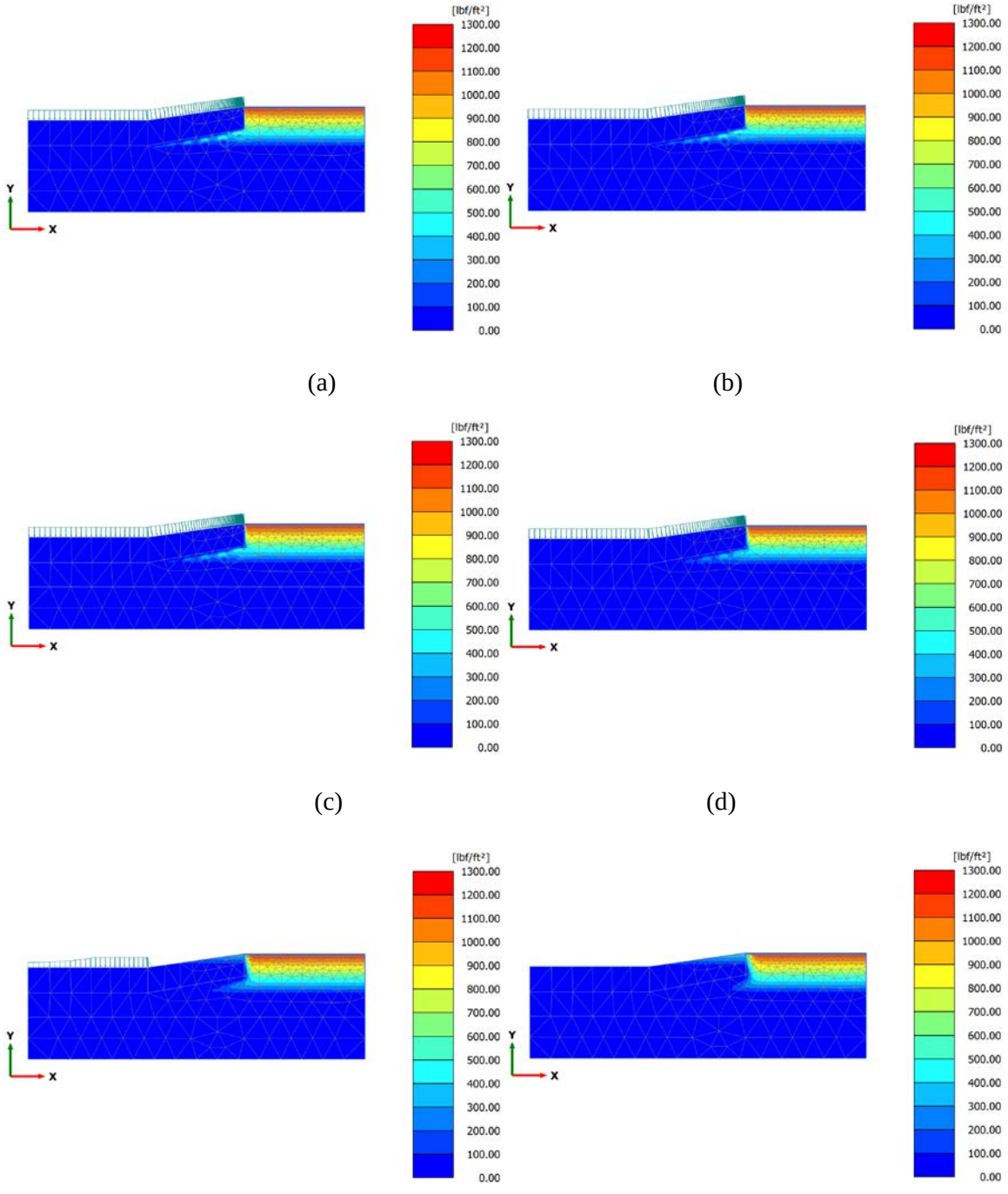

Figure A14 Suction variation of 2N wet-dry cycle for 15% initial moisture content at high intensity 12 hrs rainfall period (a) After 30 mins (b) After 2 hrs (c) After 6 hrs (d) After 12 hrs (e) after 3 days (f) after 7 days

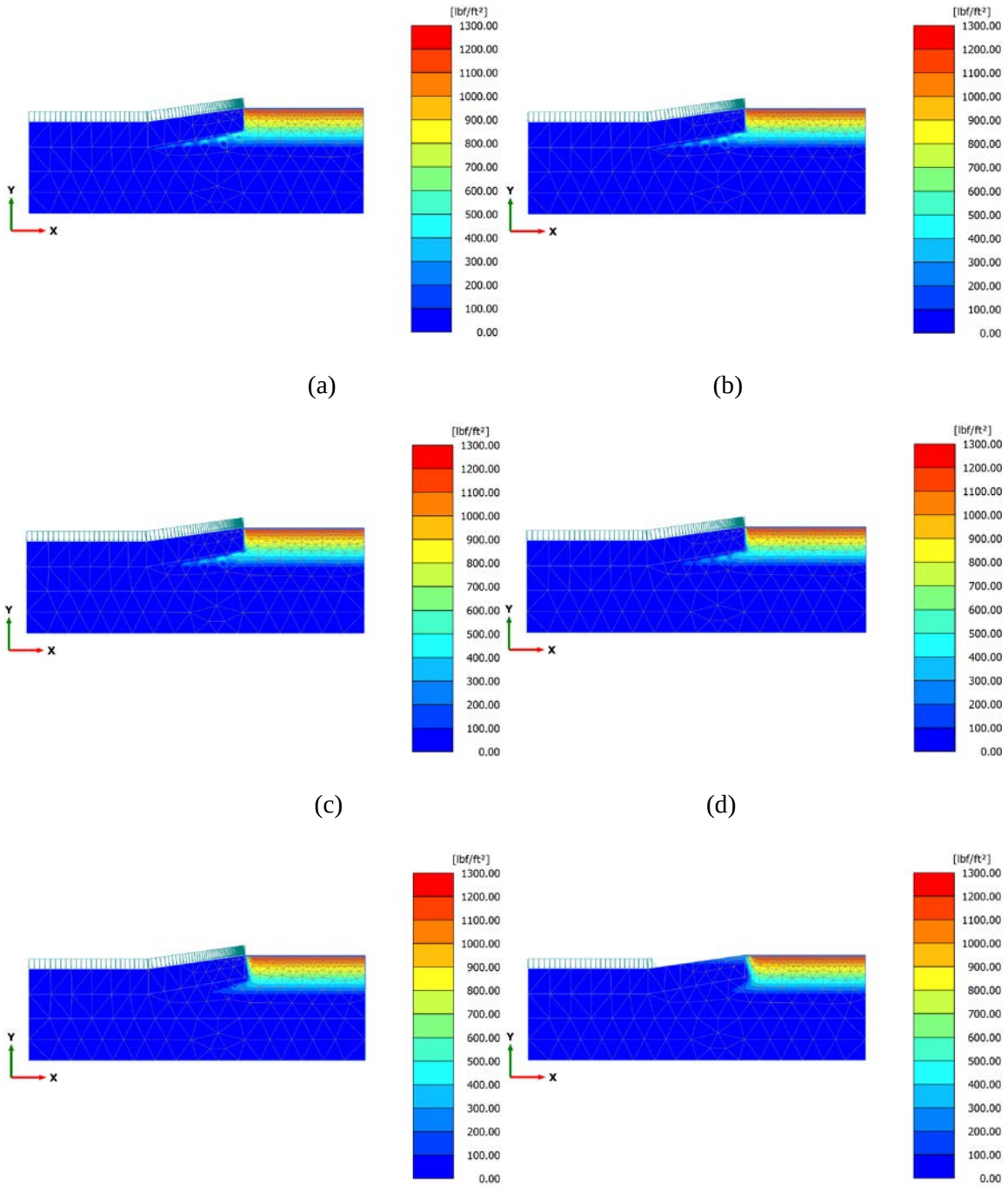

Figure A15 Suction variation of 2N wet-dry cycle for 15% initial moisture content at high intensity 3-day rainfall period (a) After 30 mins (b) After 2 hrs (c) After 6 hrs (d) After 12 hrs (e) after 3 days (f) after 7 days

25% Initial Moisture Content

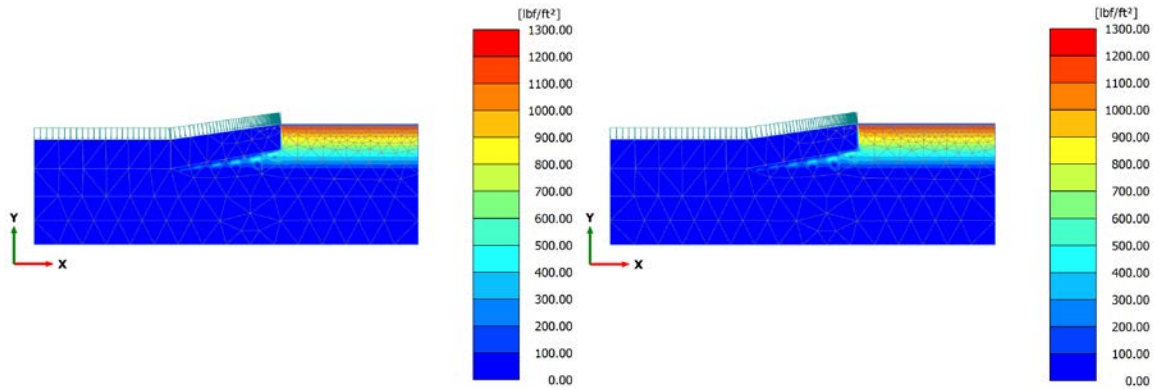

(a) (b)

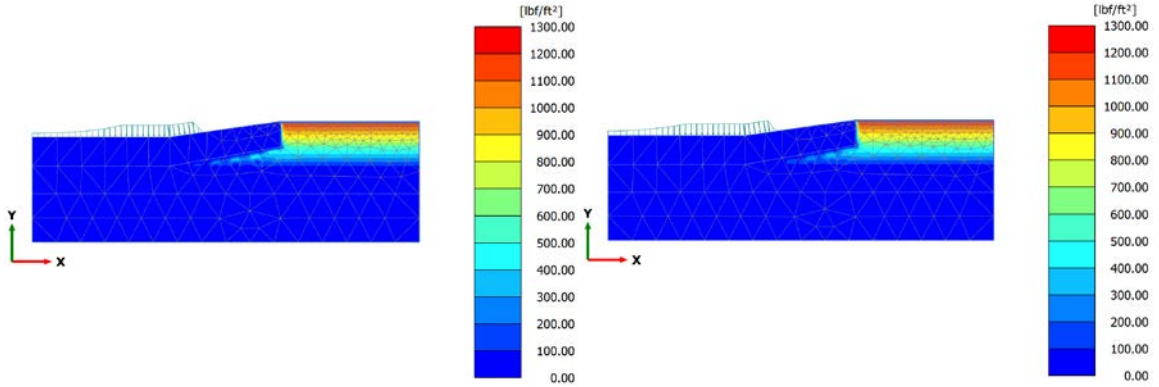

(c) (d)

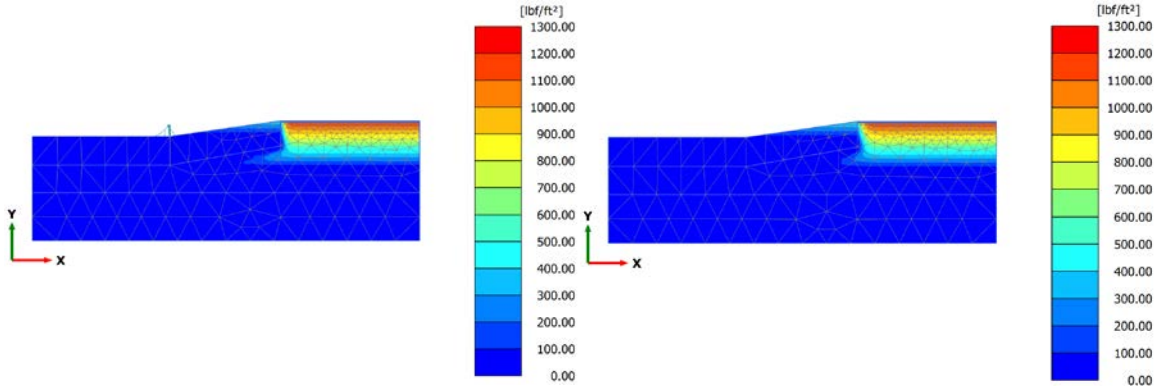

(e) (f)

Figure A16 Suction variation of 2N wet-dry cycle for 25% initial moisture content at high intensity 2 hrs rainfall period (a) After 30 mins (b) After 2 hrs (c) After 6 hrs (d) After 12 hrs (e) after 3 days (f) after 7 days

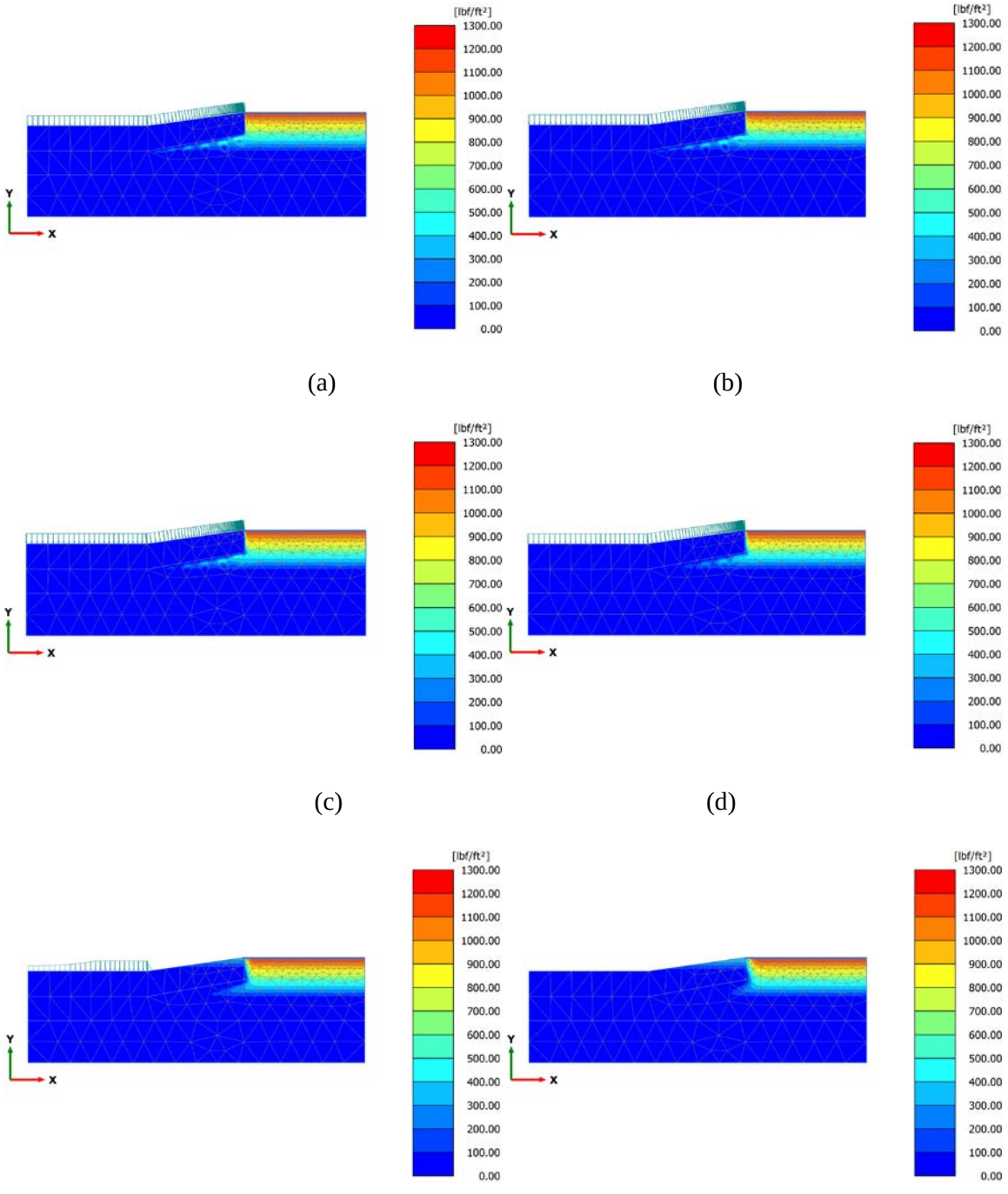

Figure A17 Suction variation of 2N wet-dry cycle for 25% initial moisture content at high intensity 12 hrs rainfall period (a) After 30 mins (b) After 2 hrs (c) After 6 hrs (d) After 12 hrs (e) after 3 days (f) after 7 days

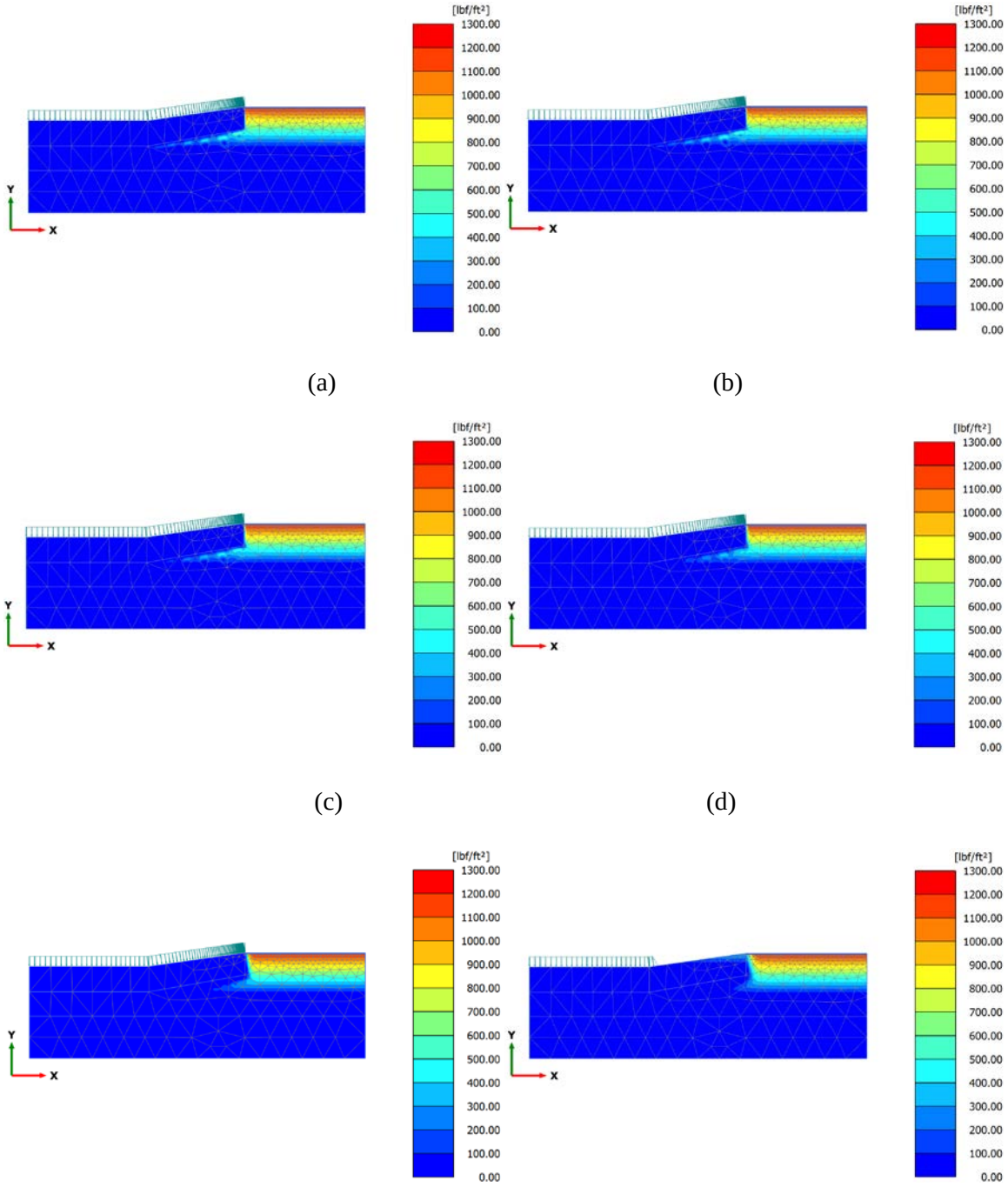

Figure A18 Suction variation of 2N wet-dry cycle for 25% initial moisture content at high intensity 3-day rainfall period (a) After 30 mins (b) After 2 hrs (c) After 6 hrs (d) After 12 hrs (e) after 3 days (f) after 7 days

35% Initial Moisture Content

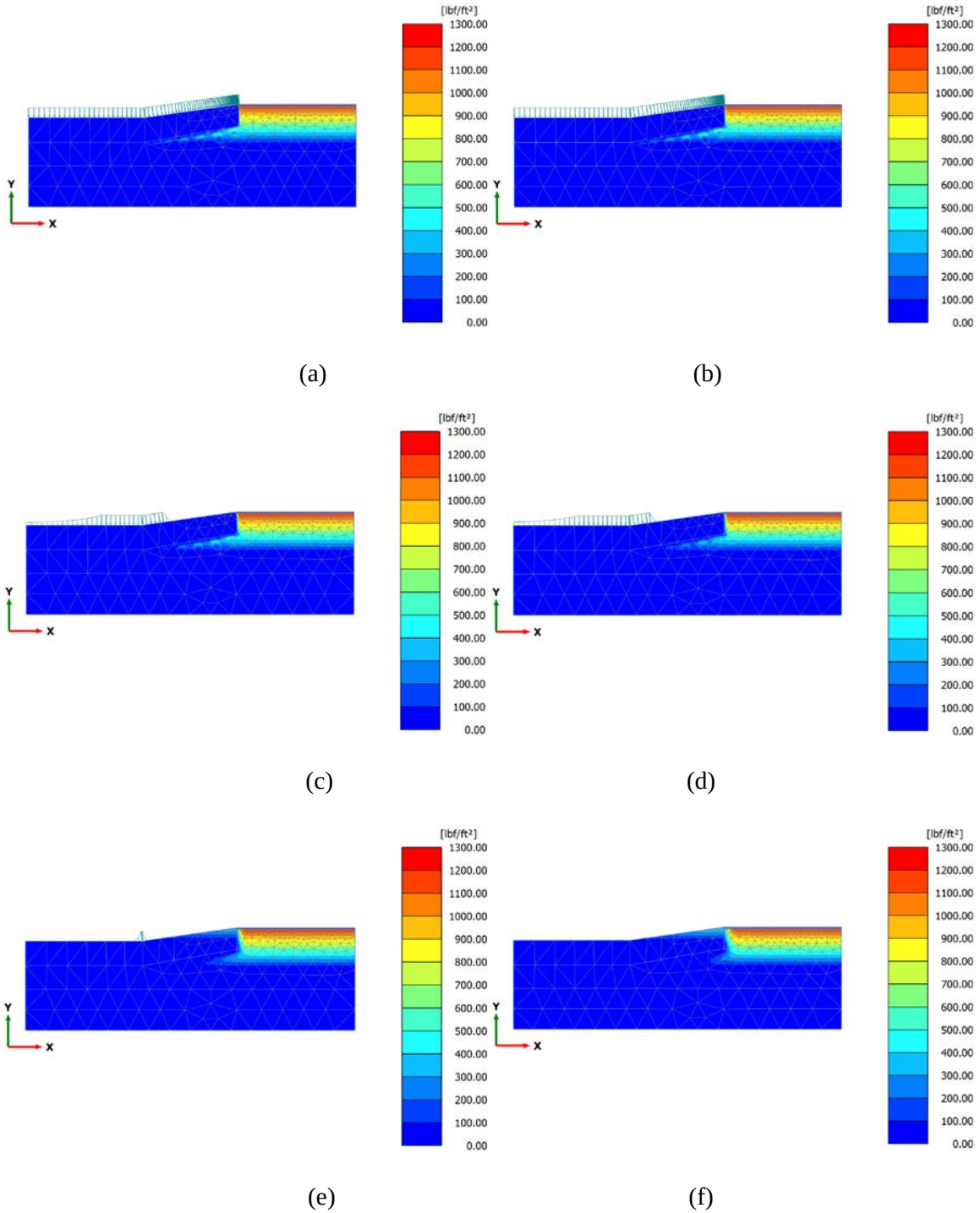

Figure A19 Suction variation of 2N wet-dry cycle for 35% initial moisture content at high intensity 2 hrs rainfall period (a) After 30 mins (b) After 2 hrs (c) After 6 hrs (d) After 12 hrs (e) after 3 days (f) after 7 days

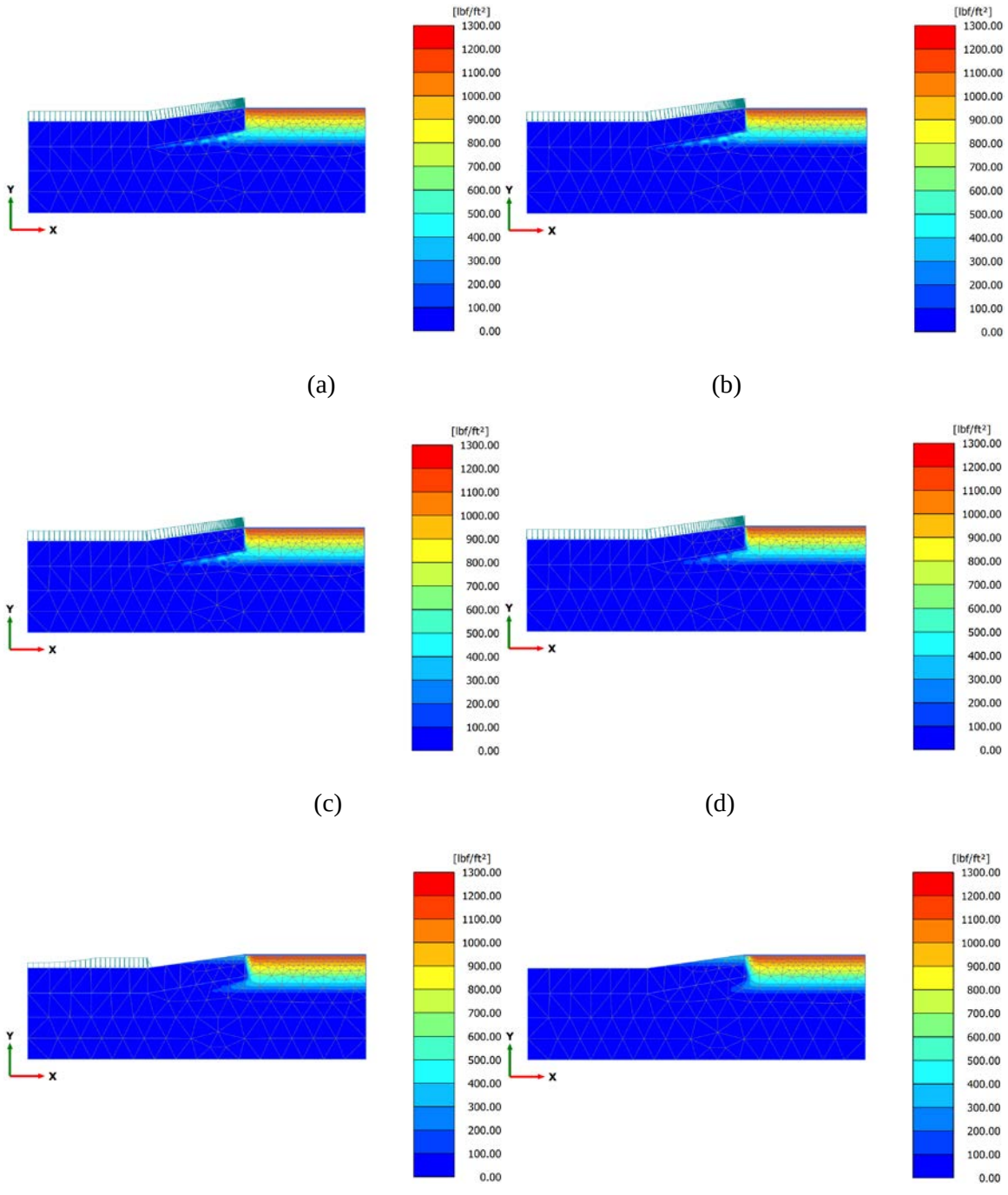

Figure A20 Suction variation of 2N wet-dry cycle for 35% initial moisture content at high intensity 12 hrs rainfall period (a) After 30 mins (b) After 2 hrs (c) After 6 hrs (d) After 12 hrs (e) after 3 days (f) after 7 days

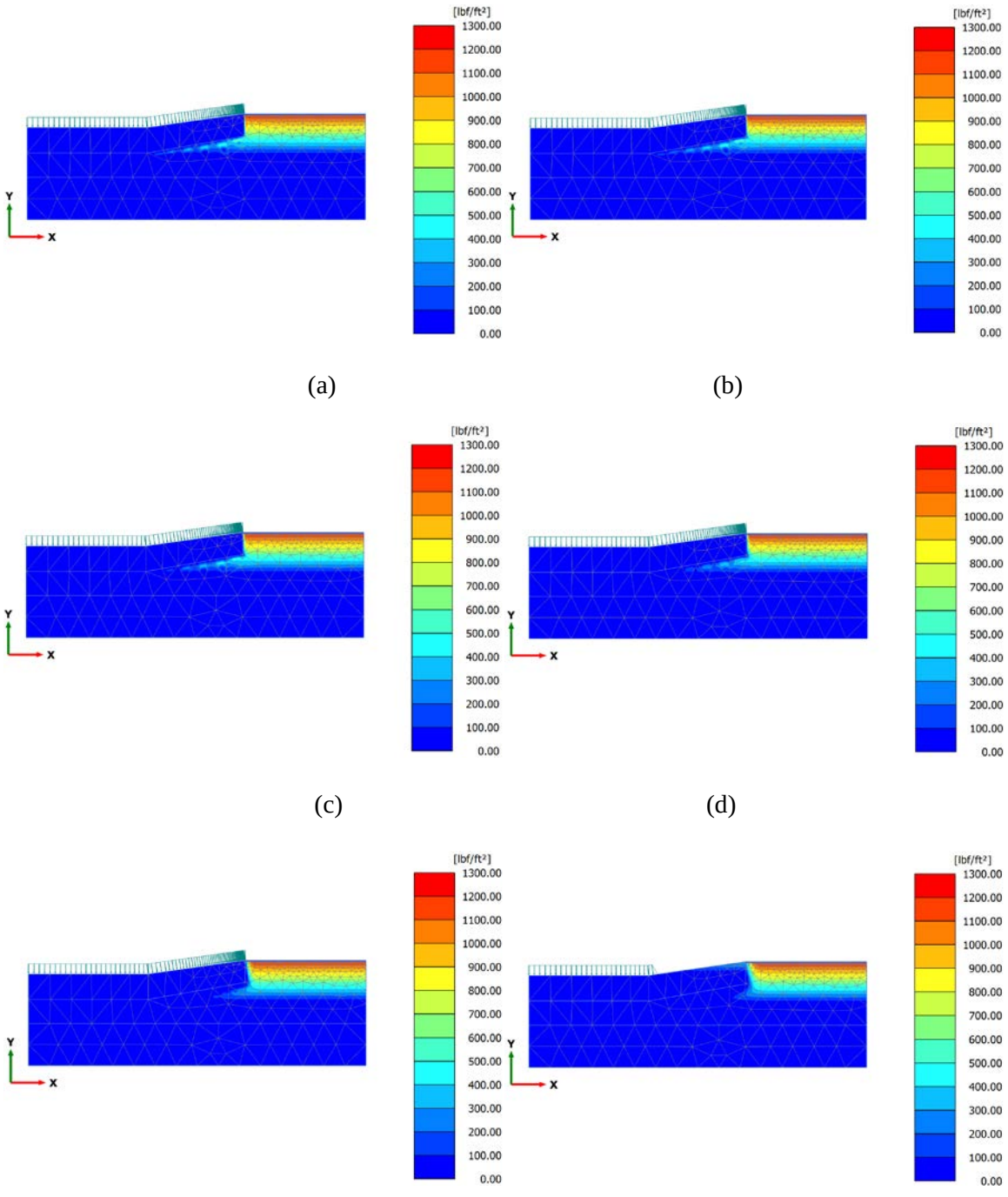

Figure A21 Suction variation of 2N wet-dry cycle for 35% initial moisture content at high intensity 3-day rainfall period (a) After 30 mins (b) After 2 hrs (c) After 6 hrs (d) After 12 hrs (e) after 3 days (f) after 7 days

3N wet-dry cycle

0% Initial Moisture Content

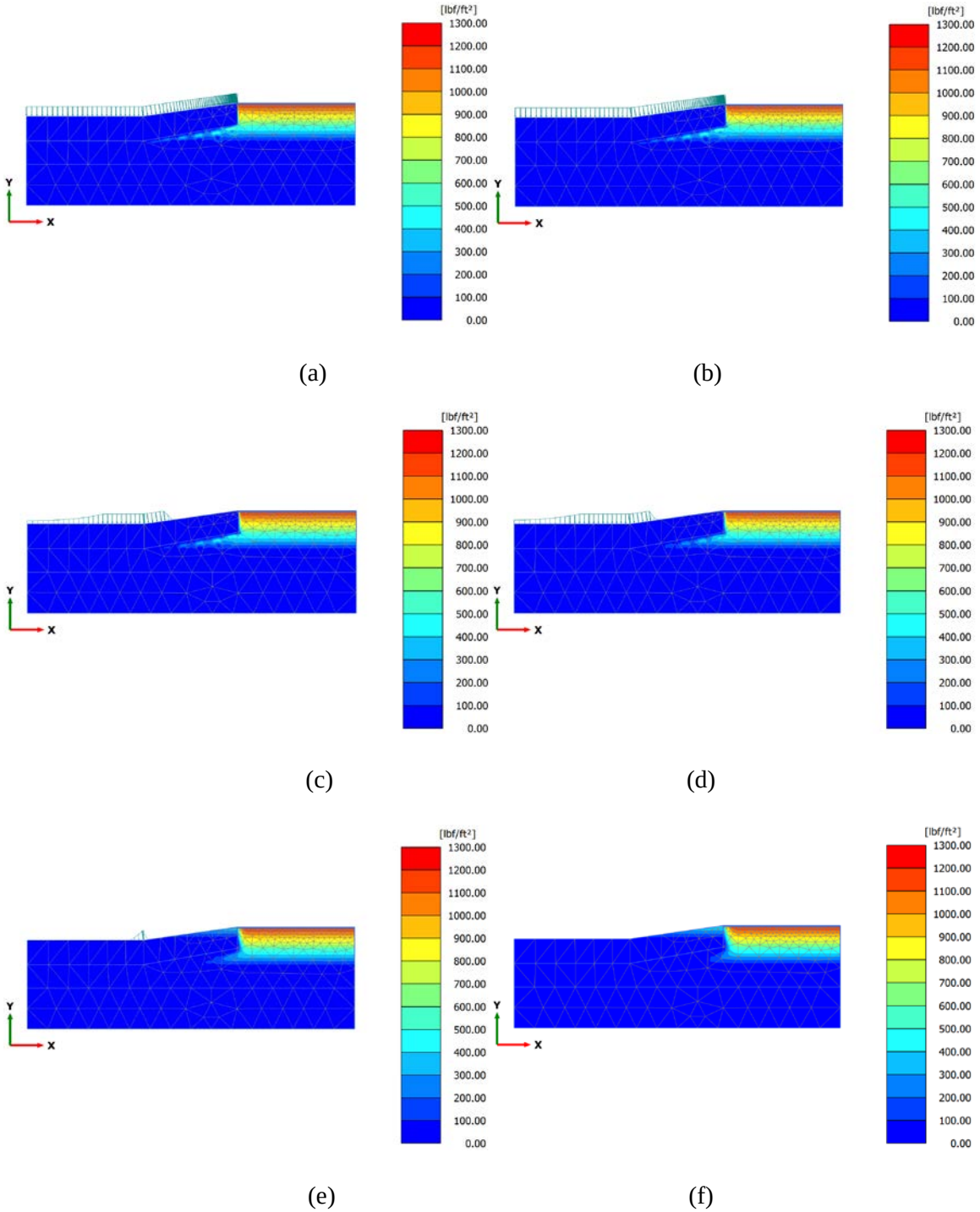

Figure A22 Suction variation of 3N wet-dry cycle for 0% initial moisture content at high intensity 2 hrs rainfall period (a) After 30 mins (b) After 2 hrs (c) After 6 hrs (d) After 12 hrs (e) after 3 days (f) after 7 days

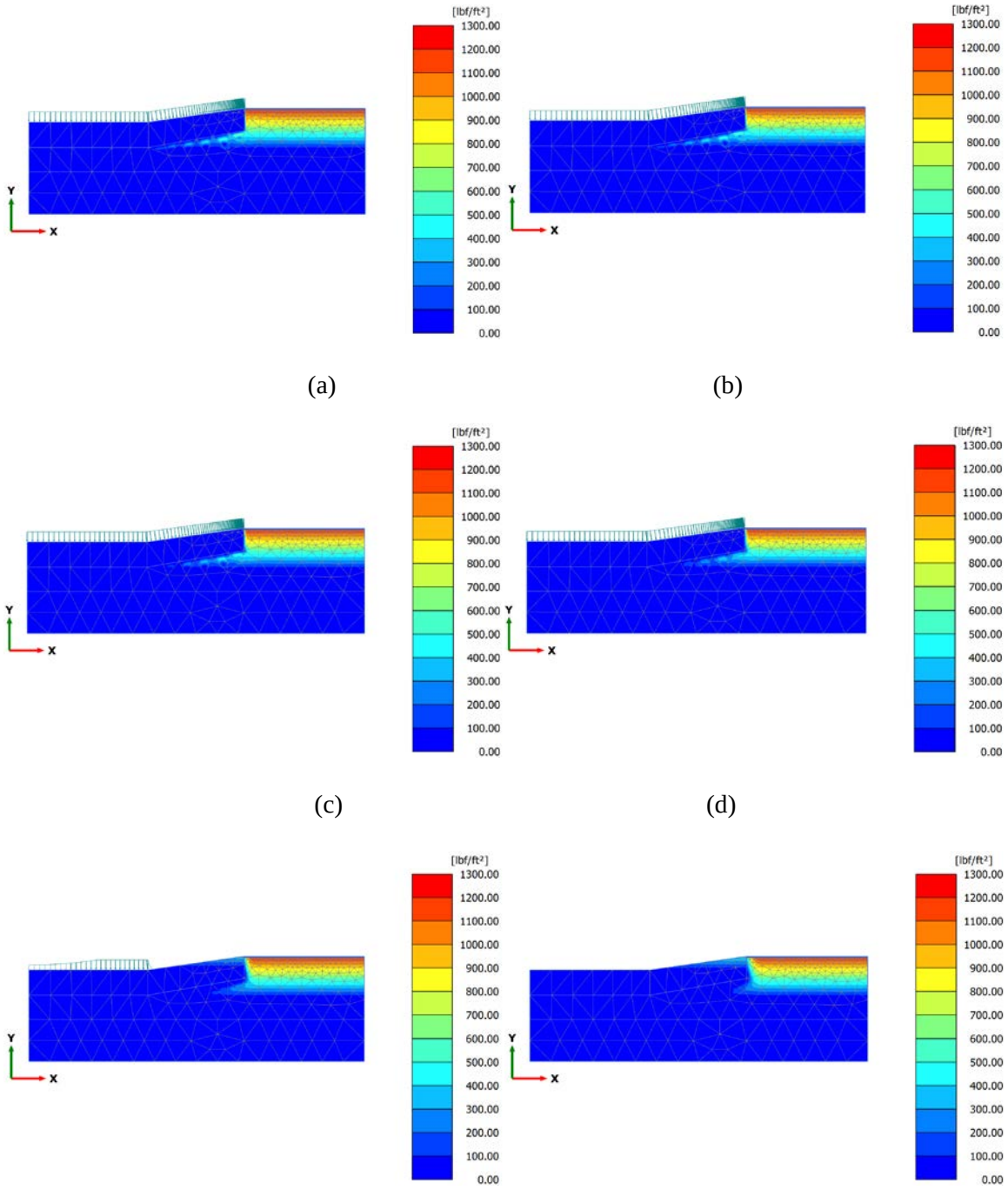

Figure A23 Suction variation of 3N wet-dry cycle for 0% initial moisture content at high intensity 12 hrs rainfall period (a) After 30 mins (b) After 2 hrs (c) After 6 hrs (d) After 12 hrs (e) after 3 days (f) after 7 days

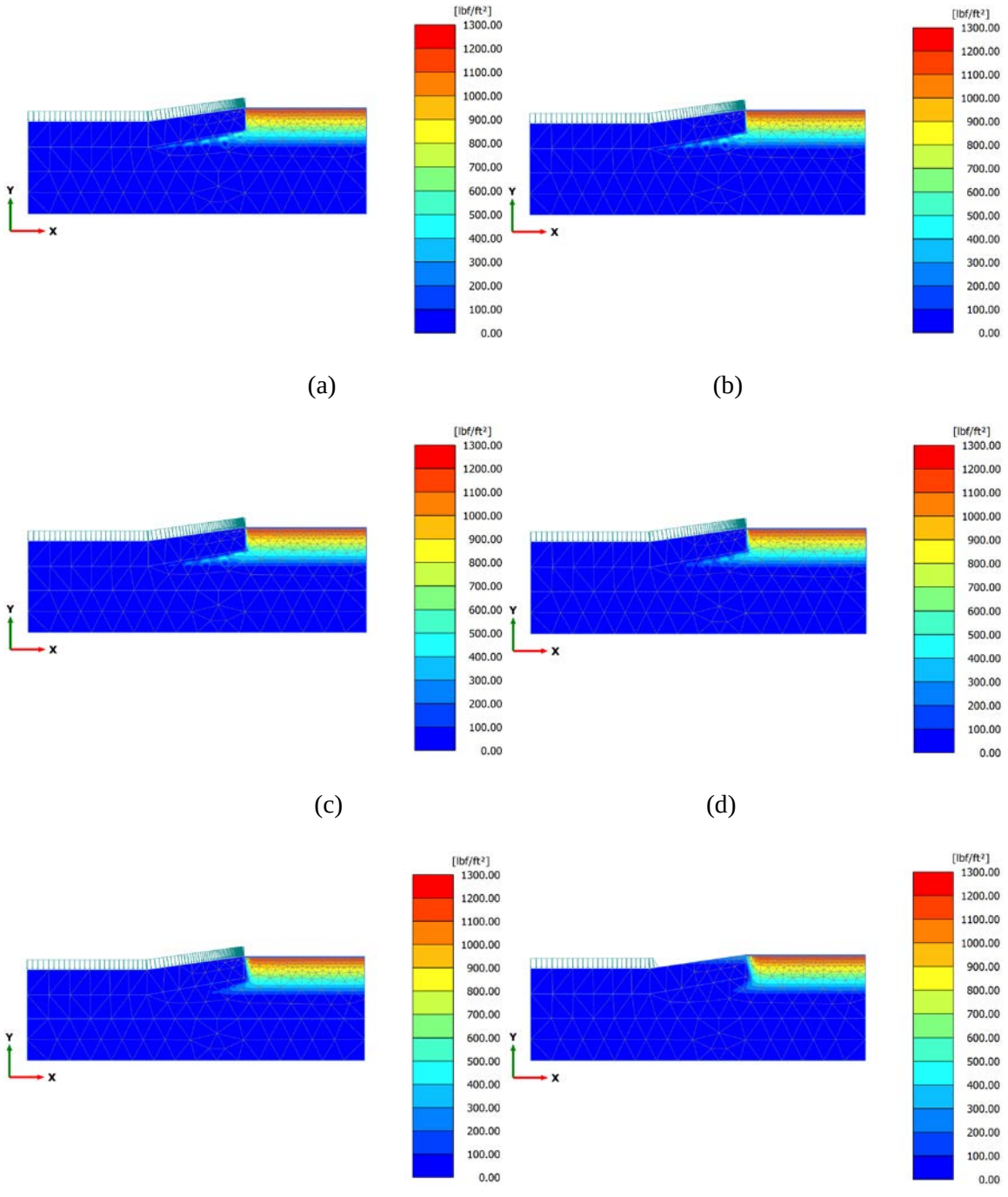

Figure A24 Suction variation of 3N wet-dry cycle for 0% initial moisture content at high intensity 3-day rainfall period (a) After 30 mins (b) After 2 hrs (c) After 6 hrs (d) After 12 hrs (e) after 3 days (f) after 7 days

15% Initial Moisture Content

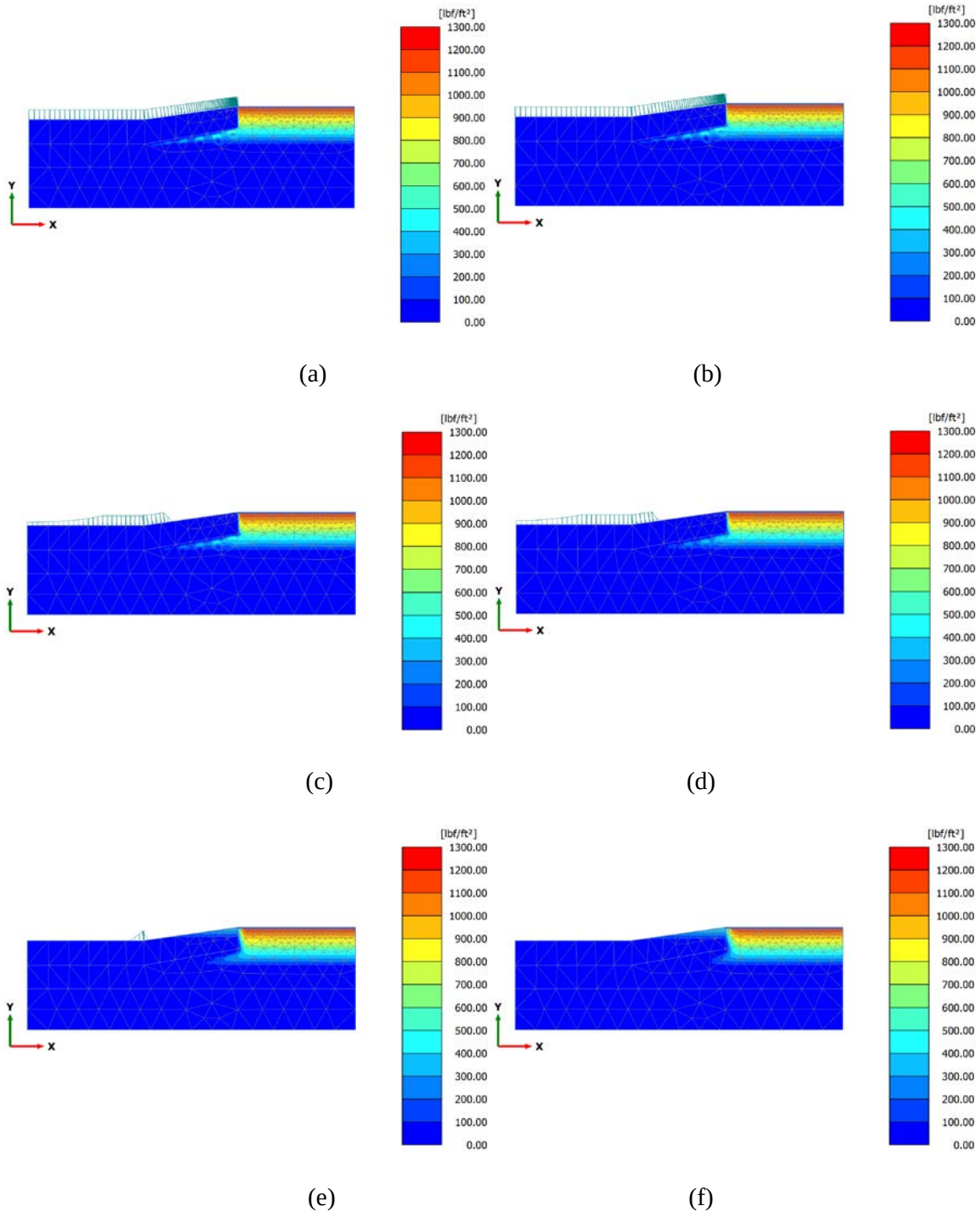

Figure A25 Suction variation of 3N wet-dry cycle for 15% initial moisture content at high intensity 2 hrs rainfall period (a) After 30 mins (b) After 2 hrs (c) After 6 hrs (d) After 12 hrs (e) after 3 days (f) after 7 days

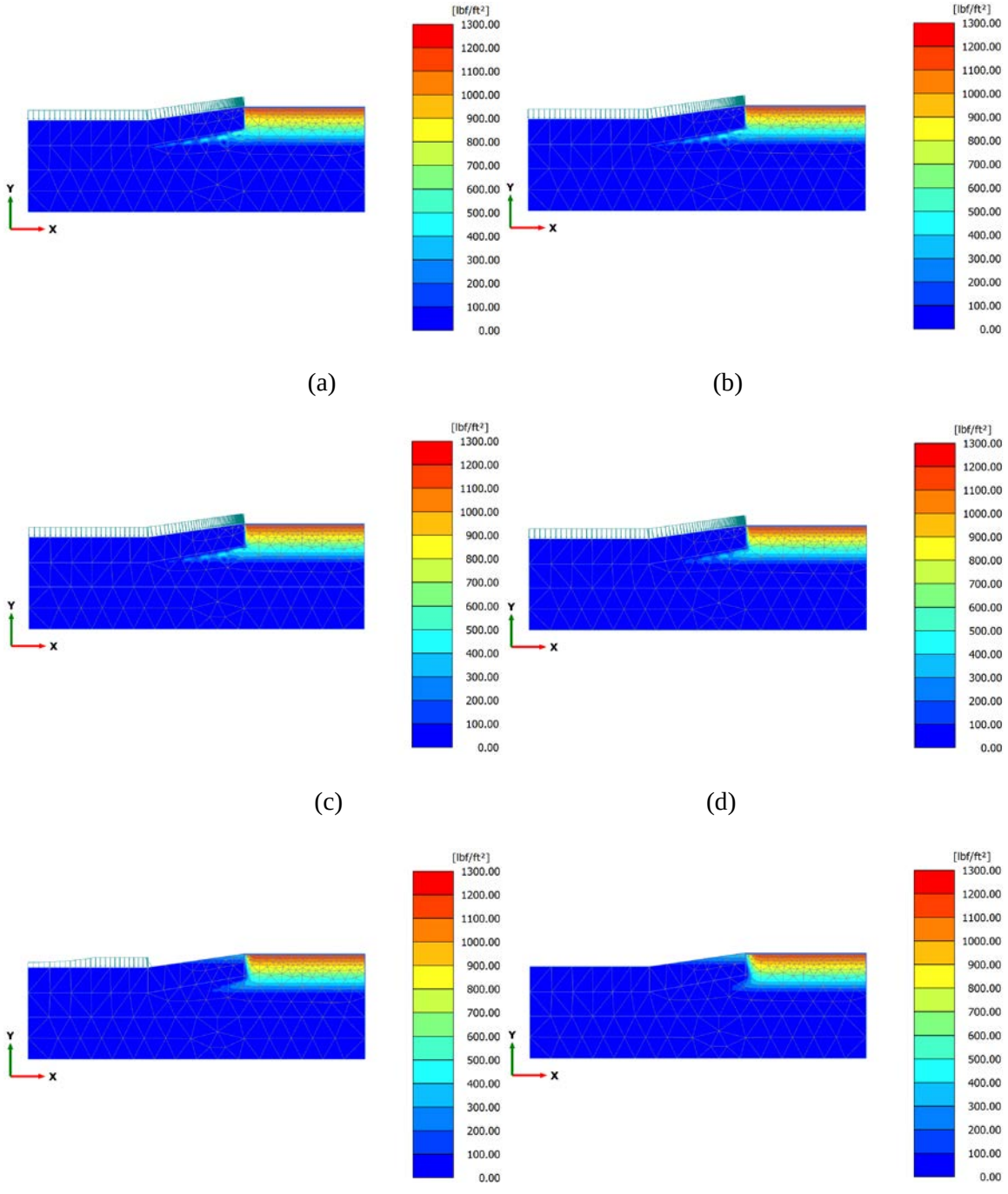

Figure A26 Suction variation of 3N wet-dry cycle for 15% initial moisture content at high intensity 12 hrs rainfall period (a) After 30 mins (b) After 2 hrs (c) After 6 hrs (d) After 12 hrs (e) after 3 days (f) after 7 days

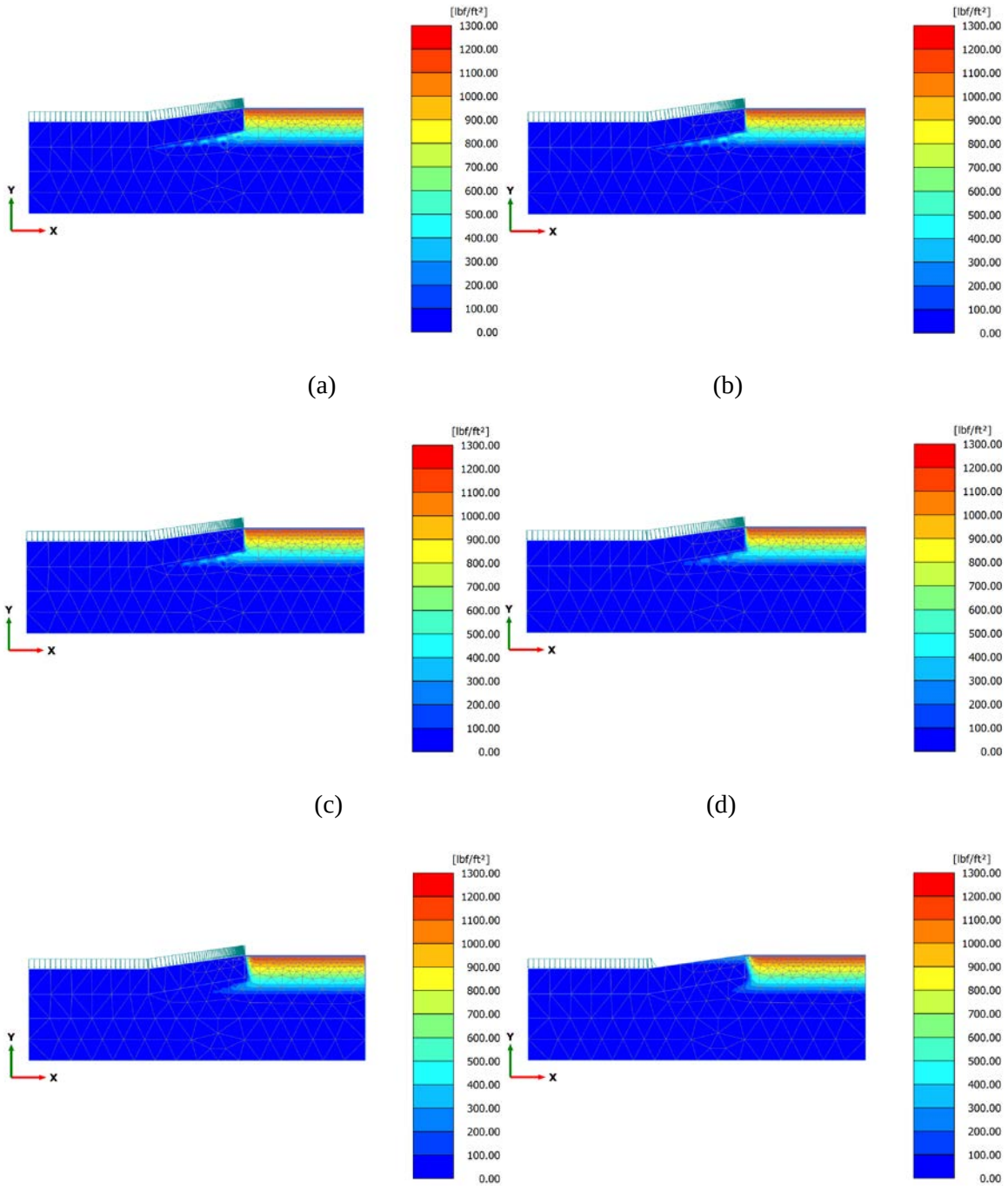

Figure A27 Suction variation of 3N wet-dry cycle for 15% initial moisture content at high intensity 3-day rainfall period (a) After 30 mins (b) After 2 hrs (c) After 6 hrs (d) After 12 hrs (e) after 3 days (f) after 7 days

25% Initial Moisture Content

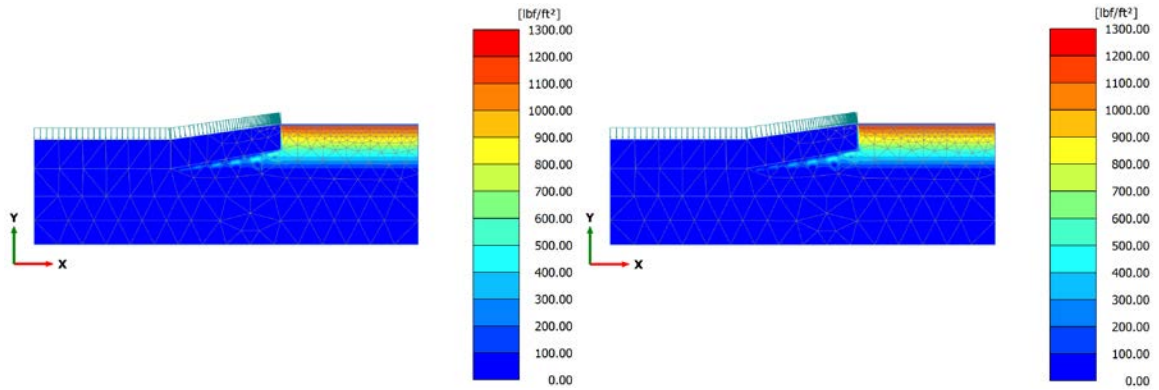

(a) (b)

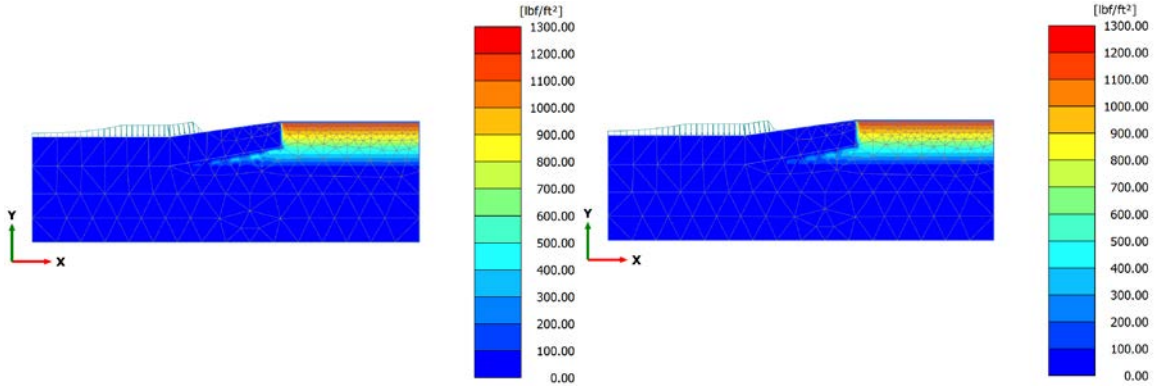

(c) (d)

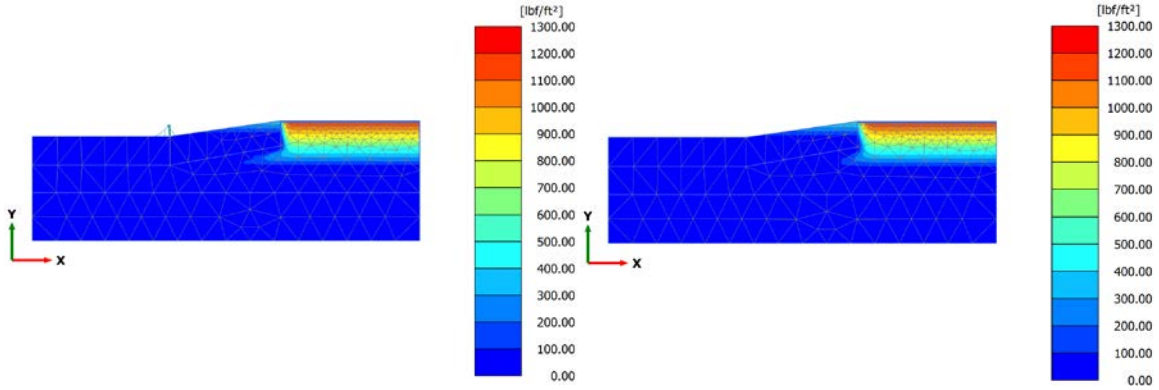

(e) (f)

Figure A28 Suction variation of 3N wet-dry cycle for 25% initial moisture content at high intensity 2 hrs rainfall period (a) After 30 mins (b) After 2 hrs (c) After 6 hrs (d) After 12 hrs (e) after 3 days (f) after 7 days

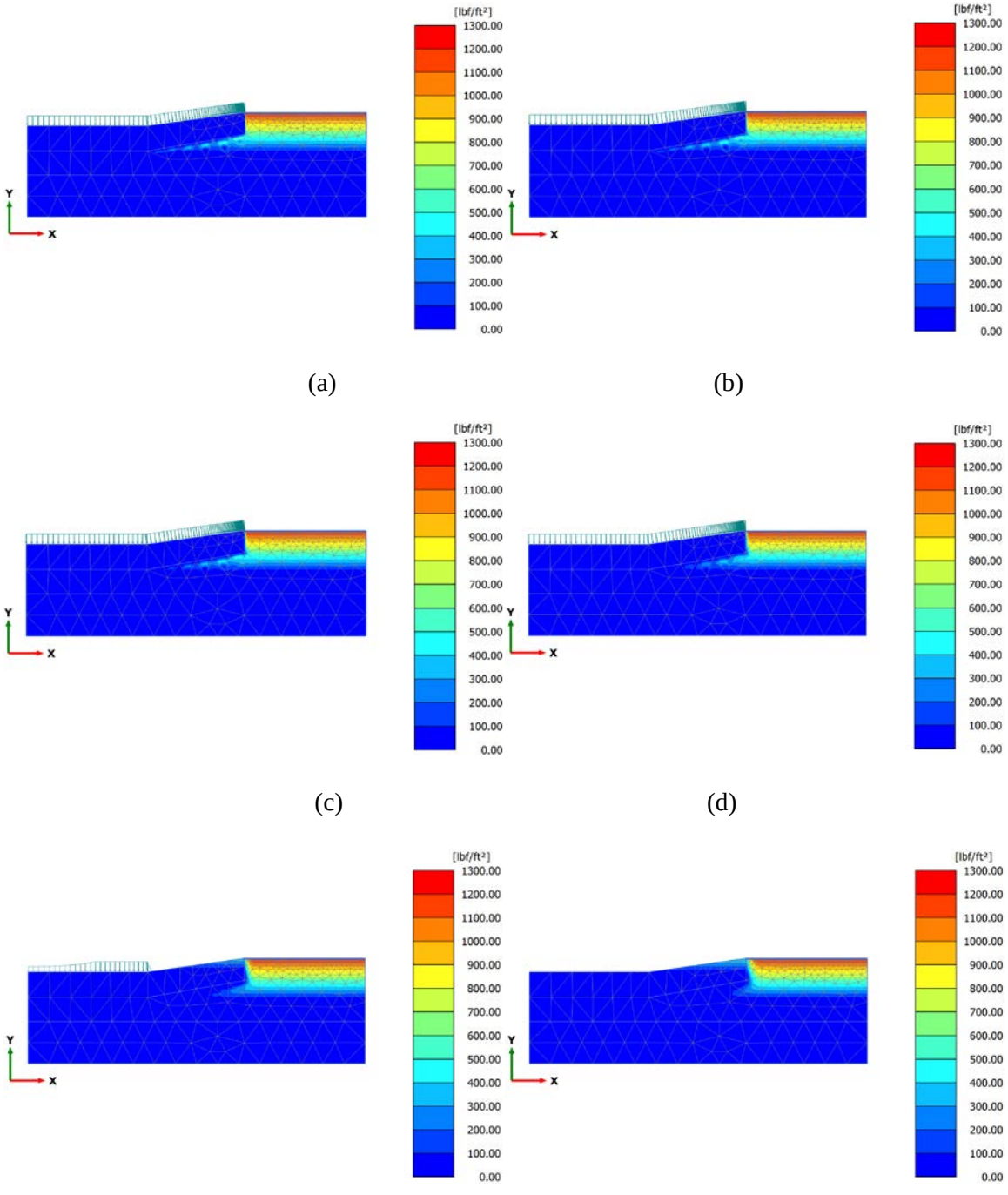

Figure A29 Suction variation of 3N wet-dry cycle for 25% initial moisture content at high intensity 12 hrs rainfall period (a) After 30 mins (b) After 2 hrs (c) After 6 hrs (d) After 12 hrs (e) after 3 days (f) after 7 days

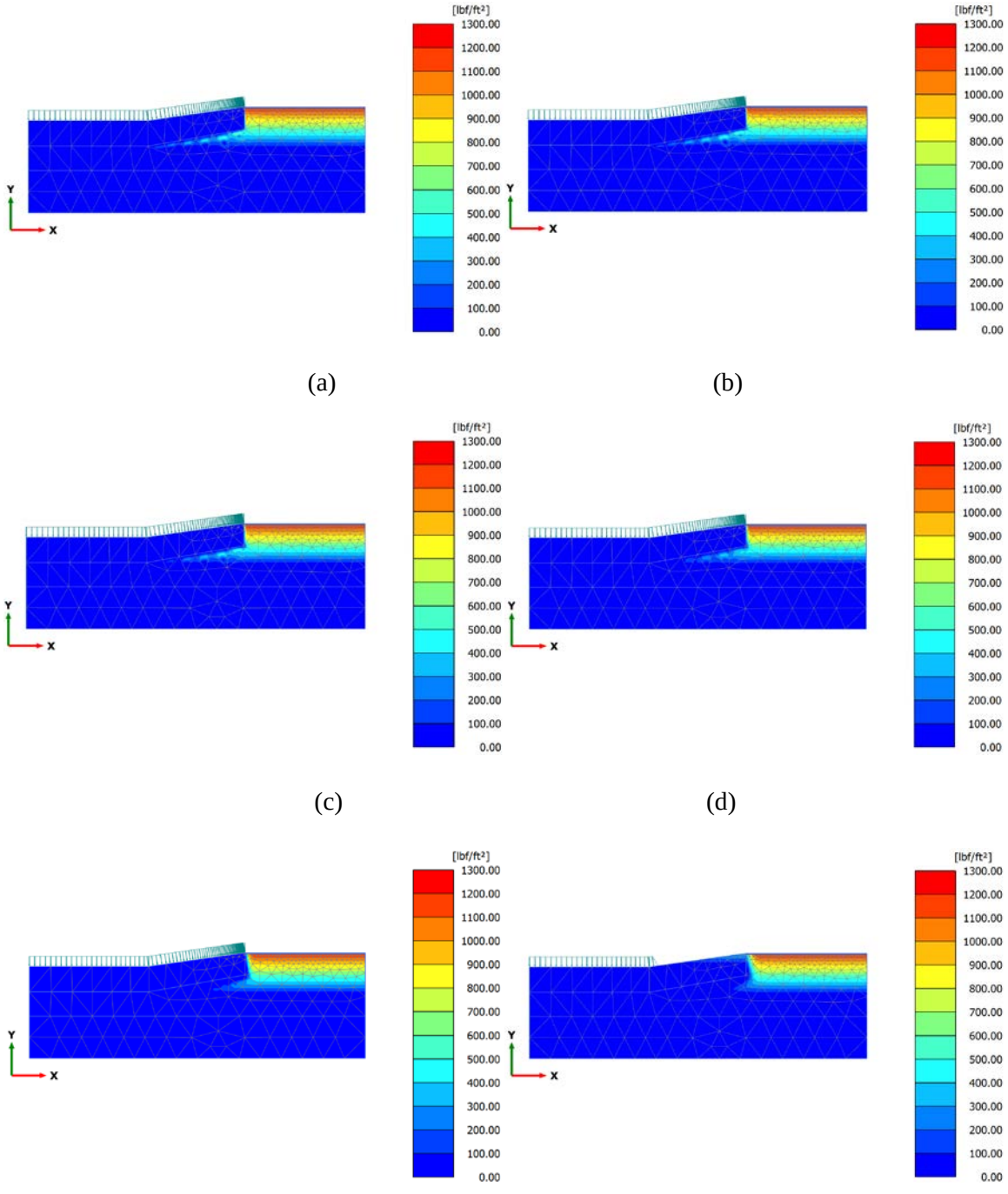

Figure A30 Suction variation of 3N wet-dry cycle for 25% initial moisture content at high intensity 3-day rainfall period (a) After 30 mins (b) After 2 hrs (c) After 6 hrs (d) After 12 hrs (e) after 3 days (f) after 7 days

35% Initial Moisture Content

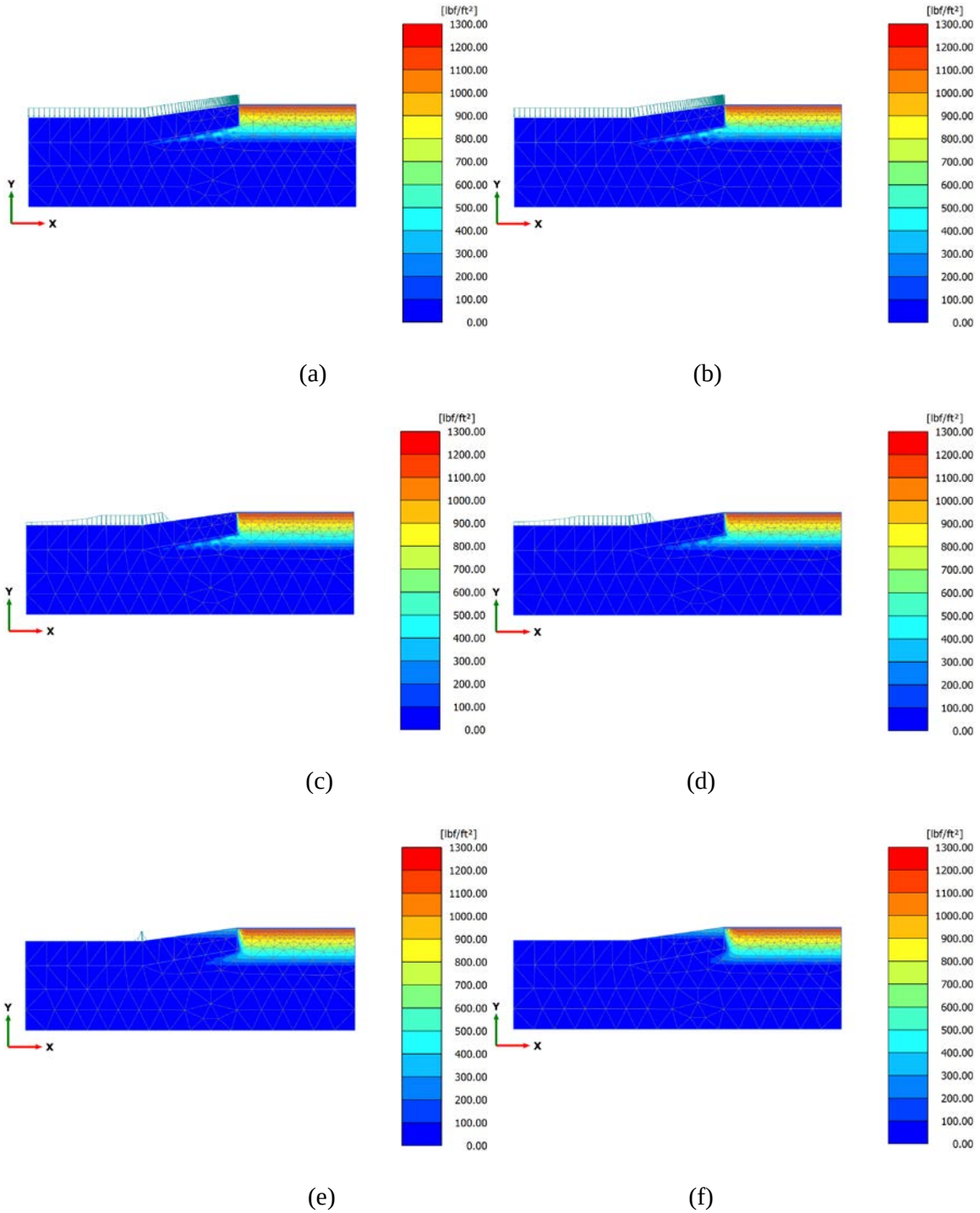

Figure A31 Suction variation of 3N wet-dry cycle for 35% initial moisture content at high intensity 2 hrs rainfall period (a) After 30 mins (b) After 2 hrs (c) After 6 hrs (d) After 12 hrs (e) after 3 days (f) after 7 days

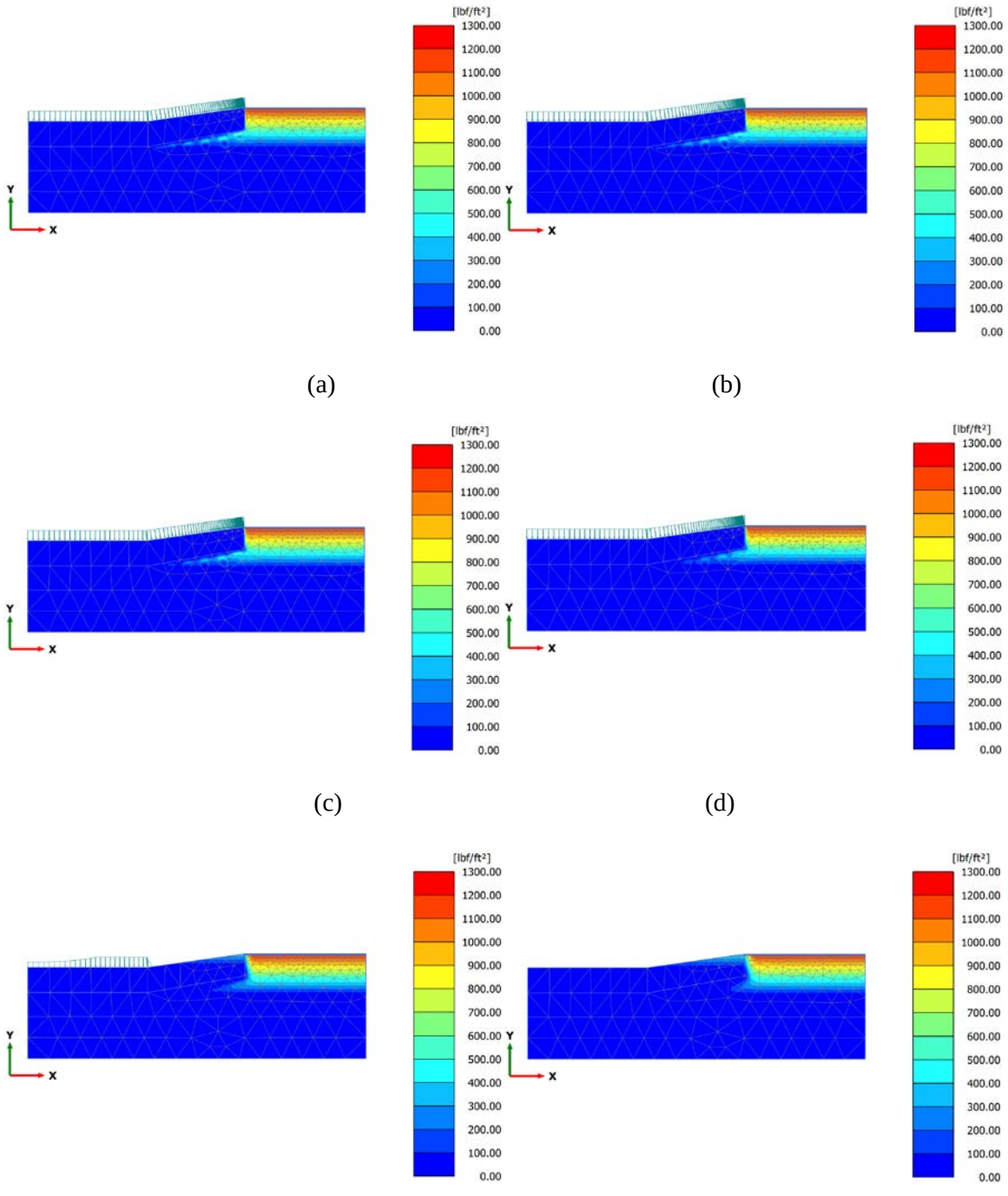

Figure A32 Suction variation of 3N wet-dry cycle for 35% initial moisture content at high intensity 12 hrs rainfall period (a) After 30 mins (b) After 2 hrs (c) After 6 hrs (d) After 12 hrs (e) after 3 days (f) after 7 days

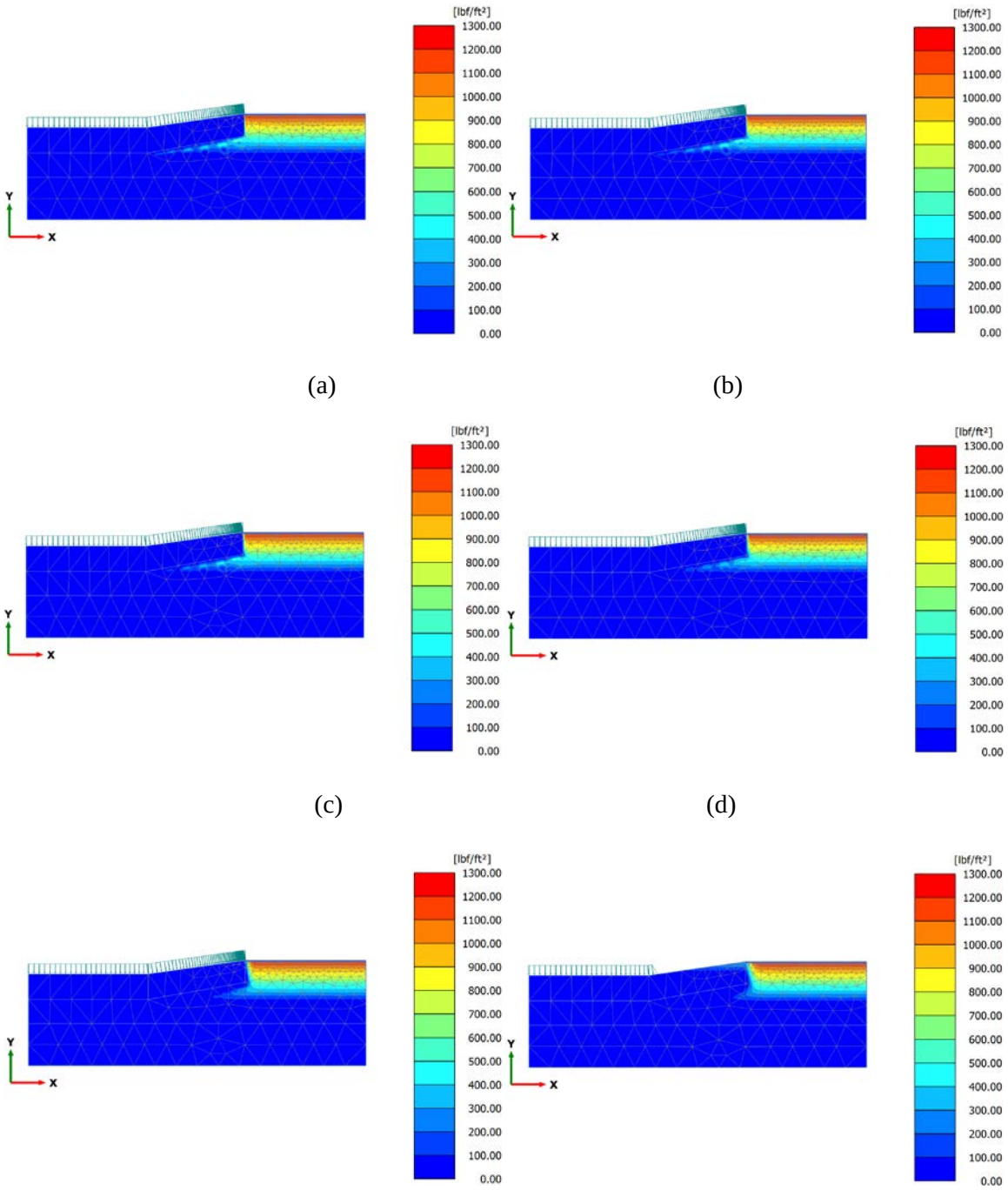

Figure A33 Suction variation of 3N wet-dry cycle for 35% initial moisture content at high intensity 3-day rainfall period (a) After 30 mins (b) After 2 hrs (c) After 6 hrs (d) After 12 hrs (e) after 3 days (f) after 7 days

APPENDIX B: PLOT OF SUCTION VARIATION ON HIGHWAY SLOPE

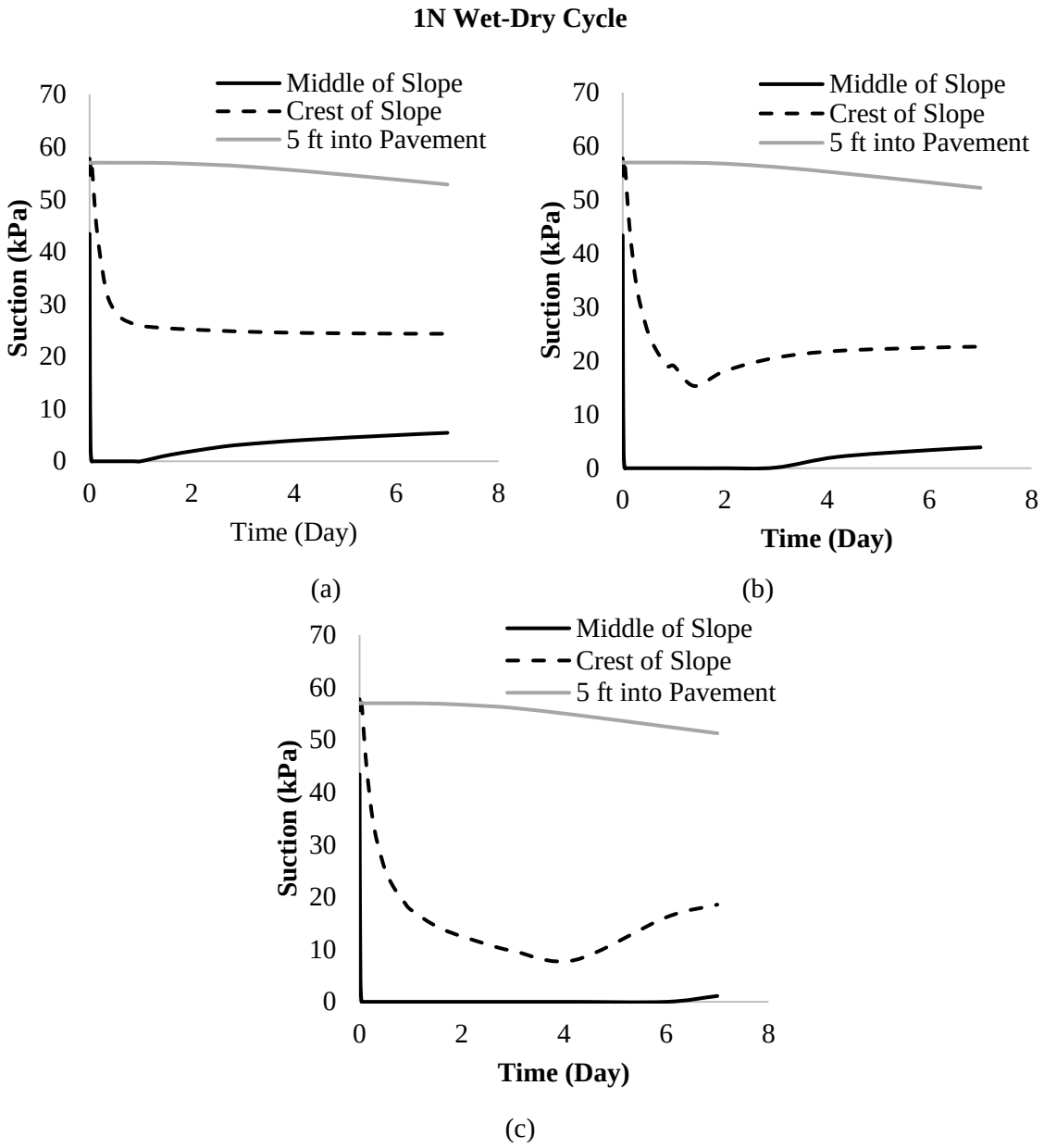

Figure B. 1 1N Suction Variation with 0% initial moisture content (a) High intensity rainfall (b) Medium intensity rainfall (c) Low intensity rainfall

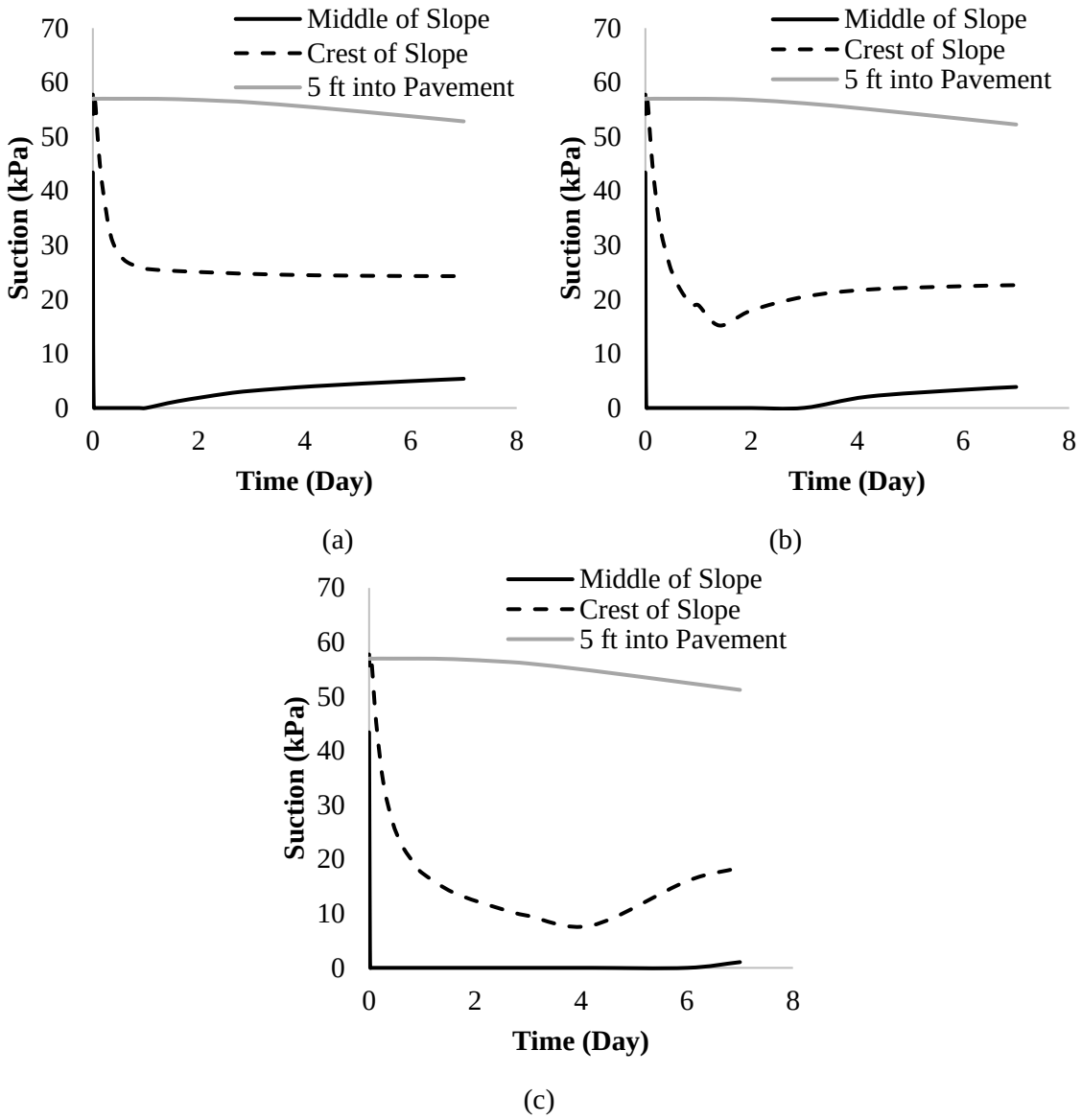

(a) (b)

(c)

Figure B. 2 1N Suction Variation with 15% initial moisture content (a) High intensity rainfall (b) Medium intensity rainfall (c) Low intensity rainfall

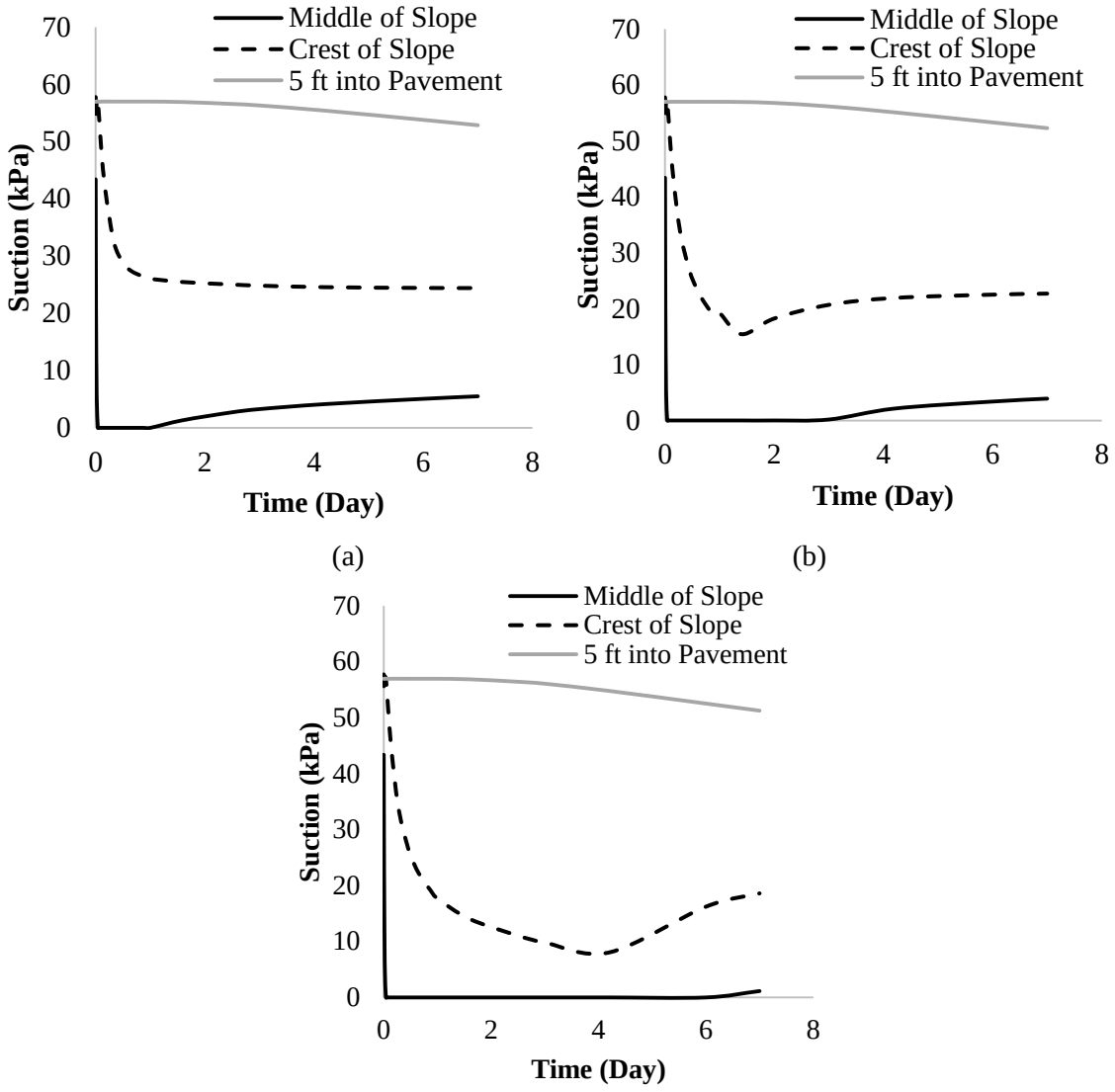

Figure B. 3 1N Suction Variation with 25% initial moisture content (a) High intensity rainfall (b) Medium intensity rainfall (c) Low intensity rainfall

2N Wet-Dry Cycle

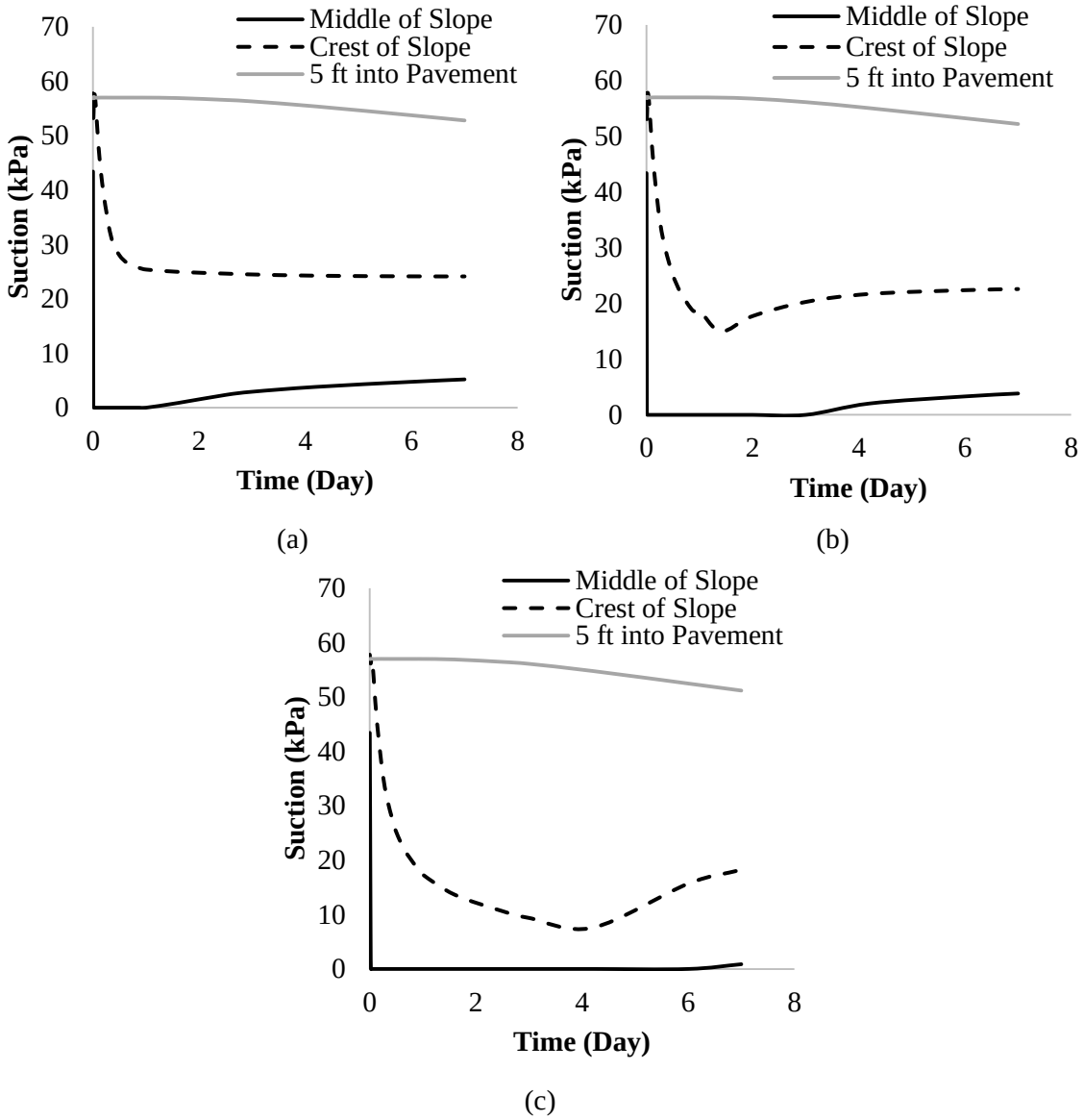

Figure B. 4 2N Suction Variation with 0% initial moisture content (a) High intensity rainfall (b) Medium intensity rainfall (c) Low intensity rainfall

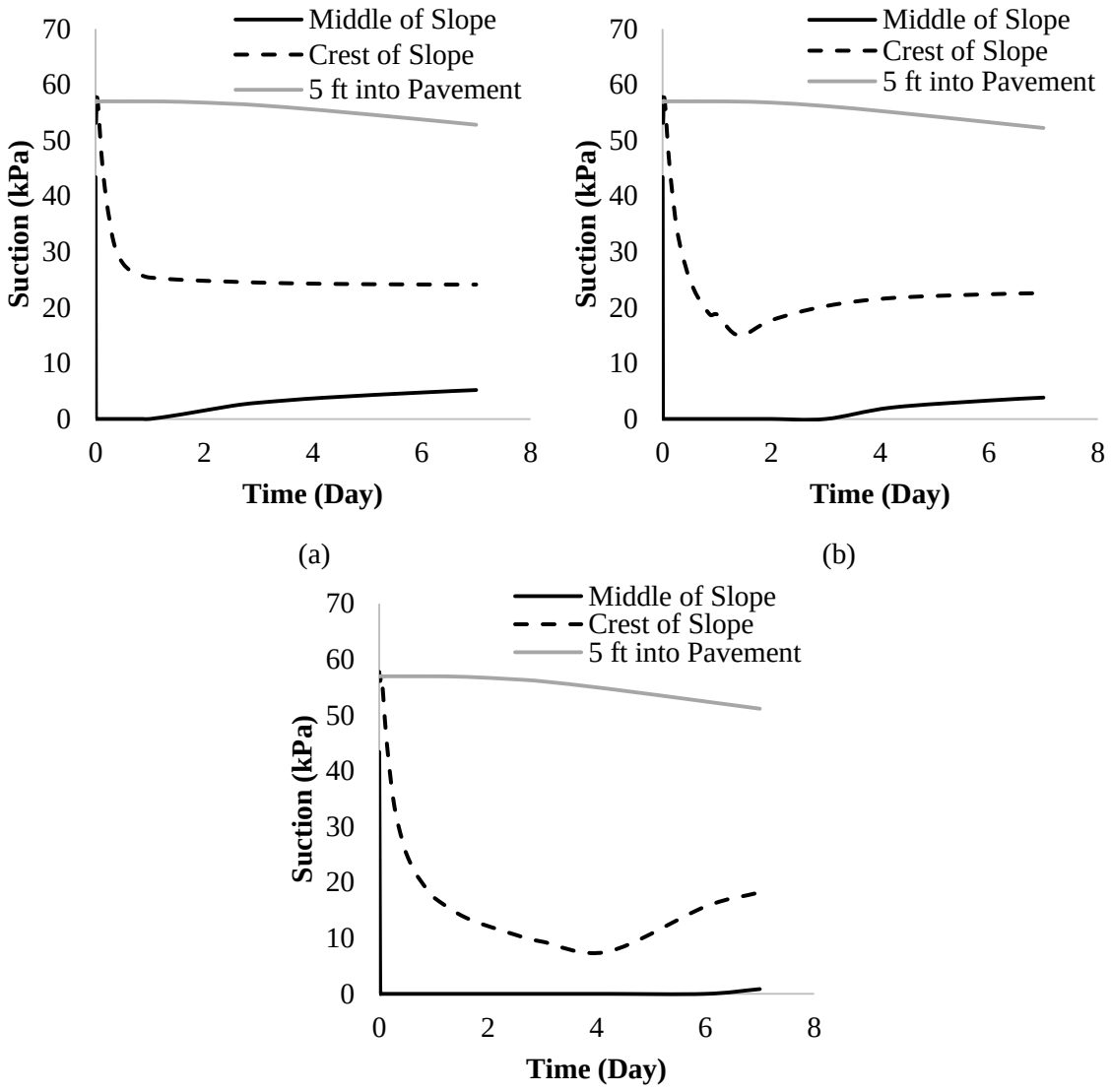

Figure B. 5 2N Suction Variation with 15% initial moisture content (a) High intensity rainfall (b) Medium intensity rainfall (c) Low intensity rainfall

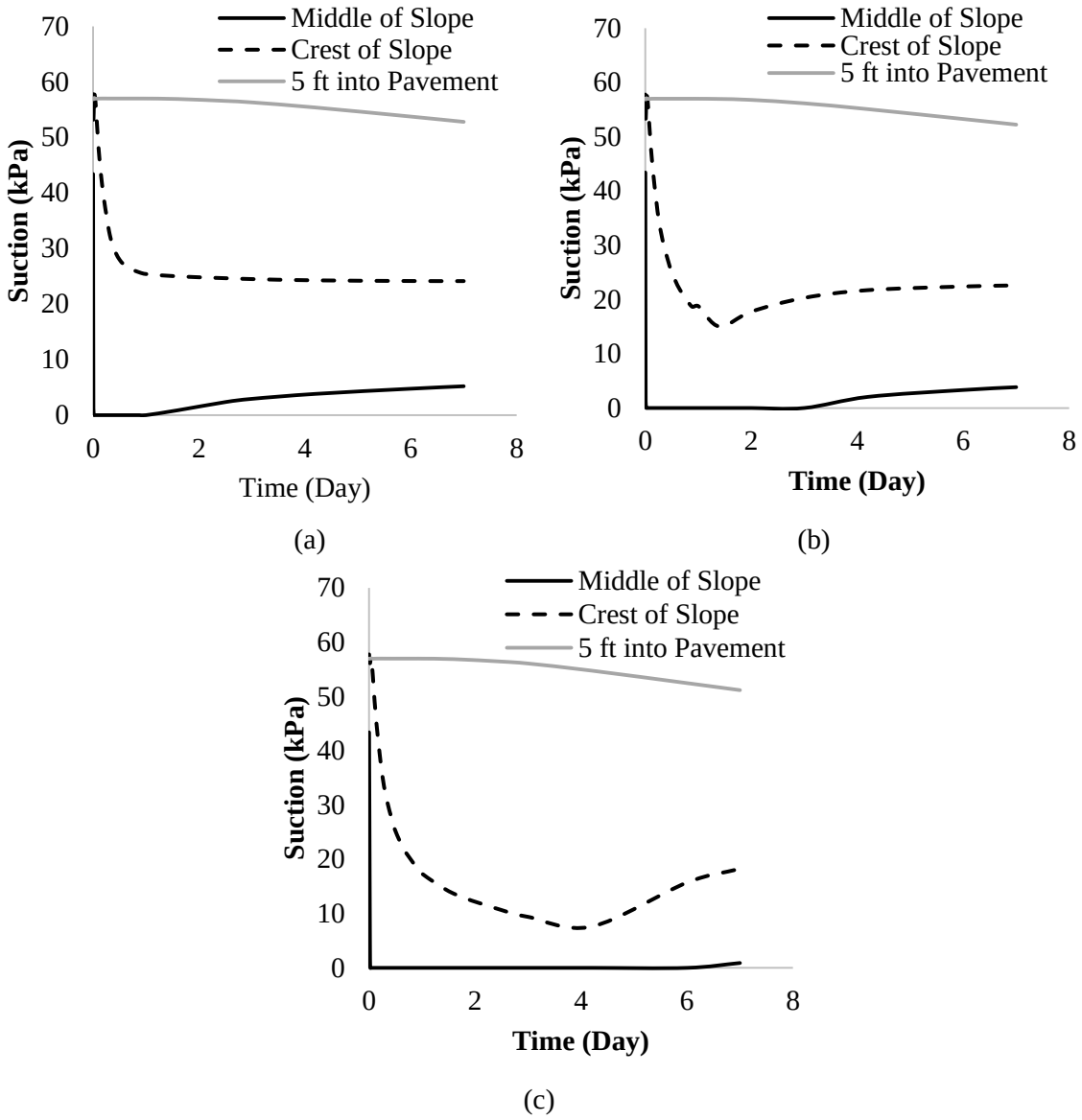

Figure B. 6 2N Suction Variation with 25% initial moisture content (a) High intensity rainfall (b) Medium intensity rainfall (c) Low intensity rainfall

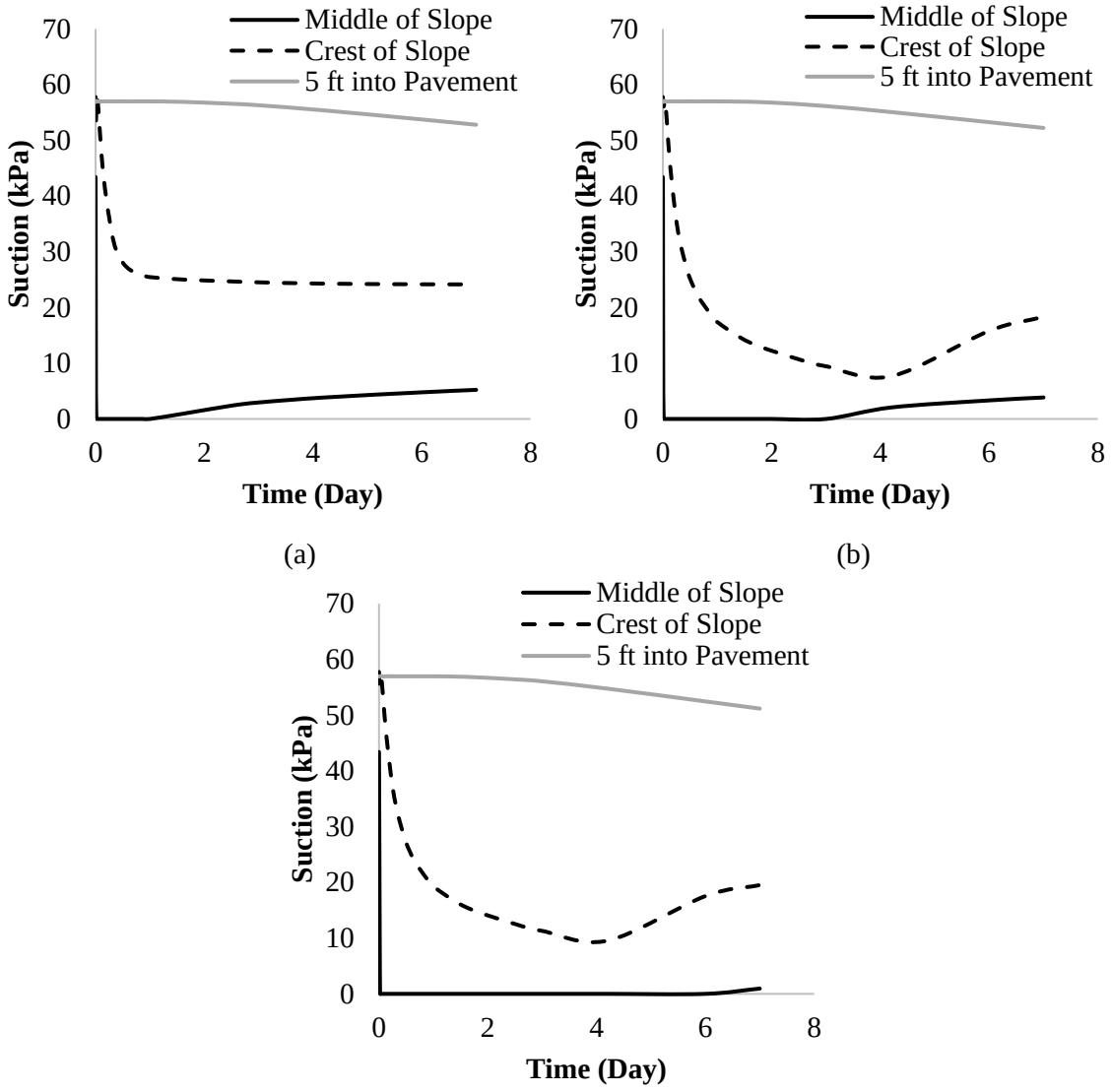

(a)

(b)

(c)

Figure B. 7 2N Suction Variation with 35% initial moisture content (a) High intensity rainfall (b) Medium intensity rainfall (c) Low intensity rainfall

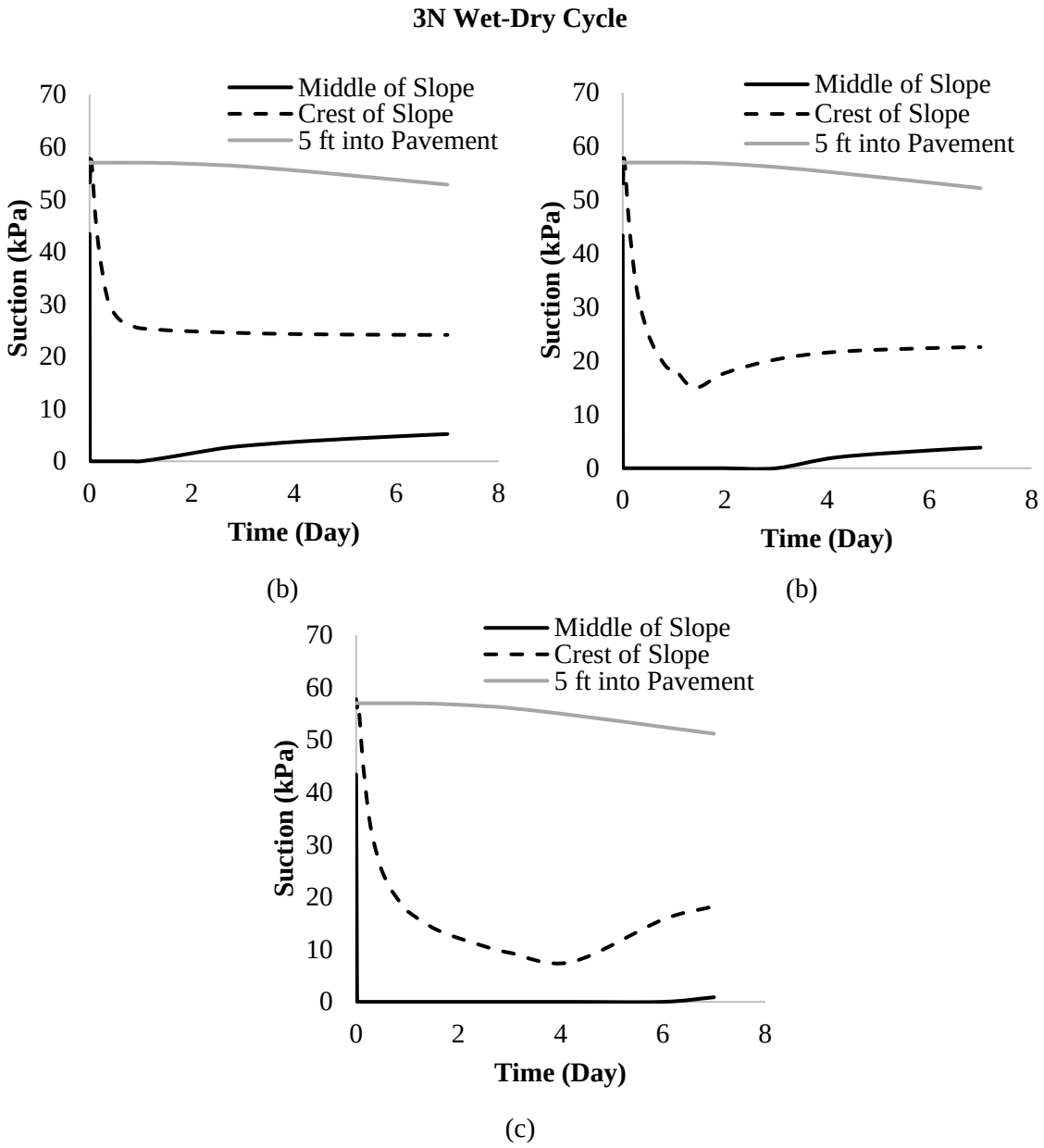

Figure B. 8 3N Suction Variation with 0% initial moisture content (a) High intensity rainfall (b) Medium intensity rainfall (c) Low intensity rainfall

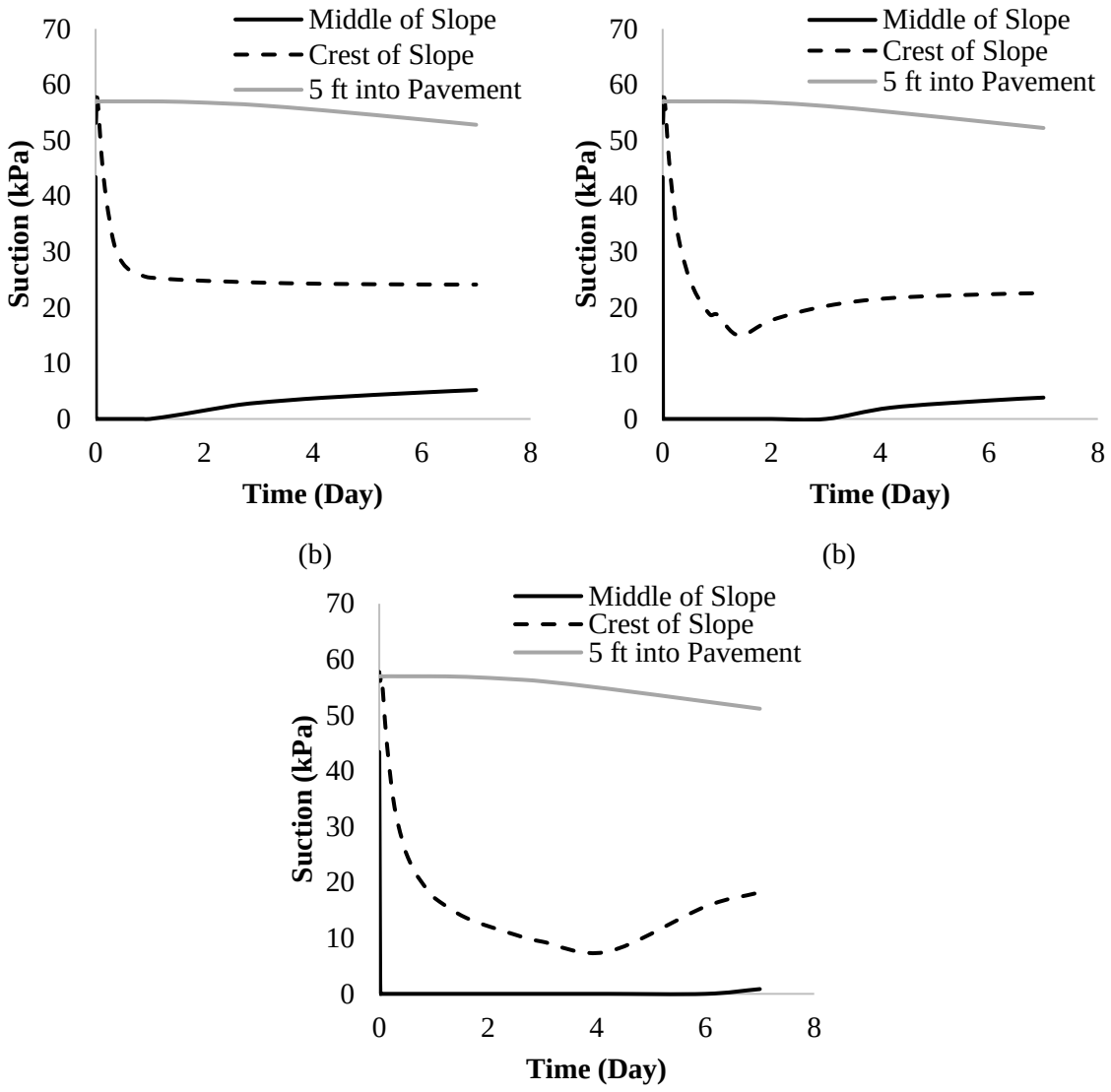

(b)

(b)

(c)

Figure B. 9 3N Suction Variation with 15% initial moisture content (a) High-intensity rainfall (b) Medium intensity rainfall (c) Low-intensity rainfall

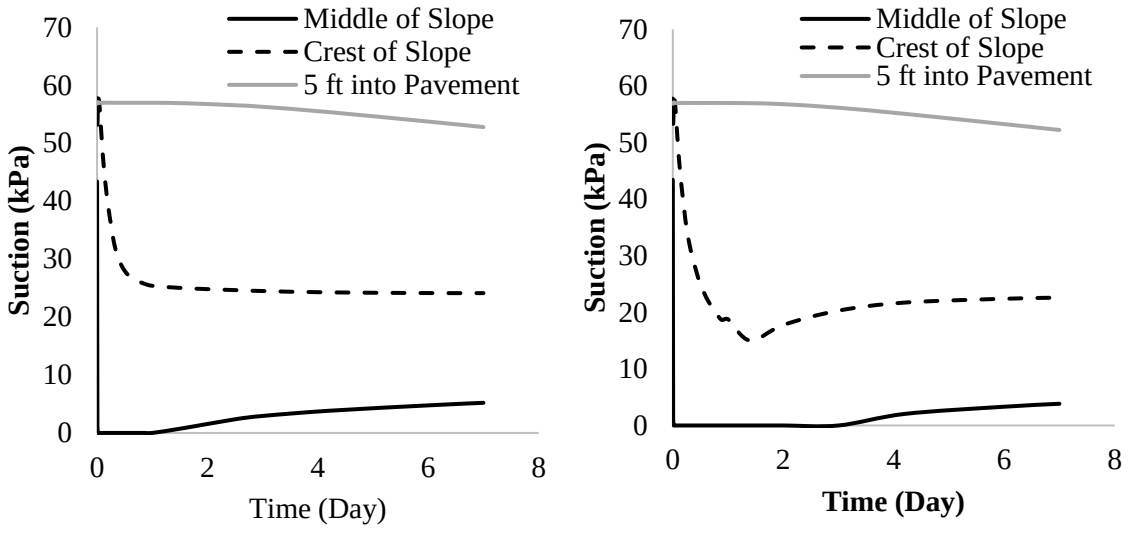

(b)

(b)

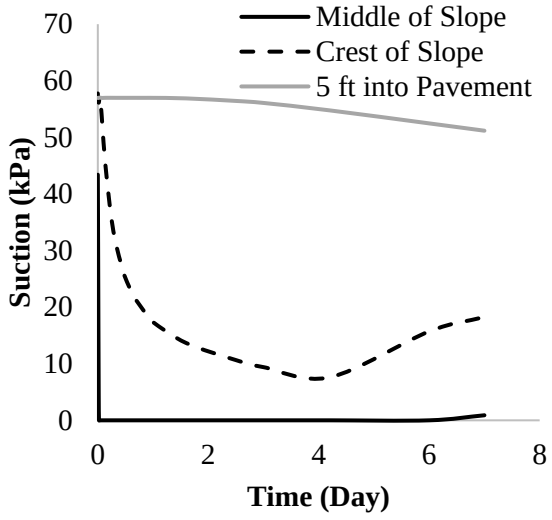

(c)

Figure B. 10 3N Suction Variation with 25% initial moisture content (a) High intensity rainfall (b) Medium intensity rainfall (c) Low intensity rainfall

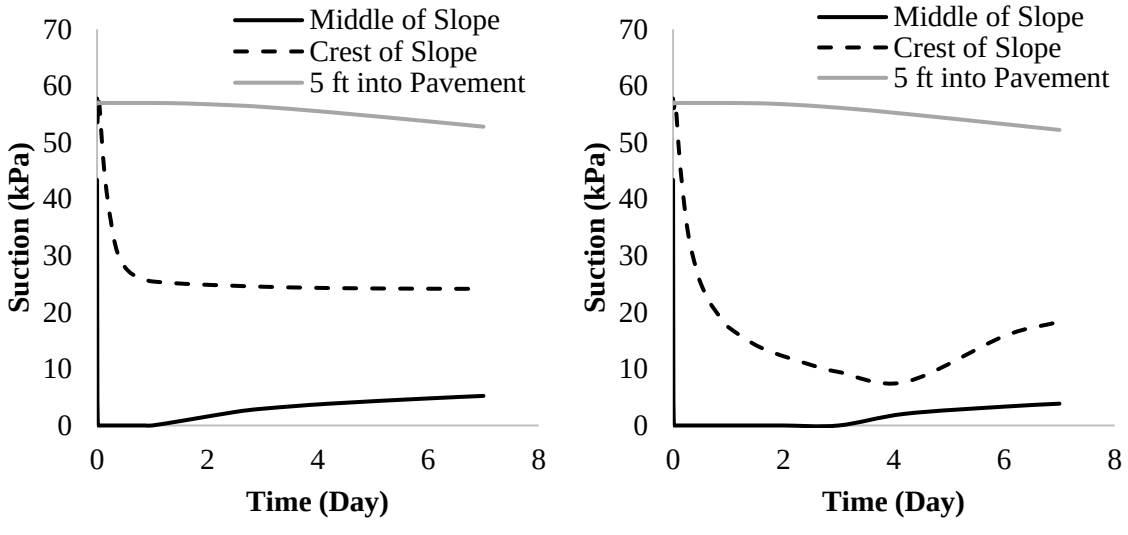

(b)

(b)

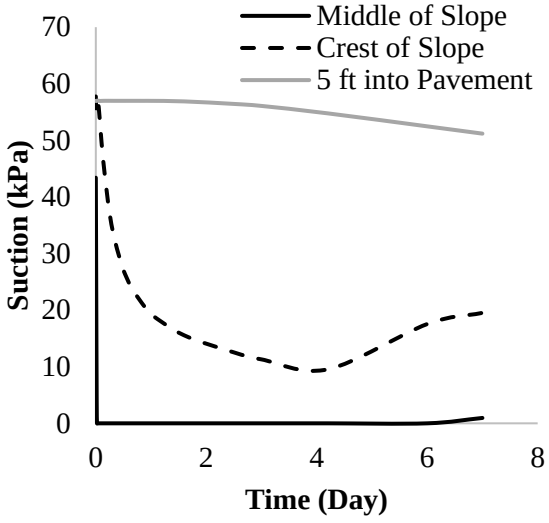

(c)

Figure B. 11 3N Suction Variation with 35% initial moisture content (a) High intensity rainfall (b) Medium intensity rainfall (c) Low intensity rainfall

APPENDIX C: FIGURES OF SUCTION VARIATION ON LEVEE

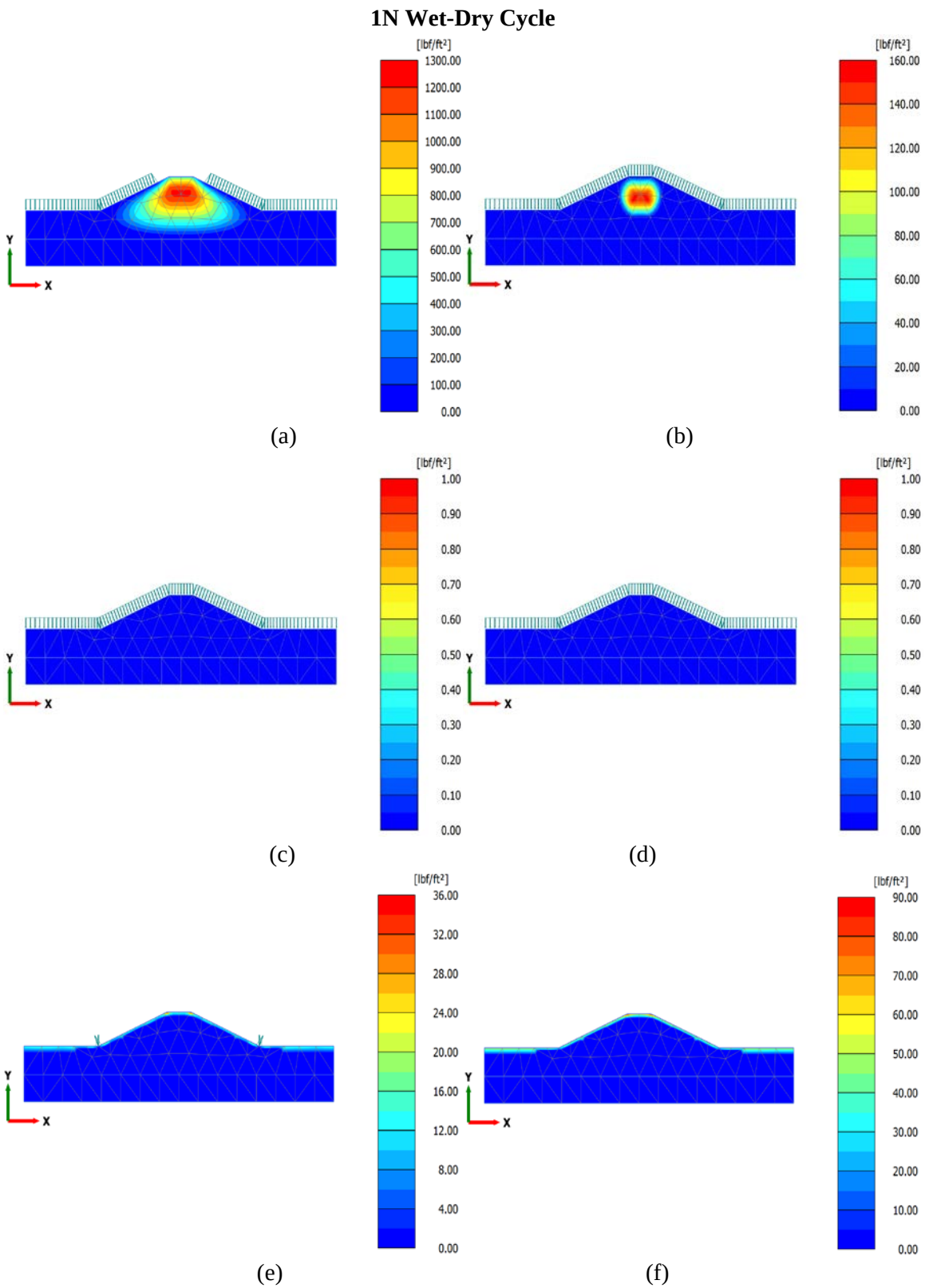

Figure C.1 Suction variation of 1N wet-dry cycle for 0% initial moisture content at low intensity 2 hr rainfall period (a) After 30 min (b) After 2 hr (c) After 6 hr (c) After 12 hr (d) after 3 day (e) after 7 day

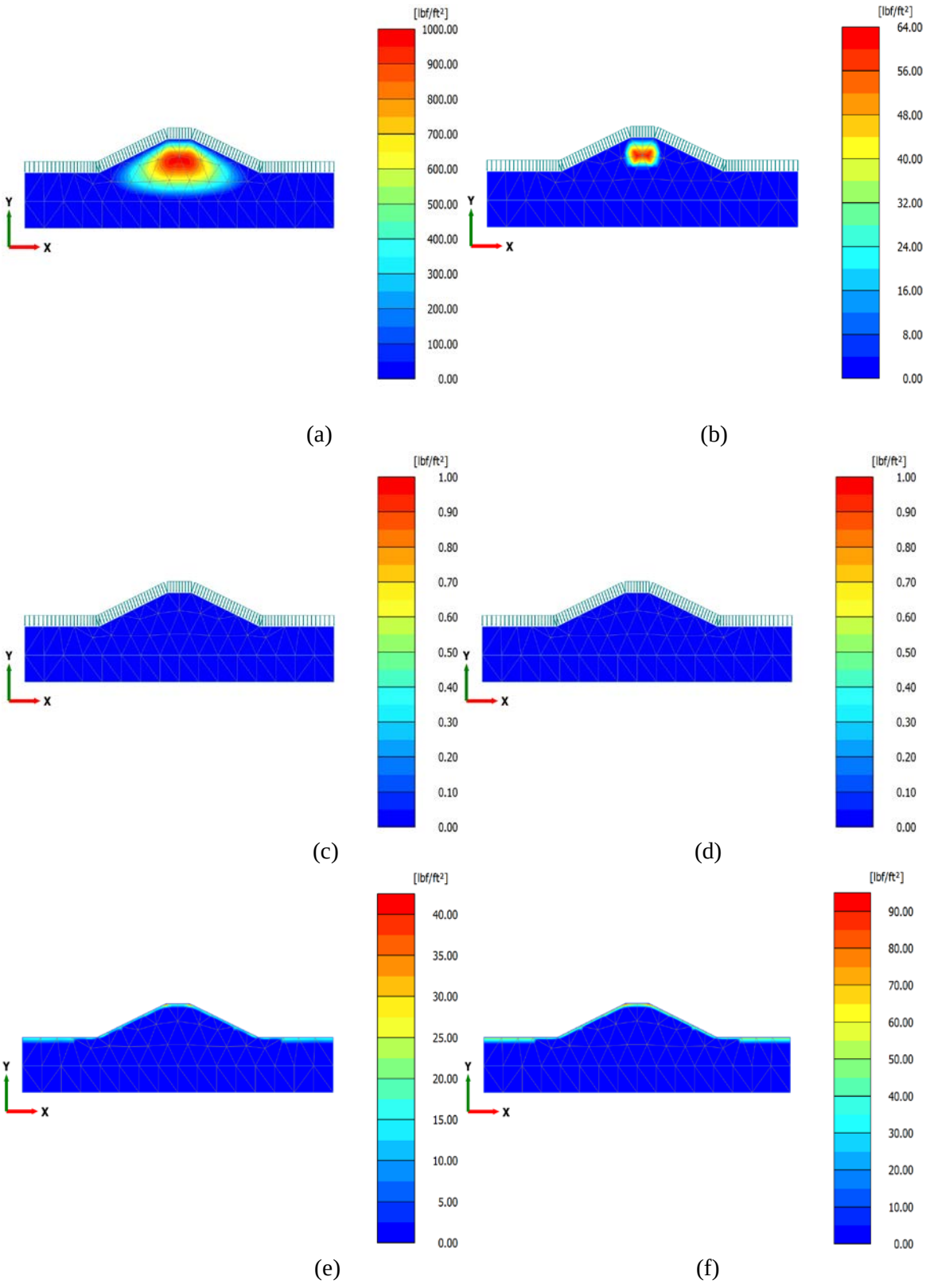

Figure C.2 Suction variation of 1N wet-dry cycle for 0% initial moisture content at low intensity 12 hr rainfall period (a) After 30 min (b) After 2 hr (c) After 6 hr (c) After 12 hr (d) after 3 day (e) after 7 day

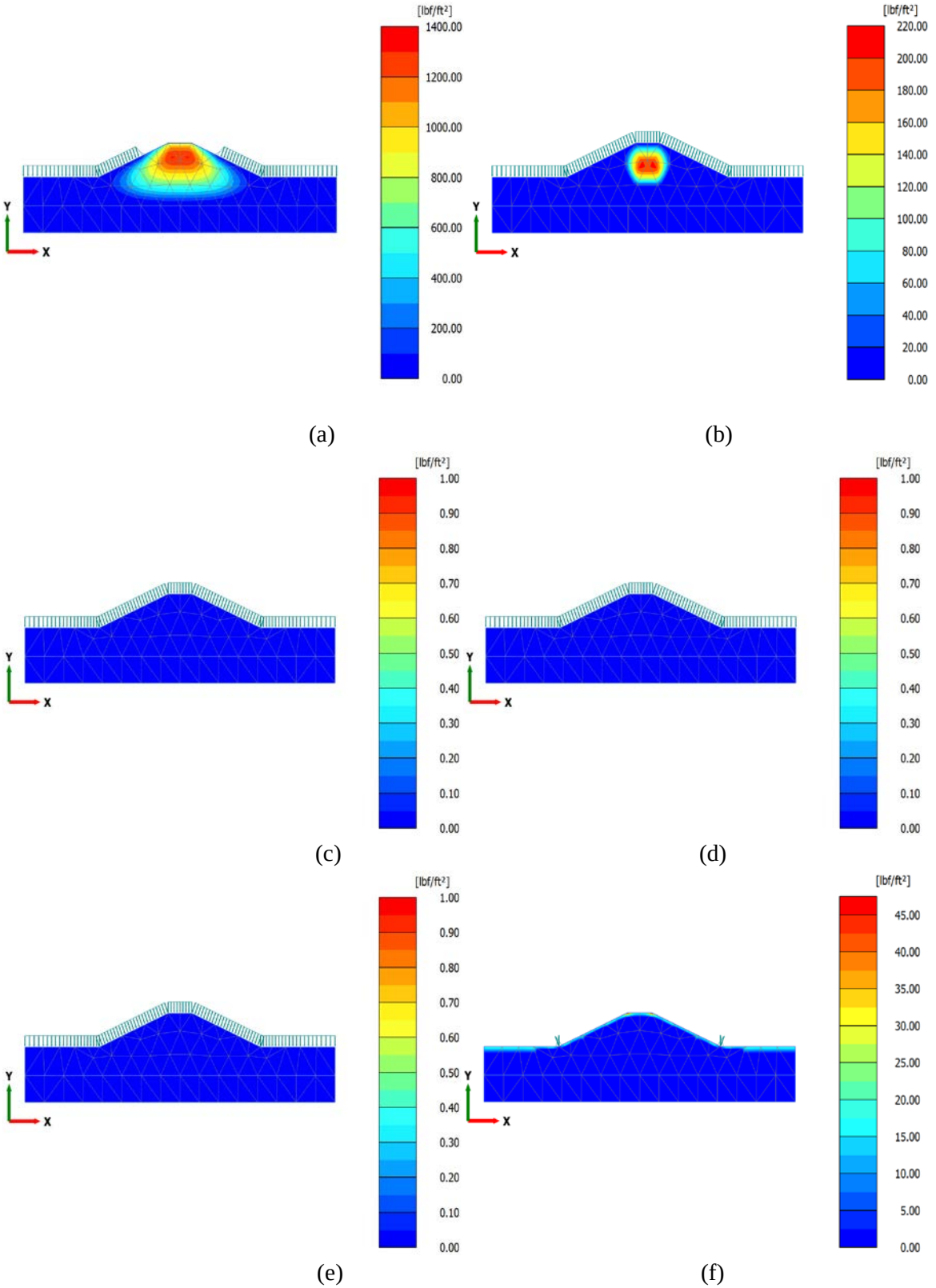

Figure C.3 Suction variation of 1N wet-dry cycle for 0% initial moisture content at low intensity 3-days rainfall period (a) After 30 min (b) After 2 hr (c) After 6 hr (c) After 12 hr (d) after 3 day (e) after 7 day

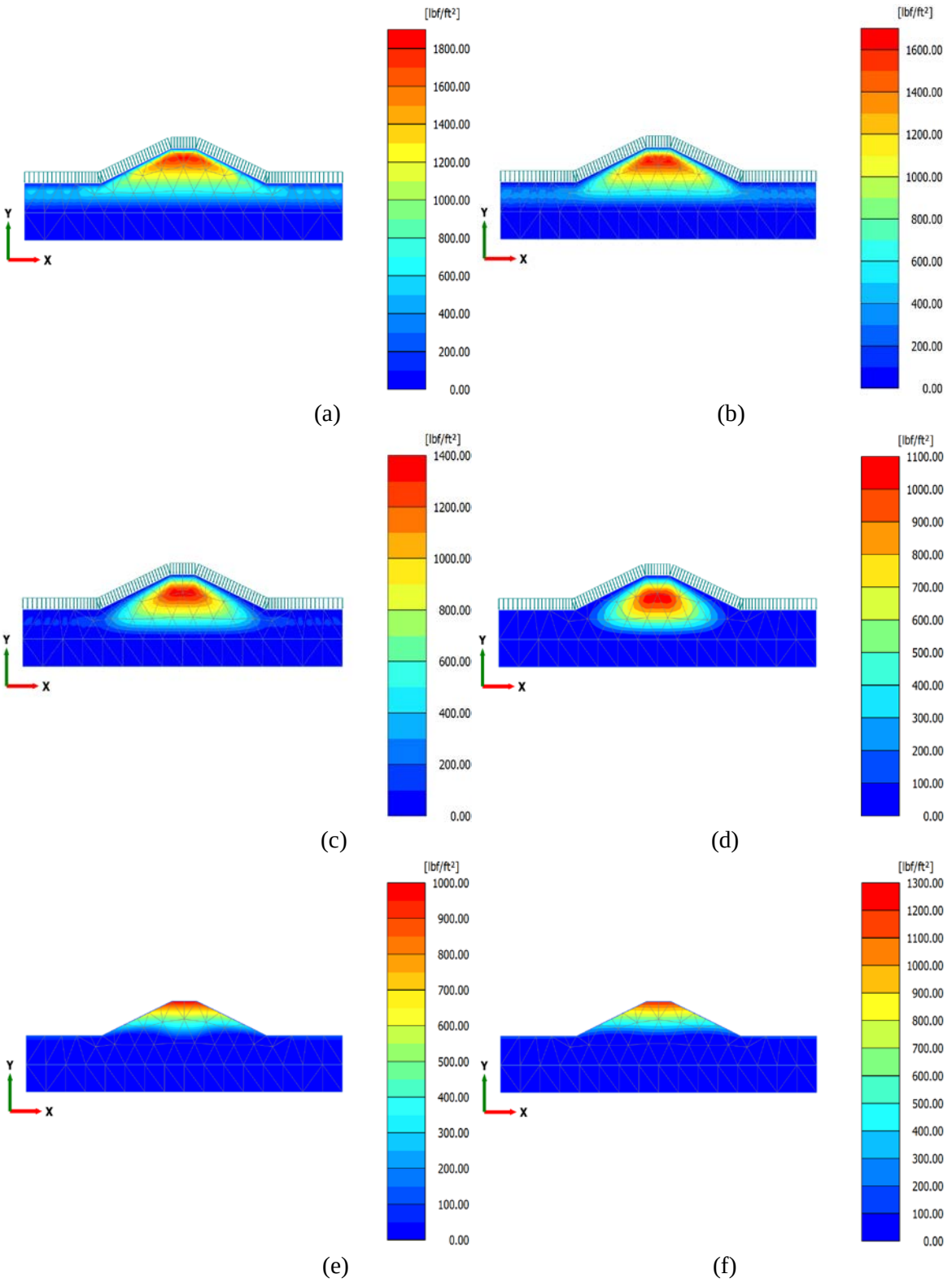

Figure C.4 Suction variation of 1N wet-dry cycle for 35% initial moisture content at low intensity 2 hr rainfall period (a) After 30 min (b) After 2 hr (c) After 6 hr (c) After 12 hr (d) after 3 day (e) after 7 day

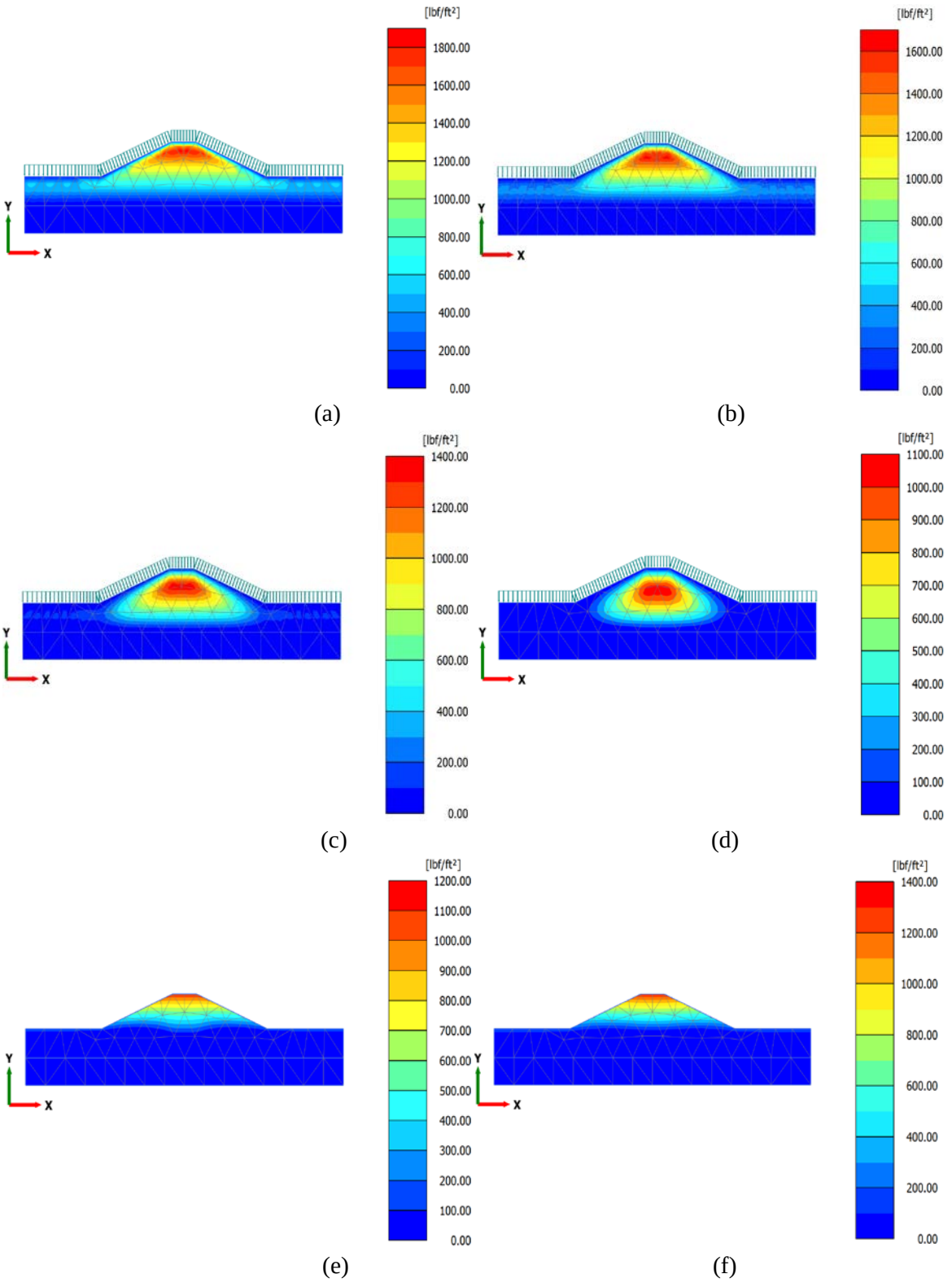

Figure C.5 Suction variation of 1N wet-dry cycle for 35% initial moisture content at low intensity 12 hr rainfall period (a) After 30 min (b) After 2 hr (c) After 6 hr (c) After 12 hr (d) after 3 day (e) after 7 day

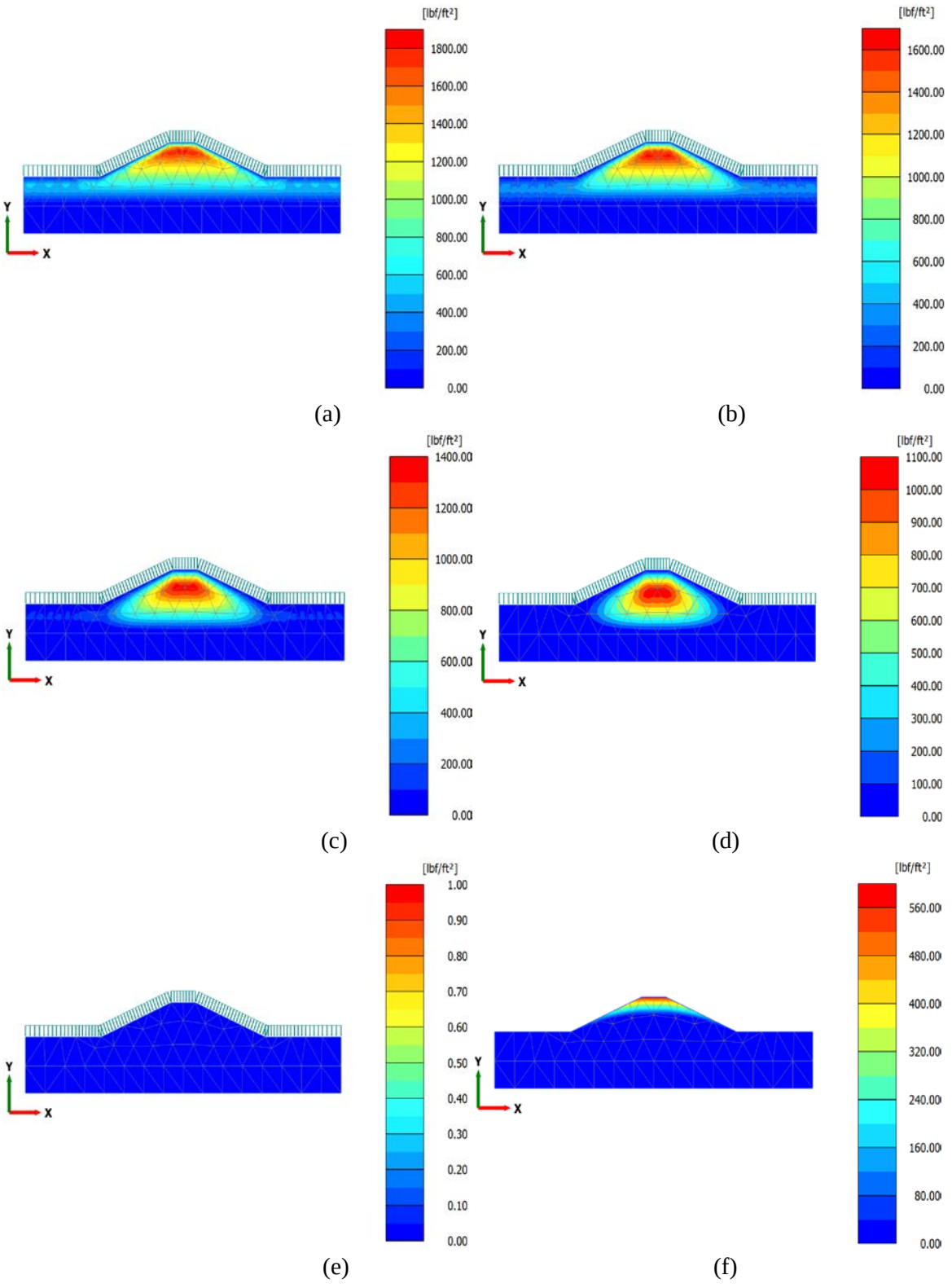

Figure C.6 Suction variation of 1N wet-dry cycle for 35% initial moisture content at low intensity 3-days rainfall period (a) After 30 min (b) After 2 hr (c) After 6 hr (c) After 12 hr (d) after 3 day (e) after 7 day

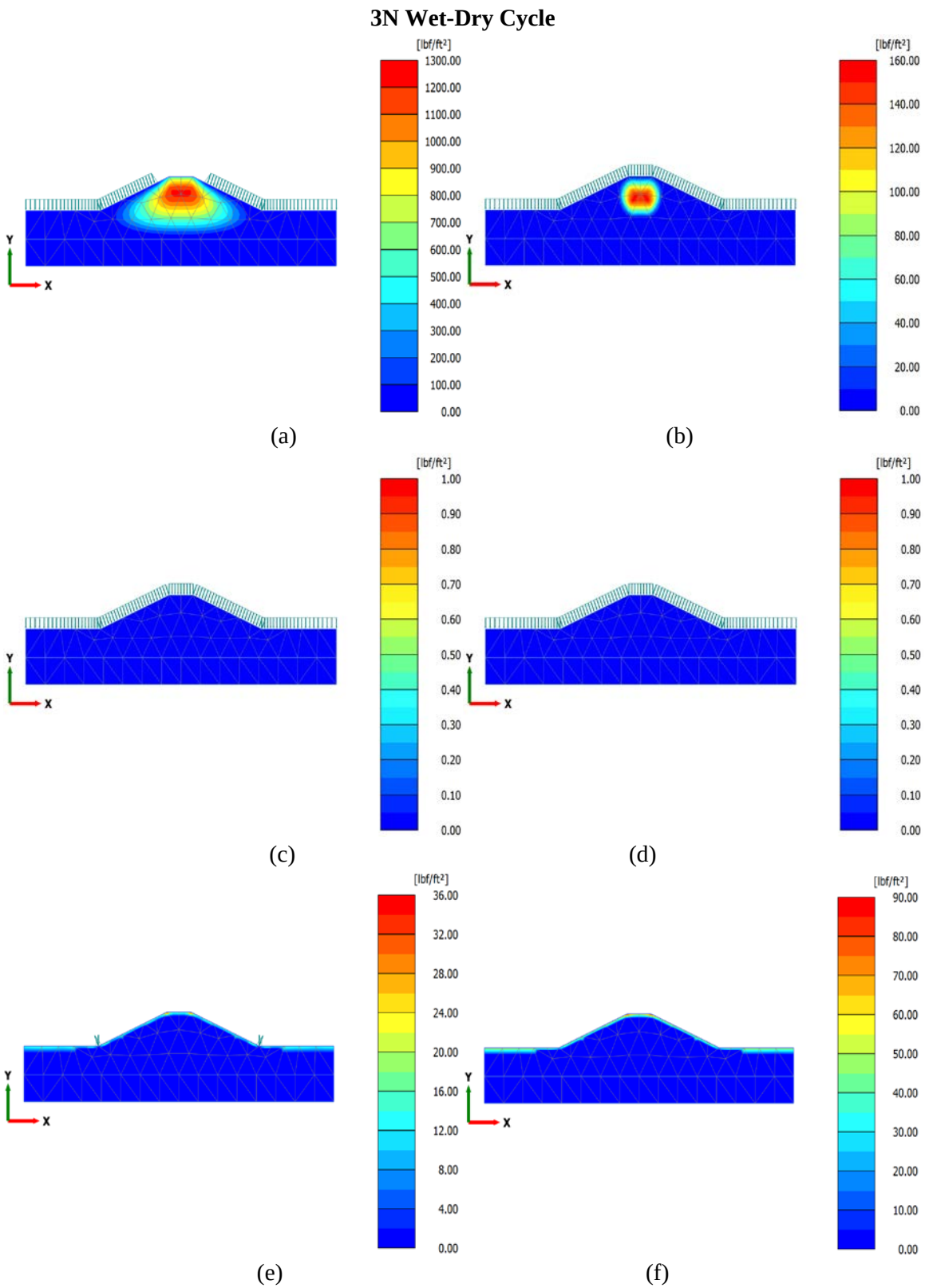

Figure C.7 Suction variation of 1N wet-dry cycle for 0% initial moisture content at low intensity 2 hr rainfall period (a) After 30 min (b) After 2 hr (c) After 6 hr (c) After 12 hr (d) after 3 day (e) after 7 day

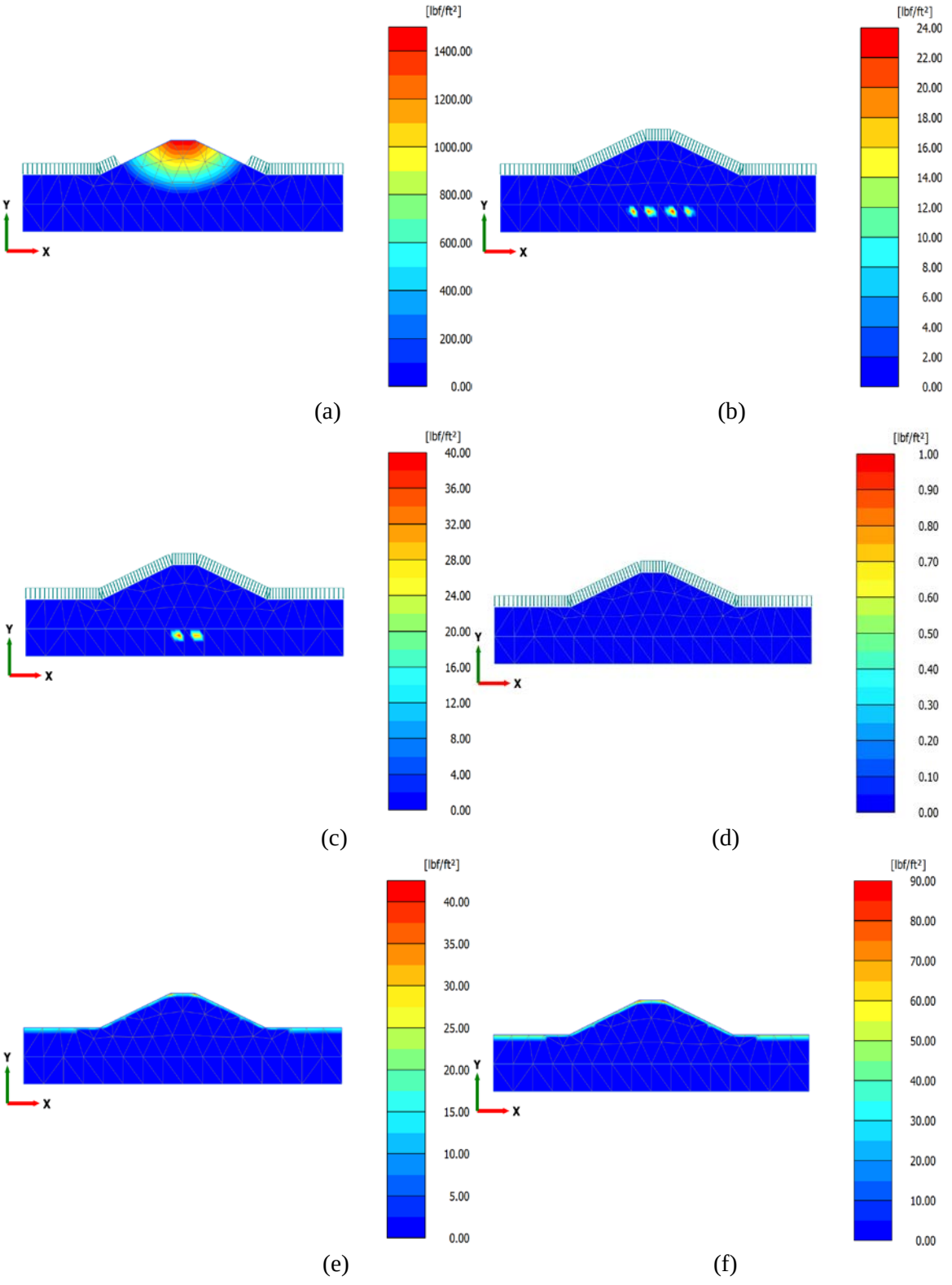

Figure C.8 Suction variation of 1N wet-dry cycle for 0% initial moisture content at low intensity 12 hr rainfall period (a) After 30 min (b) After 2 hr (c) After 6 hr (c) After 12 hr (d) after 3 day (e) after 7 day

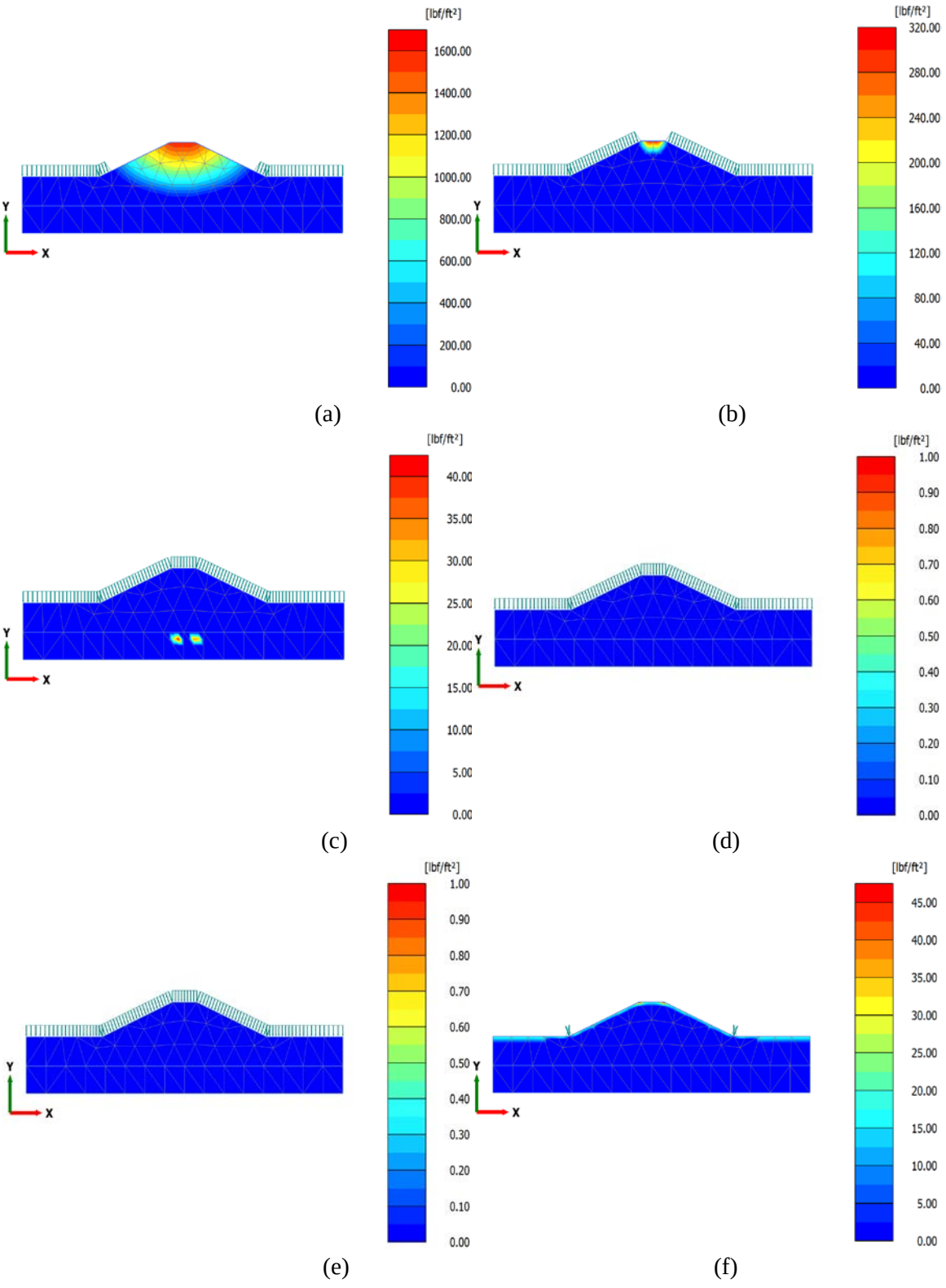

Figure C.9 Suction variation of 1N wet-dry cycle for 0% initial moisture content at low intensity 3-day rainfall period (a) After 30 min (b) After 2 hr (c) After 6 hr (c) After 12 hr (d) after 3 day (e) after 7 day

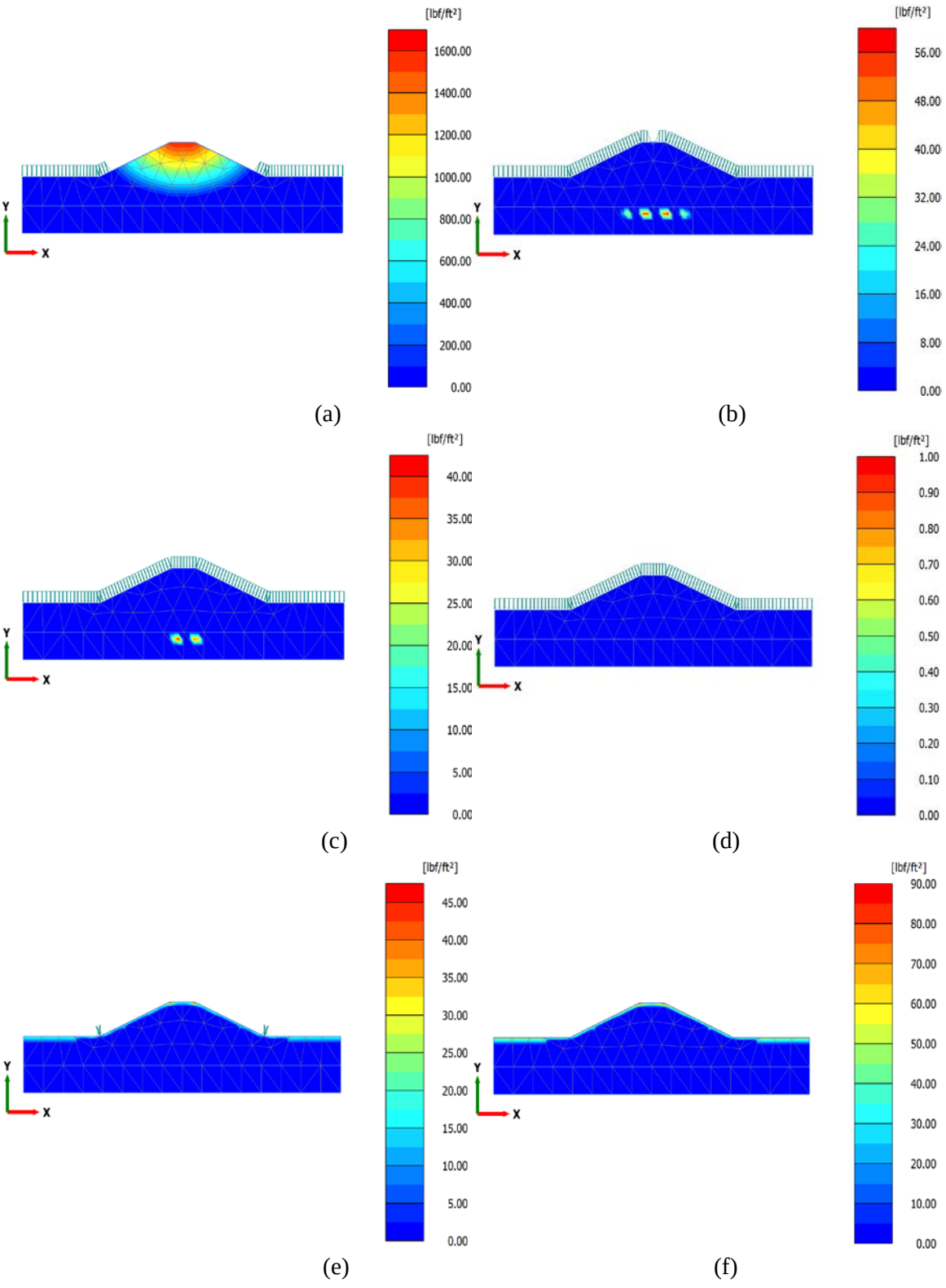

Figure C.10 Suction variation of 1N wet-dry cycle for 35% initial moisture content at low intensity 2 hr rainfall period (a) After 30 min (b) After 2 hr (c) After 6 hr (c) After 12 hr (d) after 3 day (e) after 7 day

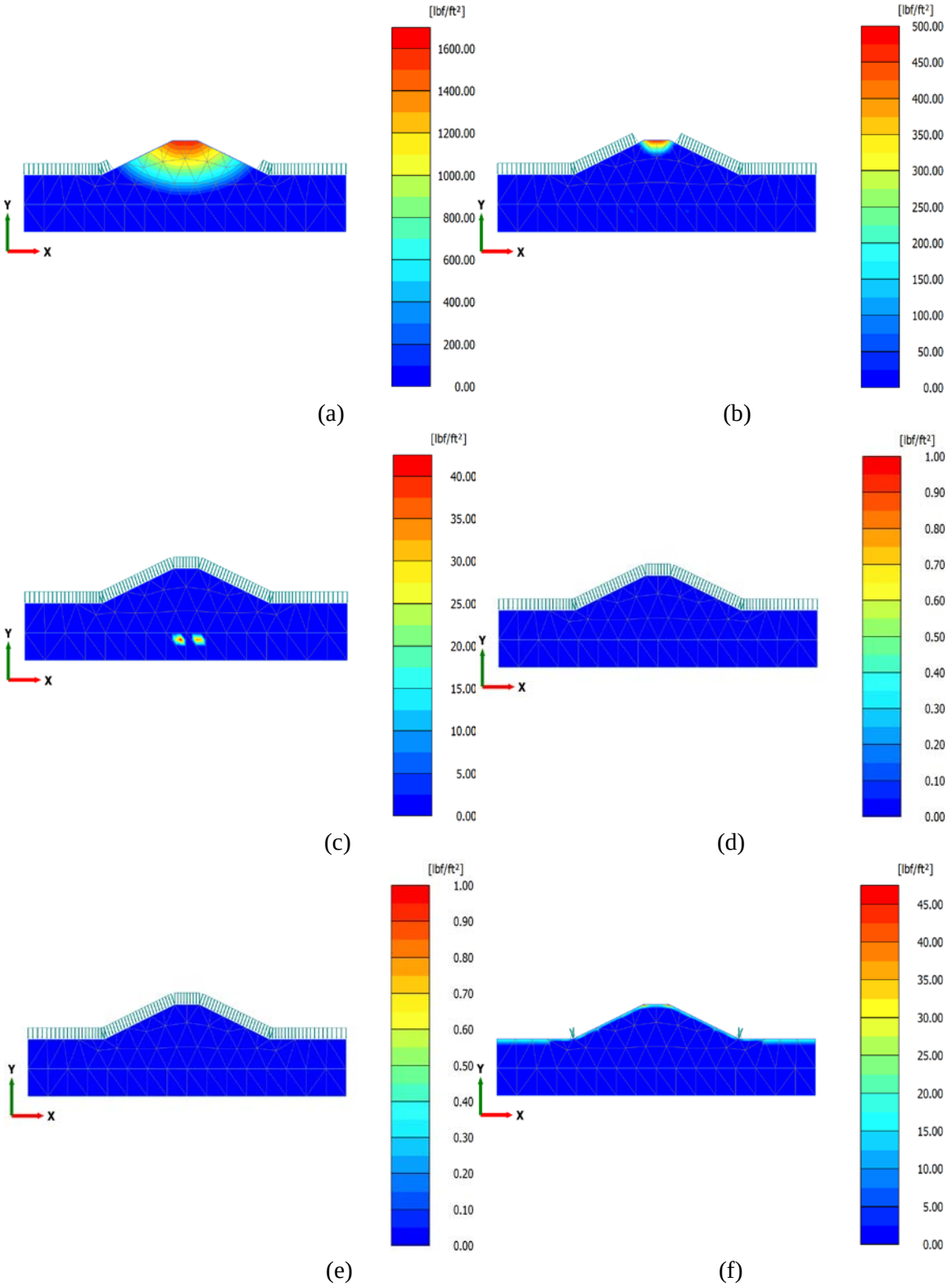

Figure C.11 Suction variation of 1N wet-dry cycle for 35% initial moisture content at low intensity 12 hr rainfall period (a) After 30 min (b) After 2 hr (c) After 6 hr (c) After 12 hr (d) after 3 day (e) after 7 day

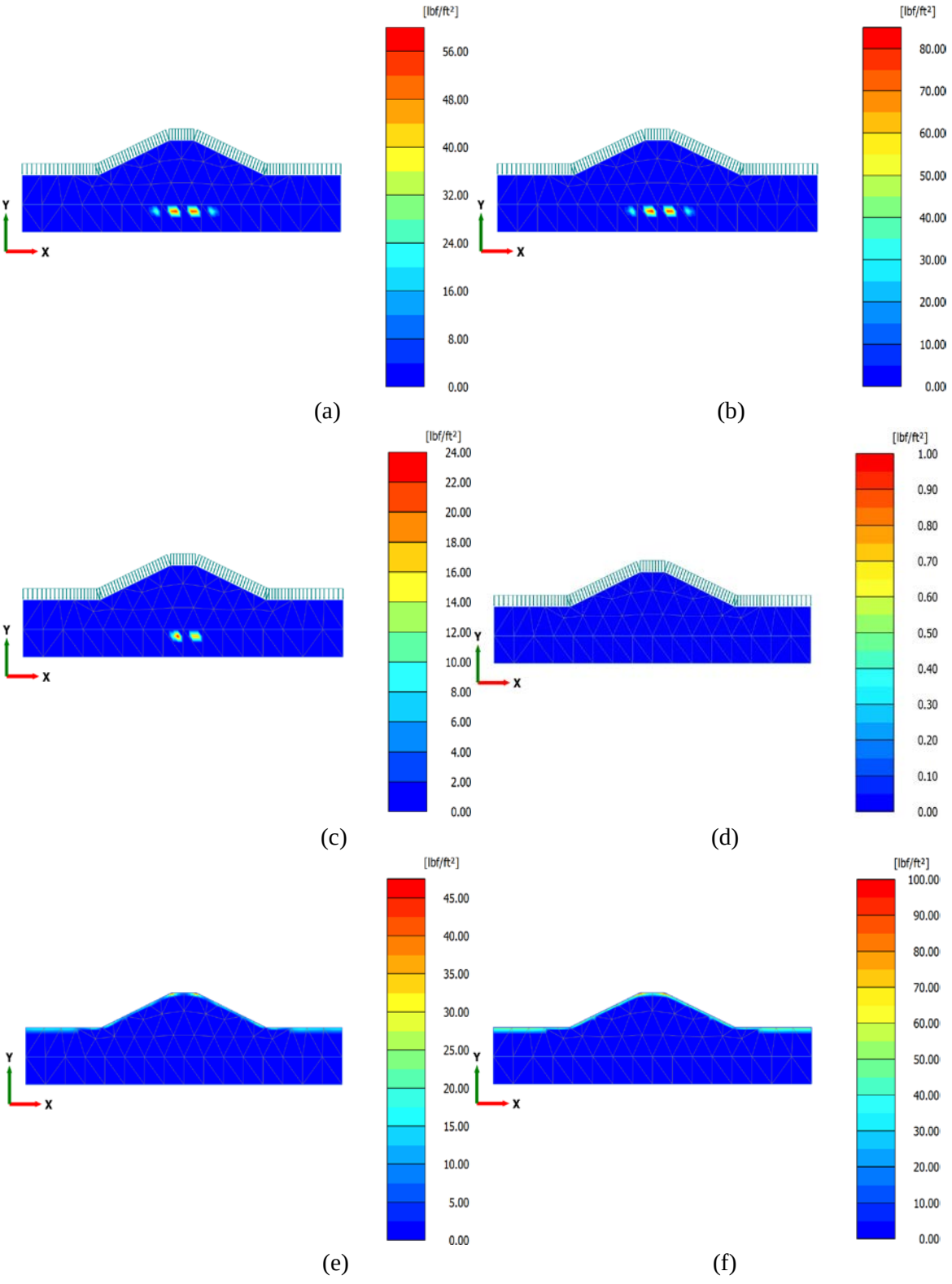

Figure C.12 Suction variation of 1N wet-dry cycle for 35% initial moisture content at low intensity 3-day rainfall period (a) After 30 min (b) After 2 hr (c) After 6 hr (c) After 12 hr (d) after 3 day (e) after 7 day

APPENDIX D: PLOT OF SUCTION VARIATION ON LEVEE

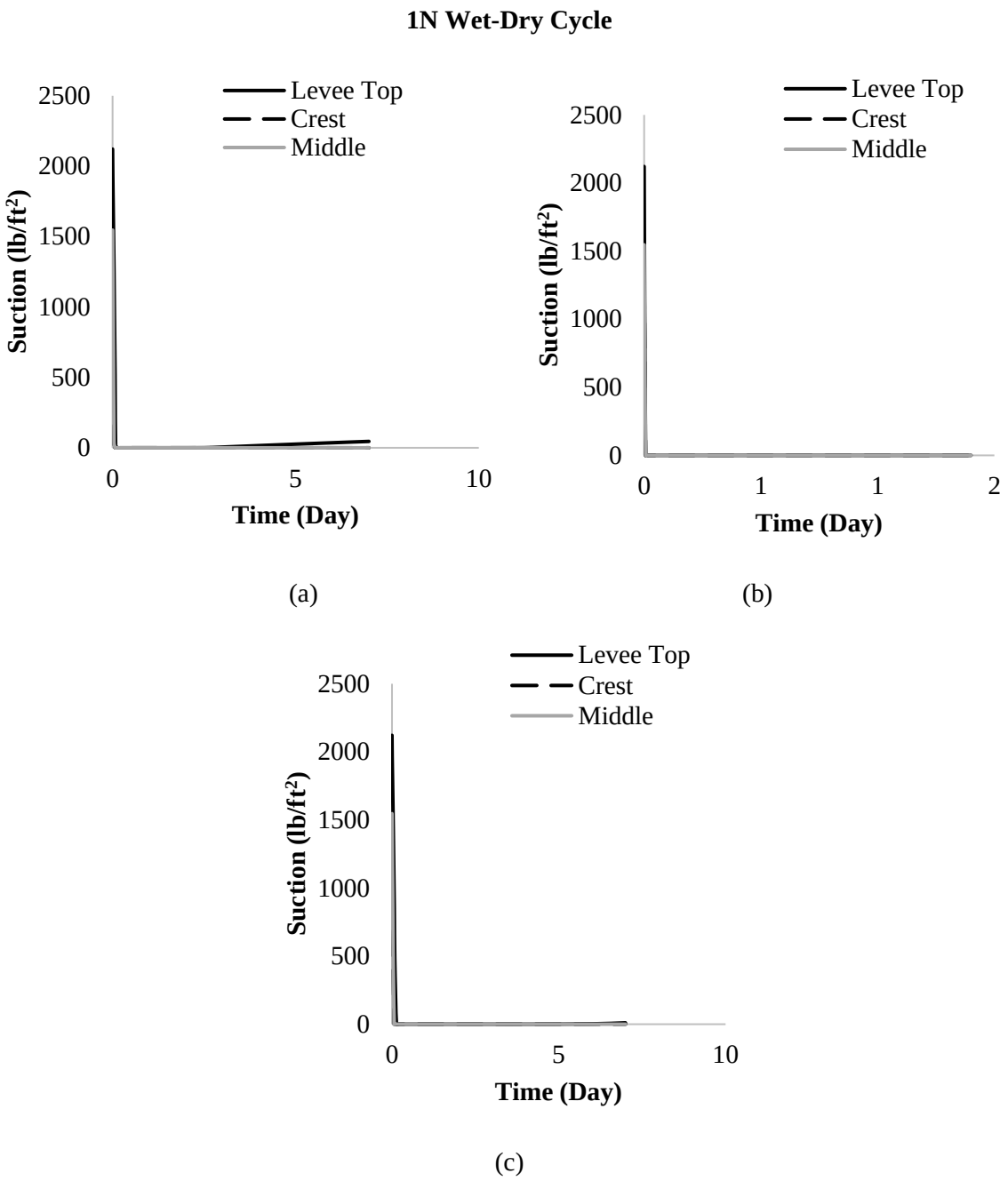

Figure D.1 1N Suction Variation with 0% initial moisture content (a) High intensity rainfall (b) Medium intensity rainfall (c) Low intensity rainfall

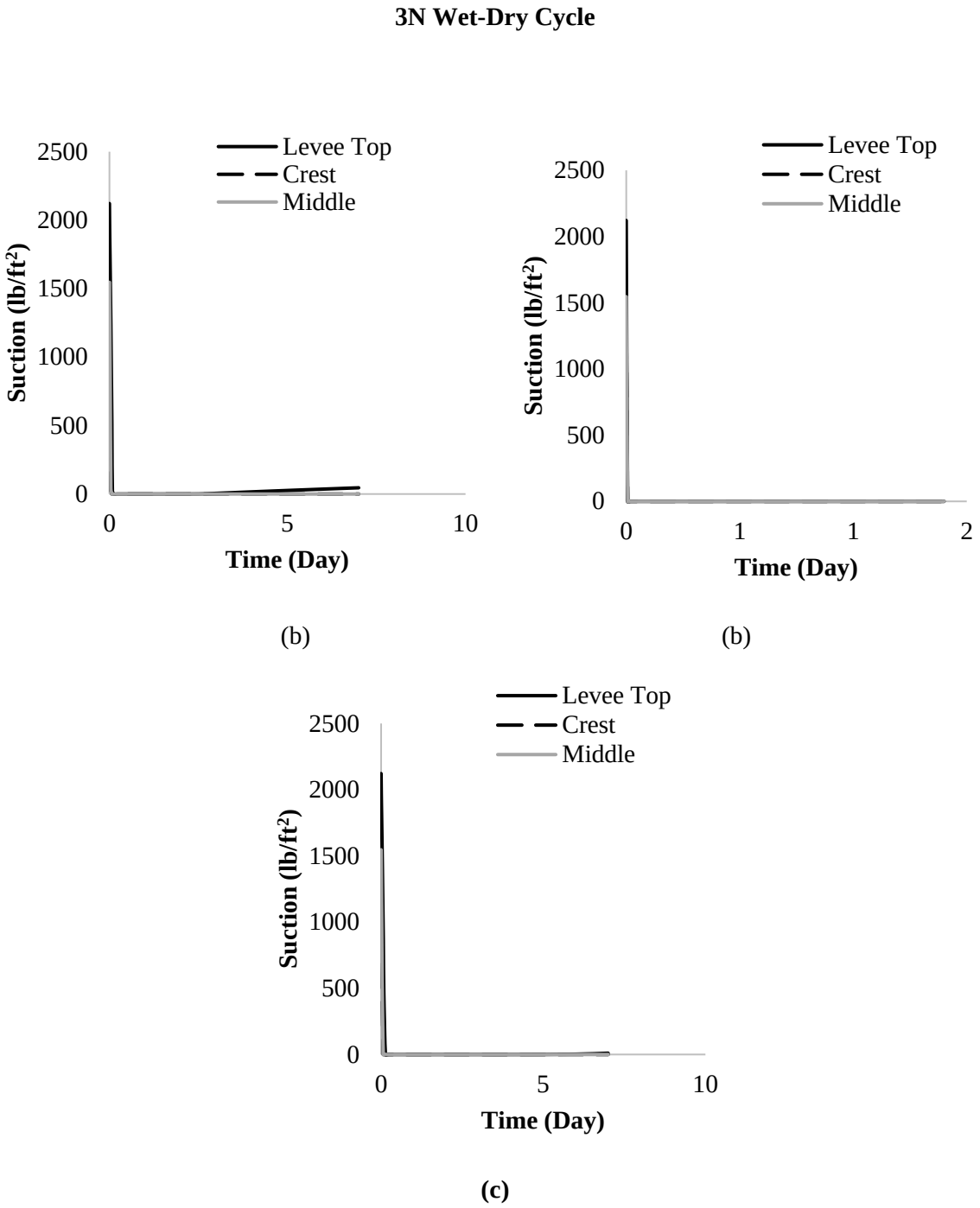

Figure D.2 3N Suction Variation with 0% initial moisture content (a) High intensity rainfall (b) Medium intensity rainfall (c) Low intensity rainfall

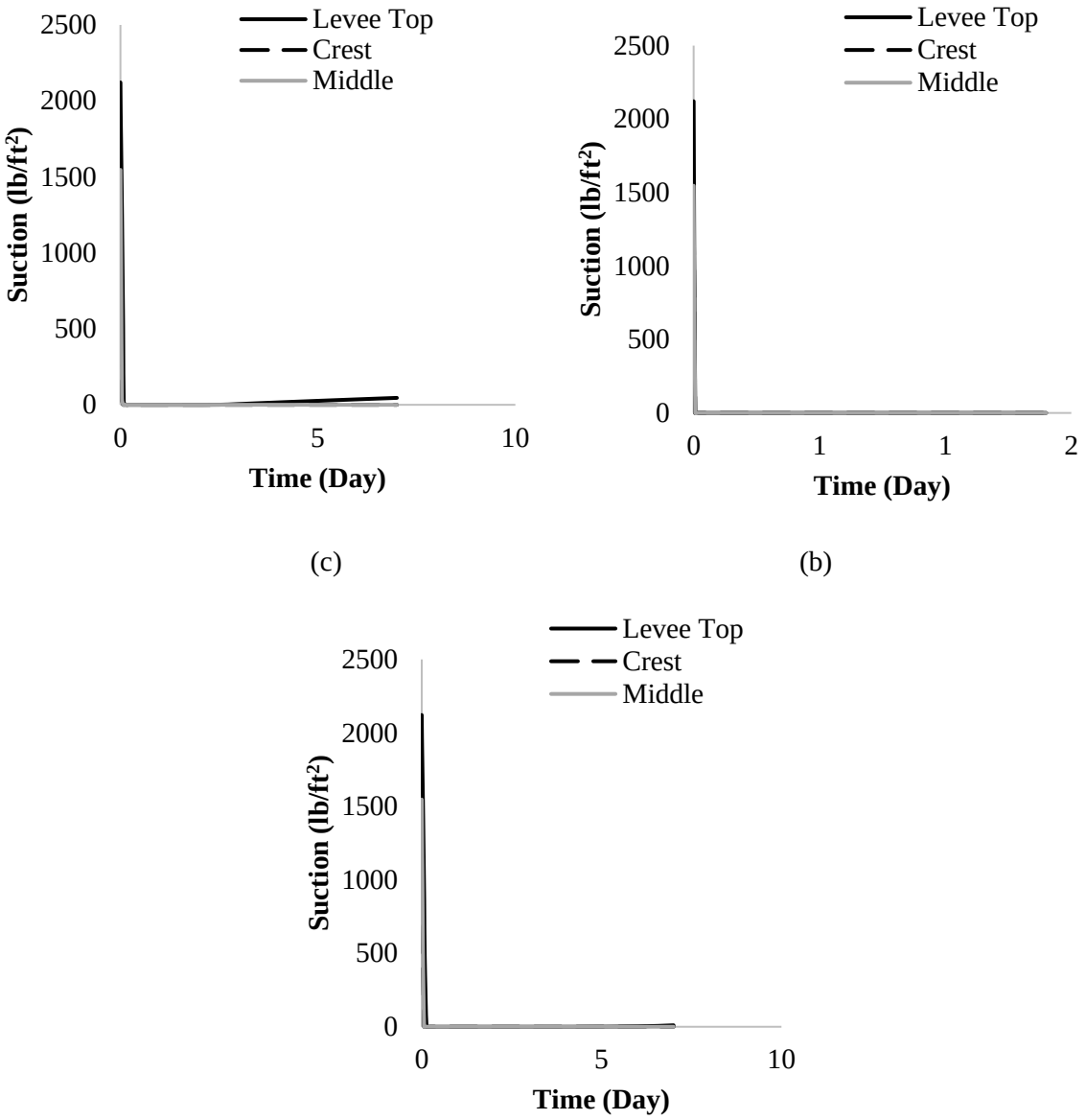

Figure D.3 3N Suction Variation with 35% initial moisture content (a) High intensity rainfall (b) Medium intensity rainfall (c) Low intensity rainfall